Acknowledgements

My supervisor Sara, who has often said "the only impact I have had on this project was telling you at the beginning that it wouldn't work." More importantly Sara's ability to make friends in an empty room has led to her having an enormous network of collaborators without whom this project could not have been possible. My second supervisor Tamsin whose spectacular communication skills keep the whole school on their toes. Liaque Latiff for not only showing me cell culture and dissection techniques but for his boundless enthusiasm, Ian Mellor, Kevin Webb, and Tom Hartman for being generous with their time, advice, and equipment. Alex Payne, John Ryan, and Andy Cubbon whose willingness to trade experimental advice for beer saved me hundreds of hours in poorly defined search terms and failed experiments. My family, for always nodding politely whenever I discussed my project. The staff at the Johnson Arms for not judging me every time I turned up to collect spiders from their beer garden. The BBSRC for funding my project and ensuring I did not starve to death. The University of Nottingham for not learning their lesson when they accepted me for my undergraduate degree.

Ex vivo Spider silk, an exploration of the novel method for the dissection and culturing of spider silk glands.

A gland by any other name would still excrete.

Thesis submitted to the University of Nottingham for the degree of

Doctor of philosophy

June 2025

Morgan Kevan Thornber

14301012

Supervisors Sara Goodacre, Tamsin Majerus

School of Life sciences

University of Nottingham

Table of Contents

Table of figures

Introduction

Tables of materials

Tables displaying materials used in methods sections, each section lists the novel materials used in each section.

Chapter 1	
Name	Cas Number
Ethanol	64-17-5
DMEM F12 HAM	73-32-5
PBS	7778-77
Tetracycline Hydrochloride	64-75-5
Gentamicin	1405-41-0
Penicillin–Streptomycin-Amphotericin	3810-74-0
Agarose	9012-36-6

Chapter 2	
Name	Cas Number
Glutaraldehyde solution	111-30-8
0.1M Cacodylate buffer	6131-99-3
Osmium tetroxide	20816-12-0
Propylene oxide	75-56-9
TAAB Low Viscosity Resin (TLV)	ERL4221D
BEEM Capsules	AGG362-1
Carbon Supported Copper Grids	TEM-FCF100CU50
Uranyl acetate	541-09-3
Lead (II) citrate	6107-83-1

Chapter 3	
1-Butyl-3-methylimidazolium chloride	79917-90-1
1-Butyl-3-methylimidazolium acetate	284049-75-8
1-Ethyl-3-methylimidazolium acetate	143314-17-4
1-Ethyl-3-methylimidazolium chloride	65039-09-0
Ethyl L-lactate	687-47-8
Acetone	67-64-1
Methanol	67-56-1
2-Propanol	67-63-0
Nitric acid	7697-37-2
Hydrogen peroxide solution	7722-84-1
Sodium hypochlorite solution	SKU 1056142500
Sulfuric acid	7664-93-9

Abstract

This thesis will detail the novel system that has been developed to dissect out and maintain in culture the glands that produce a spider's silk. As well as the findings surrounding the internal structures of the gland's cells, this study system will allow exploration of how the glands function under stress and provide potential avenues for future applications and study. This will be done in three parts. Firstly, describing the methodologies for the removal and culture of the silk glands as well as the confirmatory work to show the glands are not just surviving, but actively producing silk. Secondly the exploration of the observational data made possible through viewing the glands in culture. Finally, showing the materials research that is possible through having access to previously inaccessible liquid silk dope for testing, the work surrounding the new methodology for the dissolution and reprinting of native spun spider silk, and the insights this gives us into the way silk proteins fold and organise in the gland that produces one of the most studied biomaterials in the natural world.

Thesis Introduction

This program of work focuses on three main aims. The first, to design an ex vivo tissue culture system that allows for the study of silk glands and their production of spider silk. The second, to investigate what could we learn from these dissected glands. The third, to investigate what could be done with dissected silk glands.

To address the first aim of "to design an ex vivo tissue culture system that allows for the study of silk glands and their production of spider silk" the first chapter of thesis will detail the novel system that has been developed to dissect out and maintain in culture the glands that produce the spider's silk. This chapter will focus on the methods employed in setting up the system initially as well as the confirmatory works that went into showing that the cultured glands were not only surviving but still actively producing spider silk. The chapter will also detail the confirmatory works performed to show the repeatability of the system and its applicability across the model species, as well as two other species to demonstrate the wider applicability of the system.

To address the second aim of "to investigate what could we learn from these dissected glands?" the second chapter will detail how using the method developed in the first chapter the functions of the gland were able to be studied in greater detail, studying at different levels of magnification the structures of the gland and the silks that it produces.

To address the third aim of "to investigate what could be done with dissected silk glands" chapter three will be presented in two parts, the first detailing the material research that was possible through the novel system as well as the methodologies behind the novel ability to study liquid silk and dissolved silks. The second part of the chapter will focus on the design of protocols to develop the technology further (work that was prevented by lab restrictions resulting from the pandemic).

Before the detail of this program of work is discussed however, a broader question must be discussed, Why Spider silk? This introductory chapter will introduce the works that make research into the biomaterial that is spider silk so interesting to evolutionary biologists and biotechnologists alike. The academic interest surrounding spiders and their silk ranges from ecological studies of insect populations by studying what prey is captured in spiders' webs (Tóth et al., 2004), through using webs as a comparison point to infer evolutionary relationships between different

species (Kaston, 1964), all the way to specific use cases for artificial spider silks to be used in medical implants (Zeplin et al., 2014). Therefore, the scope of the work will be narrowed specifically into the biomaterial applications of spider silk. This will be achieved by introducing the concept of biomaterials, the background into the research into spider silk that has already been undertaken, as well as introducing some of the potential benefits that it has been speculated that spider silk, or a biomaterial that shares common properties with spider silk, could provide to academia or industry.

Introduction to biomaterials

The term biomaterial as described by the International Union of Pure and Applied Chemistry (IUPAC) as "a material exploited in contact with living tissues, organisms, or microorganisms" (Vert et al., 2012). This definition is intentionally loose. When working with this definition we can describe the ancient Egyptian use of fine animal sinew as medical sutures as one of the first recorded uses of biomaterials (Ratner and Zhang, 2020). Using this definition, the ancient Japanese practice of scorching the outer layer of wood used in buildings to deny the opportunity of fungi and insects from degrading and rotting the wood (Shou Sugi Ban) (Hein, 2010), could be described as a biomaterial, given it is the exploitation of a material used in contact with microorganisms. Whilst the former would be widely accepted as an example of a biomaterial and the latter could be argued would not, we are then left with a very broad expanse into which the term biomaterial can fit. In more modern terms the use of fish skin as a material to cover areas of full thickness burns (burns to the skin in which the damage reaches all the way through the dermis to the subcutis (Gibson et al., 2020)) to promote healing (Ibrahim et al., 2020) would fit comfortably into the general perception of what a biomaterial is, whereas the simple addition of a titanium replacement hip likely would not be viewed as biomaterial science (Affatato et al., 2018). Coating a non-

biological medical implant in a biologically derived material in order to better promote implantation and lower the risk of rejection, however, is described as biomaterial research (Teo et al., 2016). This is to say that the intentionally broad definition of biomaterial research would cover research into spider silk and its potential medical applications. But, if a structural application were found for spider silk outside of a biological application this may well not fall under this definition, broad as it is.

The public perception of biomaterials often conjures images of modernity and feats of scientific engineering within medical fields, whereas the term industrial biotechnology conjures images of factories, vats and pop-culture references to zombies or plagues. The truth however is that biomaterials and industrial biotechnology are two sides of the same coin. The simple concept is that 3.5 billion years of successive random biological trial and error (driven by the process of natural selection) has the capacity to produce a plethora of novel and useful materials. These materials thus form the inspiration for synthetic alternatives that perform similar functions or that have similar properties. It is upon the foundation of this that most modern biotechnological and biomaterial research is focused. Biomaterial science was described in 1996 by Ratner as an interdisciplinary endeavour and that remains true to this day. The design and production of microbially biodegradable plastics for example, could

not have been possible without the combined works of microbiologists, biochemists, polymer, and industrial chemists, environmental and oceanographical scientists and production engineers.

The inherently interdisciplinary nature of biomaterial research is one of the driving factors that makes the field so interesting and promotes so much growth, the use of the term biomaterial has increased over 1200% in the last 40 years (Google-Books, n.d.). This proliferation of research has led to breakthroughs in tissue scaffolds, medical prosthesis, artificial valves and organs, stents, tissue culturing, biomanufacturing and more. The need for further research into biomaterials is a driving force in modern research funding with journals like Biomaterials, Nature Biomaterials and Biomaterials Science Rsc all extolling the need for further work into the fields underpinning biomaterial research. These journals publish works detailing advances like healing diabetic wounds using antimicrobial hydro gels (Tu et al., 2022), the formation of scaffolds to aid in the bioprinting of kidney tissues (Lawlor et al., 2021) and the formation of self-healing hydrogels for severe wound care (Wang et al., 2019a) respectively.

Introduction to spider silk research

One of the well-recognised biomaterials is spider silk, having captured the imaginations of people for thousands of years it is commonly referred to as the "Holy Grail" of biomaterials (Cumbers, 2019). A solid protein fibre, formed from a hydrophobic liquid silk dope produced in specialised glands; spiders' silk has been utilised by humans for thousands of years, from ancient aboriginal Australians using silk threads for fishing line, through the ancient Greeks and medieval Europeans using spider silk as antimicrobial bandaging (Lewis, 2006). In more recent centuries, silk has been employed as graticules on microscopes, high powered telescopes and rifle sights, a use that it is well suited for as it resists changing dimensions under changing temperature (Emile et al., 2007). The first true analysis of spider silk's properties was performed by Benton in 1907 when he observed a "thread of unusual diameter" and began the first true materials testing on spider silk, remarking upon its unusual strength and elasticity (Benton, 1907). Subsequent analysis has shown silk to be possessed of many properties of interest to researchers, such as its strength (Giesa et al., 2011), flexibility (Tahir et al., 2017), toughness (Yang et al., 2005) and extensibility (Blackledge et al., 2005) that prompted further study which will be expanded upon below.

Some silk is reported to be roughly as strong as high-grade steel (when the diameter of the fibre is taken into account) but at one sixth the mass and thus it is commonly stated that spider silk is "six times stronger than steel", gram for gram , (Matweb.com, 2018). Spider dragline silk is also non immunogenic to humans (Askarieh et al., 2010), highly rotationally stable (Emile et al., 2007) and capable of absorbing and dissipating a huge amount of energy, with almost 70 percent of the energy put into silk during extension is dissipated as heat and cannot be recovered as elastic recoil (Gosline et al., 1984).

These properties make for a fascinating subject matter given that by virtue of its being a protein, it is roughly 53% atmospherically sourced carbon (Rouwenhorst et al., 1991). Silk could be a potentially useful addition to medical, textile and manufacturing fields (Tahir et al., 2017). Given that, under the correct conditions, silk can last for thousands of years, for example, when webs were found in the undisturbed tomb of Tutankhamun (Carter, 1923).

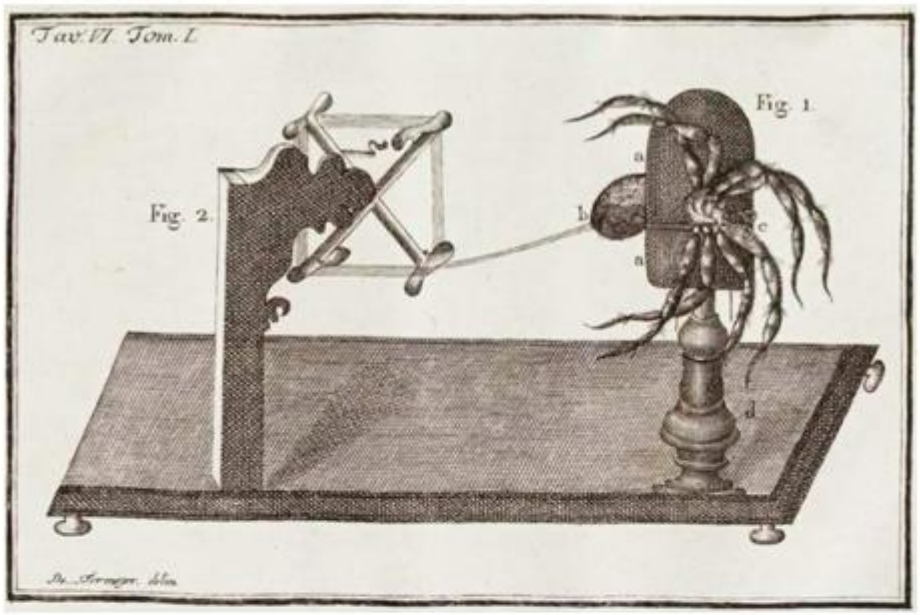

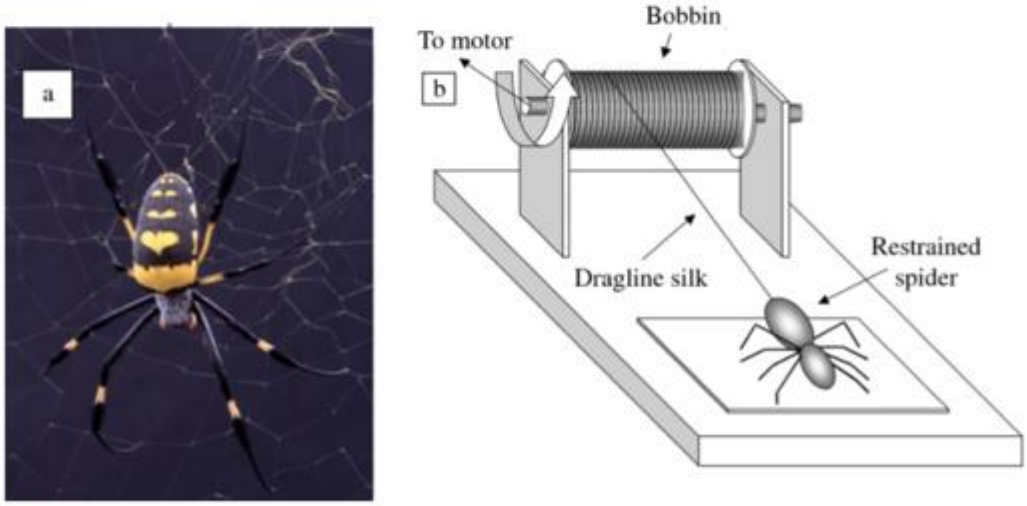

1 (a) *Nephila senegalensis* spider. (b) Schematic diagram of the silk-reeling equipment.

2 *Figure 1. Top: An early attempt to harvest silk from orb-weaving spiders,*

3 *taken from (Termeyer, 1866) Bottom: a figure from a modern paper*

4 *detailing similar apparatus taken from (Young et al., 2021)*

In this early attempt to produce silk, a spider is immobilised with the abdomen separate and clamped (Fig. 1.) this allowed the silk thread (b) to be wound upon a spindle (Fig. 2.). in a process that is very similar to the current method utilised in most material labs that test silks (Vollrath et al., 2013, Young et al., 2021). This process is however very labour and time intensive to produce very small quantities of overall product.

There have been many attempts to "produce" spider silk. Initially these efforts were made to produce silk in the quantities required for study. Figure 1 shows a method, which in a more updated fashion, is still in use in modern labs(Young et al., 2021). This method unfortunately produces little silk for the effort required and places a large amount of stress on the spider producing the silk and the silk itself (Madsen et al., 1999). Even if this were an effective method to harvest silk, farming enough spiders to make this a commercially viable venture would be impractical as when in close proximity, spiders unfortunately tend towards cannibalism (Foelix, 2007).

Domesticated silkworms (*Bombyx mori*) are farmed through a process called sericulture where hundreds of the silkworms are cultivated on branches of the mulberry tree (Takeda, 2009) Given, the previously discussed cannibalistic nature of spiers, it would not be possible to farm

spiders in this way. Attempts have been made utilising more modern techniques. The first early attempts at producing silk were made utilising the model system of *E. coli* with what could now be described as the standard genetic engineering toolkit: namely, sequencing a gene, synthetically producing the gene in high copy numbers (to avoid the error rate inherent in PCR), utilising restriction endonucleases to excise the desired gene fragment, transforming this into a bacterial expression plasmid vector and transfecting the plasmid into chemically competent *E. coli*. Then utilising the host cells native ribosomes, tRNA and amino acids to produce your target protein in high quantities(Fahnestock and Irwin, 1997). A technique that is very similar to how pharmaceutical insulin is made. It is worth noting that herein the production of "silk" refers to the production of a full-length spider silk protein, unless explicitly mentioned otherwise to differentiate from truncated spidroin silk proteins or even silks produced in Silkworms.

Aside from poor yields and an increased tendency for the host cells' to denature during production, the relatively small quantity of silk produced failed to meet the strength and flexibility of native full length spider silk (Prince et al., 1995, Huemmerich et al., 2004, Stark et al., 2007, Heim et al., 2010). Having said this there have been many different attempts to produce silk that have mimicked or come close to one of the properties of

silk. In a systematic review of spider silk performed by Koeppel in 2017 it was shown that when compared to native spun spider silk the recombinant and artificial silks did not perform as well as the original in terms of strength but did outperform the original in others (Koeppel and Holland, 2017).

There are multiple reasons that this initial effort met with limited success. Firstly, the structure of a silk gene and therefore its protein is highly repetitive (Challis et al., 2006). It has been "suggested" that this leads to tRNA pools within the producing *E. coli* to become depleted (Chung et al., 2012). Which leads to truncated proteins forming hairpins leading to inefficient translation. This problem of truncated proteins was then exacerbated by the highly hydrophobic nature of the silk proteins themselves. This caused a tendency for the truncated proteins to form large aggregates within the cells interrupting their metabolic processes and often leading to cell death.

A more successful attempt was made in utilizing the similarity between mammalian and insect protein post processing machinery to overcome the issues of protein aggregate build up, this coupled with the larger cell size and correspondingly larger pools of tRNA held promise. Transgenic lines were made using immortalised bovine mammary

epithelial cells and baby hamster kidney cell lines. Whilst these experiments led to the production of spider silk proteins, the resultant fibres, whilst strong, were very brittle (Lazaris, 2002). The limitations of this method likely arose from the limitations of immortalised cell lines themselves, given that genotypically, phenotypically and morphologically these cells lines often bear little resemblance to the original cell type they were initially grown from (Pan et al., 2009). These genotypic differences can result in the truncation of genes (Lewis et al., 2013) which can lead to incomplete translation of the target protein

One slightly more bizarre attempt led to headlines surrounding the "Rise of the 'Spider-Goats'" (Rutherford, 2012). Utilising a similar transgenic system in an attempt to produce silk, Tucker et al (2014). created a herd of transgenic goats with a spider silk gene in their mammary tissue, whilst this was met with limited success the small yield and high cost of maintaining a herd of goats led the publisher to switch from the aims of producing large quantities of silk for textiles, to small quantities for medical biofilms work.

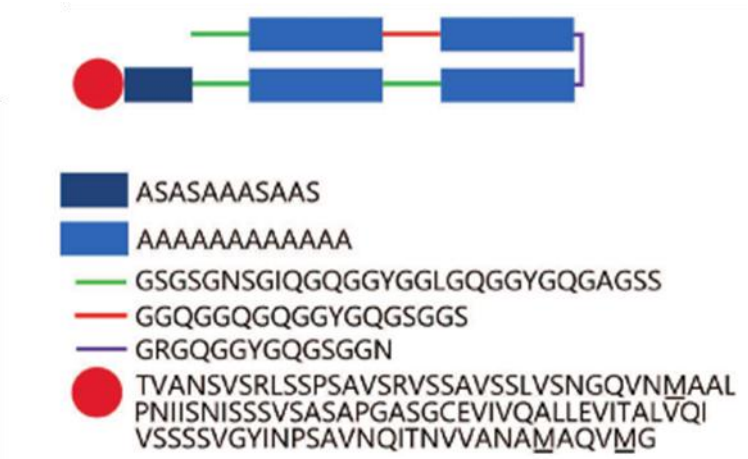

Figure 2. A diagram showing the structure of the synthetic silk 4RepCT. Adapted from(Harvey et al., 2017) blue boxes represent the 4 polyalanine repeats, with the dark blue box denoting the alanine and serine-rich region at the start, the red, green, and purple lines denote various glycine-rich regions and the red circle at the start represents the non-repetitive C-terminal domain (Harvey et al., 2017).

The most recent advance in the production of spider silk is arguably the most imaginative. Rather than attempt to produce a whole spider silk gene the work of Harvey et al (2017). produced instead a miniature synthetic silk gene. Noticing from previous work the highly conserved nature of both the repeating pattern of silk genes and their cross-species conservation of the C-terminal (Challis et al., 2006) of the protein, they set out to simplify the gene to make it capable of being produced in *E. coli*. Figure 2 shows this simplified gene, using only four repetitive

domains as well as the conserved non-repetitive C- terminal domain, combined with the randomisation of the codon usage within the cell allows for a significantly lower stress to be placed upon the cells. The addition of a cleavable thyrodoxin solubility tag meant that this could be produced in high quantities in and kept soluble allowing for storage and solidification at a later time. The synthetic nature of the gene also allows for the introduction of 'click chemistry' sites allowing for the addition of growth factors and antibiotics to the final product. Whilst a significant step forward, this method too has some drawbacks. Whilst the resultant protein can be prompted to form fibres, they are significantly smaller than native spun silk and do not possess the same strength or extensibility. Although given the nature of the product the formation of true silk fibres is rarely the end goal, with studies focusing instead on the formation of films and hydrogels. The protein itself is currently time consuming to produce and cannot be stored in concentrations greater than 10% because it has a high tendency to polymerise and thus come out of solution.

It could be argued that the secret to producing spider silk in the quantities necessary for industrial and medical applications has yet to be found. It could be further argued that the insights necessary to understand how to circumvent the problems already encountered in trying

to manufacture it at scale might be gained through a better understanding of what happens within the highly specialised environment of the silk gland itself.

Chapter 1. A novel system for the dissection and maintenance of spider silk glands in culture

Introduction

As stated in the introduction to the thesis the aim of this first chapter is "to design an ex vivo tissue culture system that allows for the study of silk glands and their production of spider silk." This first chapter of the thesis will detail the works undertaken to develop the novel system to dissect out and maintain in culture the glands that produce the spider's silk. This chapter will focus on the methods employed in setting up the system initially as well as the confirmatory works that went into showing that the cultured glands were not only surviving but still actively producing spider silk. The chapter will also detail the confirmatory works performed to show the repeatability of the system and its applicability across the model species as well as two other species to demonstrate the wider applicability of the system. To discuss these aims several topics must first be introduced. Namely, spiders and their diversity, spider silks and their production, and the previous attempts made to culture insect glands.

Spiders and their diversity

Spiders are a diverse group of organisms, that evolved from a Devonian arachnid ancestor approximately 400 million years ago (Shear et al., 1989). with over 48,500 known species they have since become the largest and most diverse group in their class of arachnids (Dimitrov and Hormiga, 2021) with other notable inclusions being scorpions, vinegarroons, and ticks. The order Araneae, with over 40,000 species across 109 families (Garrison *et al*., 2016) , comes in seventh in total species diversity of any other group of animals (Sebastian, 2009). The diversity has led to an estimated total global biomass of 25 million tonnes of spiders (fresh weight) that is estimated to consume between 400 and 800 million tonnes of insects annually, (Nyffeler and Birkhofer, 2017). A fact that when published lead one reporter to write that "spiders could theoretically eat every human on the planet and still be hungry" (Walker, 2017).

This huge biomass is spread across every continent and major land mass (Turnbull, 1973). Their huge spread across habitats and ecological niches has understandably produced a highly specialised and unique diversity of adaptations. One of these fascinating adaptations has seen young spiders travel great distances through the air using a process

called ballooning (Coyle et al., 1985). Once hatched most species of spiders release a long strand of silk into the wind and grip it as they are taken away by the air. This has seen spiders land in ship rigging 1,600 km from the nearest land mass (Hormiga, 2002) and have been found in air samples from 16,000 ft above sea level (VanDyk, 2009). Not only this but spiders have been shown to swim, dive and construct a diving bell containing air which they can use to breathe (Seymour and Hetz, 2011). These feats as well as their ability to construct habitats, prey wrappings and prey capture devices come primarily from their ability to produce silk.

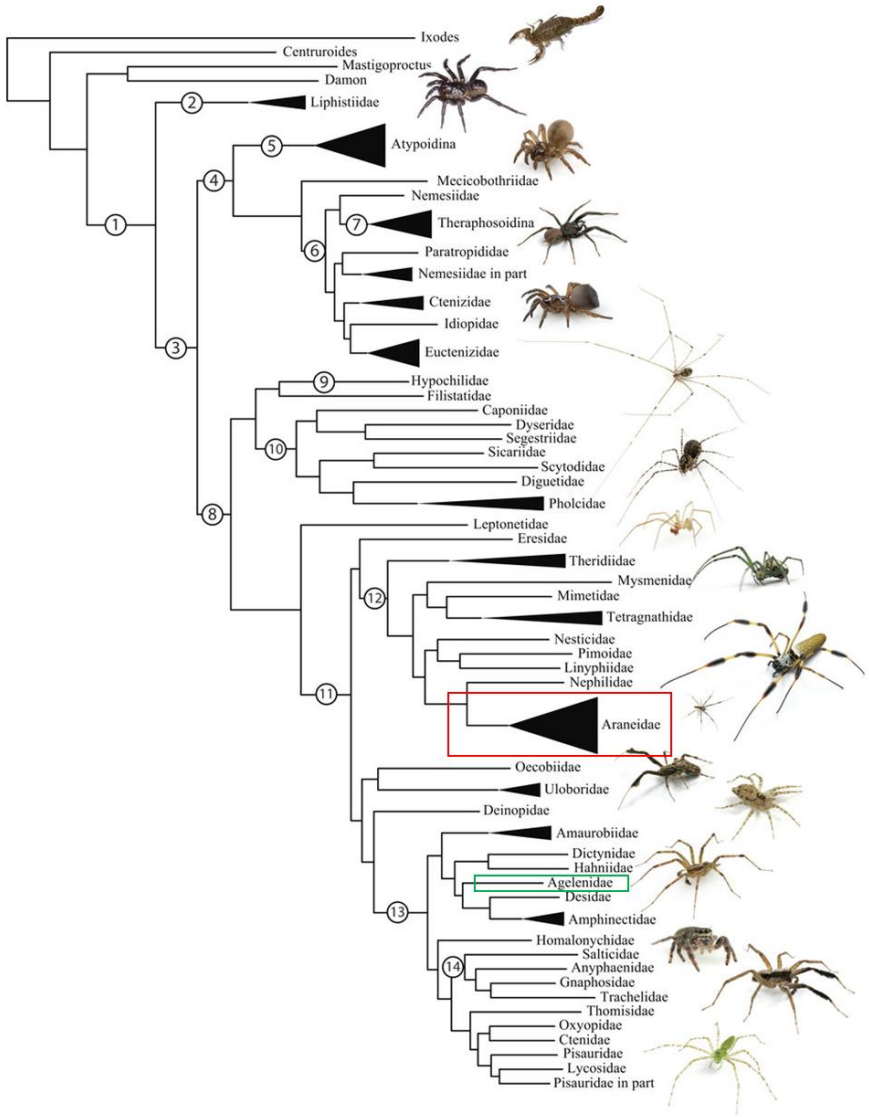

Figure 3 A broad phylogenetic tree showing spider genetic and morphological diversity (Garrison et al., 2016); (Sebastian, 2009) Two families have been highlighted to demonstrate the families worked on in this chapter: the Araneidae (red) and Agelenidae (green). The three species within those families were Larinioides sclopetarius, Eratigena atrica *and* Zygiella x-notata.

A phylogenetic tree used to show the genetic and morphological diversity found in spiders. Two families have been highlighted to demonstrate the families worked on in this chapter: the Araneidae (red) and Agelenidae (green). The three species within those families were *Larinioides sclopetarius, Eratigena atrica* and *Zygiella x-notata.*

These specific families were selected for this investigation for due to the availability of the species and the available literature on their silks. The chosen species were of a size that could be easily dissected, plentiful and could be collected in the local area. Araneid silks are among the most studied and best understood spider silks and so two of these were included (*Larinioides sclopetarius* and *Zygiella x-notata*) Alongside this a funnel weaving species (*Eratigena atrica*) was also chosen to provide a contrast to a different family's silks.

1 Spider silks and their production

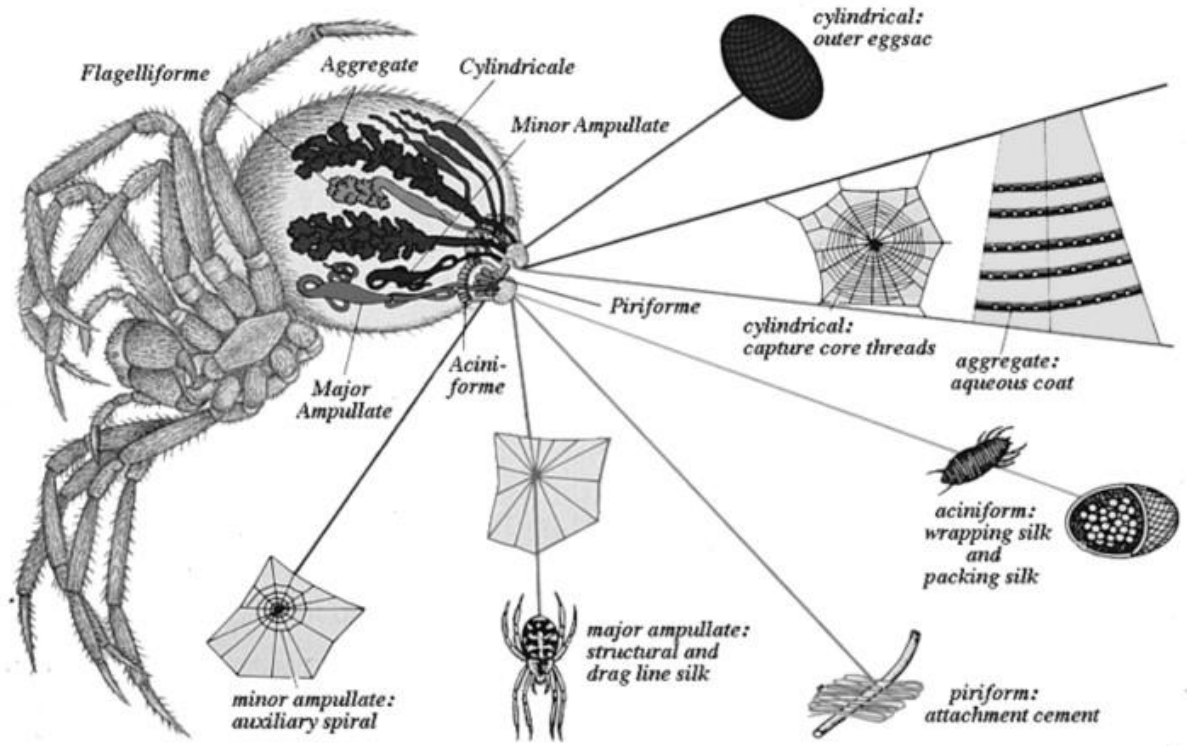

2

3 *Figure 4 Stylised representation of the silk gland structure of the orb*
4 *weaving spider* Araneus diadematus *(Vollrath, 1994), With permission*
5 *from Elsevier.*

6 Figure 2 shows a generalised map of gland morphology and the
7 glandular origin of each specific type of silk from *Araneus diadematus*.
8 Whilst this morphology is specific to the species in the exact position,
9 size, and topology of the glands, these vary greatly depending on species,
10 age (Townley et al., 1993), and sex. As, unsurprisingly, only females

produce Tubuliform and Aciniform silk (used in formation of egg sacs). It is worth noting that there is a wide array of morphological variation between species. With orb weaving species being arguably the most complex with 7 silk glands producing seven different types of silk all with unique roles (Vollrath, 1994). Compared to certain mygalomorph species possessed of multiple copies of only one silk gland type, all producing a mixture of two types of silk used for all general purposes (Palmer, 1985a).

Spider silk is produced in specialised glands in the abdomen of spiders and pultruded through spinnerets in the distal end of the abdomen. These vary from generalised sheet weaving glands in larger mygalomorph (tarantulas, funnel-web, etc.) (Palmer, 1985b) to highly complex systems of specialised glands producing highly specialised silk (Starrett et al., 2012)in the orb-weaving species of the family Araneidae as shown in Figure *3*.

The connection of spider silk, to silk glands was made very early (Wray, 1670) with the earliest works utilising dissection to perform morphological study (Wilder, 1865) and comparison between the silk glands of multiple species(Millot, 1926, Apstein, 1889, Warburton, 1890) As techniques have advanced so has our understanding of how the silk

glands themselves are adapted to their function. One example of this is the advancement in understanding of how pH shown descend along the length of a silk gland when pH probes were placed centrally and at the end of the silk glands from *Nephila clavipes* showing a defined drop in pH from the silk producing tail to the delivery duct (Dicko et al., 2004). This work was then further refined by repeating it using a micro pH probe to display the descending pH across 8 separate areas of the silk gland (Andersson et al., 2014). Whilst these previous investigations provide a trove of data to be studied, they rely on the removal of the silk gland from its surrounding tissue. Specifically, once a gland has been isolated it is either fixed or placed in a non-native system where it ceases to function as a silk gland i.e. an organ for the production and excretion of silk. Whilst the importance of tissue fixation cannot be overstated in modern investigative techniques, it inherently relies on "fixing" an organism or tissue in a static position on the organellar level (Howat and Wilson, 2014). Whilst this allows for a detailed view of the cellular process occurring within the cell, this is definitionally static and therefore, is limited in its ability to capture dynamic processes. Similarly, dissection of silk glands followed by incubation in a non-nutritious buffer slows or halts the production of silk changing the nature of the silk glands.

Insect cell culture

Early attempts at cell culture involved removing a small volume of tissue and suspending it within a mixture of its own lymph, plasma and saline (Carrel, 1910). This method was later refined to use an isolate of their native growth medium (lymph, plasma and other fluids) (Carrel, 1924). Much of the work focusing on successful culture tends towards discussion of either the setting up of primary cell lines from tissue isolates (Day and Grace, 1959) or the maintenance of cell lines (Phelan and May, 2015), cell lines being defined as "The isolation of cells from animal tissues and their subsequent and successful growth in artificial culture" (Arunkarthick et al., 2017). This definitional narrowing becomes problematic when discussing the culturing of whole organ isolates from an animal. Whilst the culturing of whole organs and partial organs has been commonplace in plants for research and commercial micropropagation (Loyola-Vargas and Ochoa-Alejo, 2024) there is still a minor gap in whole organ culturing in vertebrates, with the majority of work being done in either 2D cell lines or 3D organ on a chip systems (Zhao et al., 2024). When discussing invertebrate organ culture there were several groups working on the dissection and culturing of partial or whole organs in the middle part of the last century. With researchers like Loeb and Schneiderman being able to keep a section of *Bombyx mori* epithelium

alive for 35 days in culture (Loeb and Schneiderman, 1956). This work too continued down the path of tissue cultures and cell lines (Grace, 1969) as this gave rise to easier to observe interactions between cells which was, at the time, more valuable. The work of whole tissue culture was laborious as it required a difficult and time consuming process of extracting and purifying haemolymph from the target organism to fortify the existing media types that were available (Vago, 2012). As such the aim of whole organ culturing in invertebrates was not widely continued, leaving a substantial gap in the literature. It can be argued that, for the sake of this work, a successful culture would be one in which the target gland is functioning sufficiently to provide the opportunity to observe the production of sufficient material for study.

Methods

Collection and storage of specimens

All samples were taken from populations in the Nottingham area, collecting was performed with full knowledge and permission from the owners of the premises. Samples were identified by matching the distinctive dorsal and ventral markings of the species to those of the identified specimens already collected and with those shown on the British

arachnological society page (British-Arachnological-Society, 2022) and with the species description and photos found in Britain's Spiders: A Field Guide(Bee et al., 2017). Whilst the primary species collected through this process was *Larinioides sclopetarius,* two other species of relevance were collected for this work, *Erigena atrica* and *Zygiella x-notata*. These were identified by eye by comparing their size, carapace markings and web structures to the listed entries in Britain's Spiders: A Field Guide (Bee et al., 2017).

Locations:

The Johnson Arms, 59 Abbey St, Nottingham NG7 2NZ

(52°56'32.3"N 1°10'48.5"W)

The Johnson arms is located next to the river Leen and has a large, covered, deck area immediately at the rear of the property. It has multiple sets of outdoor lights which attract small flying insects throughout the evening. The covered but humid nature of the environment coupled with the abundance of prey organisms makes this an ideal location for the bridge cross spider *Larinioides sclopetarius.*

The Queen's Medical Centre, Derby Rd, Nottingham NG7 2UH

(52°56'37.6"N 1°11'06.4"W)

The Queen's Medical Centre is also located adjacent to the river Leen. It is also the major trauma centre for the East Midlands, and as such it has a large underground carpark, which is consistently lit throughout the night attracting flying insects. This area of a very large building has an ambient temperature higher than its surroundings. The

car park also offers some protection from predation as birds rarely enter the area.

The humidity, temperature, abundance of prey items and protection from predation mean that this area gives rise to approximately 70% of the specimens used in this study.

Amigo’s Kebab house, 357b Derby Rd, Nottingham NG7 2DZ

(52°56'49.6"N 1°11'01.2"W)

Also bordering the river Leen, this collection of shops is lit throughout the night, covered from the elements, and warmed by the heat from the nearby kitchen. This combination allows for year-round warmth, humidity and prey abundance that allows for a very stable population of spiders.

Spiders were collected monthly. The site for collection was rotated each time to avoid over sampling or over taxing one population. Specimens were collected in 25ml universal tubes with perforated lids and were transferred into a large, transparent plastic container with a perforated lid. Into the lid was inserted a piece of cotton wool to allow for

additional water to be delivered to the specimen without running the risk of limiting the oxygen that was available to the spider.

Once housed securely, the specimens were kept in a temperature and humidity-controlled environment (19°C, 80% humidity) and were each fed with three lab reared fruit flies (*Drosophila melanogaster*) three times a week. The samples were fed by cooling down the *Drosophila* in a fridge until they had stopped flying, taking the pot containing the spider and tapping it on the lab bench until the spider sat on the bottom of its sample pot, removing the lid with one hand and pouring in 3 fruit flies, before quickly resealing the lid. Water was then sprayed onto the cotton in the pot lid, the hydrated pot now containing the spider and its food was then placed back into the stable environment of the incubator.

In this environment the specimens would regularly survive for periods exceeding 4 months. Whilst in culture the collected specimens regularly laid egg sacs which once hatched produced upwards of 80 individual spiderlings. Due to the cannibalistic nature of the spiders this usually led to 2-5 surviving into adulthood.

Production and storage of solutions

A master mix of antibiotics and antimycotics (50.155 ml) was made up to be added to 500ml of stock solution. This was made up by defrosting the frozen stock solution of tetracycline, gentamycin, penicillin, streptomycin, and amphotericin under the sterile dissection hood. Once defrosted the aliquots were made up of 5 µl tetracycline, 25 µl gentamycin and 125 µl amphotericin, plus 50ml of penicillin and streptomycin solution. These aliquots were then frozen at -12°C in order to be used when necessary.

FBS (foetal bovine serum), DMEM F12 HAM (Dulbecco's Modified Eagle's Medium/Nutrient Mixture F-12 Ham) and PBS (phosphate buffered saline) were all acquired from the medical school stores and kept refrigerated at 4°C. When necessary, the outer surface of a given bottle (media, FBS, PBS or an aliquot of antibiotics) would be sprayed down with a solution of 70% ethanol and water before being placed in the sterile dissection hood, an aliquot of ambiently defrosted antibiotic and antimycotic solution would then be added before the solution had its lid firmly attached and was mixed through inversion. The date and time of the antibiotic addition was then recorded on the bottle to ensure they

would remain in date. When not in use the mixed solutions would remain in the fridge at 4°C.

Commonly referred to mixtures and their makeup

Disinfection buffer (PBS, 0.01µg/ml tetracycline, 0.05µg/ml gentamycin, 100µg/ml penicillin, 100µg/ml streptomycin, 0.25µg/ml amphotericin) was made up by defrosting the frozen stock solution of tetracycline, gentamycin, penicillin, streptomycin, and amphotericin.

Media (DMEM F12 HAM, pH-7.4, 20°C, 10% FBS, 0.01µg/ml Tetracycline, 0.05µg/ml gentamycin, 100µg/ml Penicillin, 100µg/ml Streptomycin, 0.25µg/ml Amphotericin)

1% agarose (CAS: 9012-36-6) dissolved in sterile distilled water raised to 80°C before being poured to set in a sterile environment for 20 minutes at ambient temperature.

Disinfection anaesthesia and isolation of the abdomen

A spider was transferred from the storage tank into a small clean plastic pot, which was then placed into the freezer (set to -12°C) to immobilise the spider. The spider in the cold environment would be checked every 30 seconds and would only be moved to the next stage once no movement response was shown to stimulation. Next the spider would be covered with 70% EtOH and left to incubate for 1 minute to disinfect its outer surfaces. Using two pairs of fine forceps the cephalothorax was crushed to immediately euthanise the spider. This method of euthanasia was adapted from the limited literature available (Pizzi, 2006) and current lab practices. The spider was gripped at both ends of the pedicel (the small stalk connecting the cephalothorax and abdomen) and pulled apart to separate the abdomen. As suggested in (Chaw and Hayashi, 2018) the abdomen was immediately transferred to a dissection plate in a sterile cell culture hood under a dissection microscope and covered with disinfection buffer (PBS, 0.01µg/ml tetracycline, 0.05µg/ml gentamycin, 100µg/ml penicillin, 100µg/ml streptomycin, 0.25µg/ml amphotericin). The antibiotics are present to limit infection during the culturing process, given the spiders in question are being collected from a non-controlled environment.

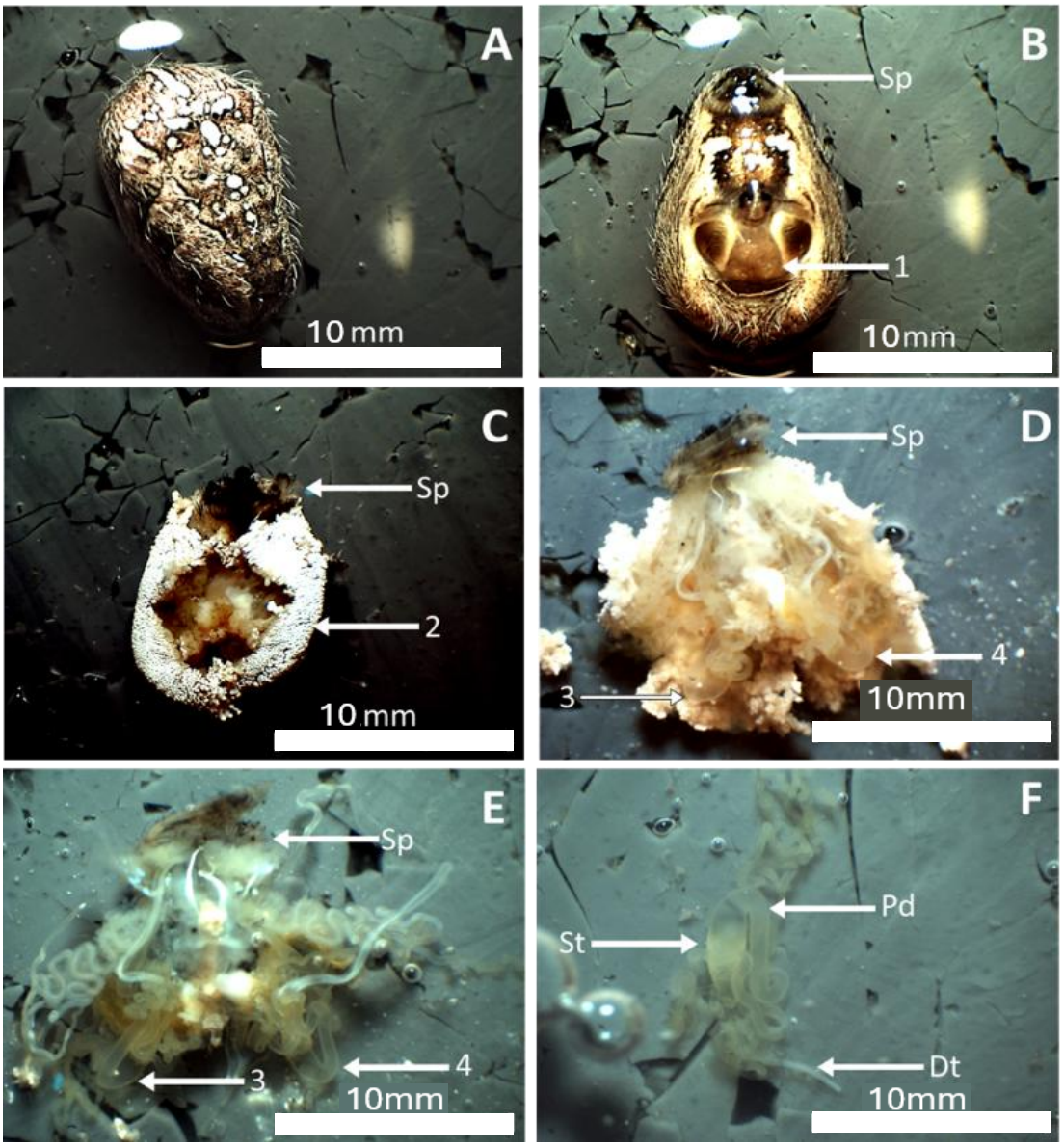

1

2 *Figure 5. The Process of removing target glands from subject species*

3 (Larinioides sclopetarius *pictured*) *using sterile dissection techniques.*

4 *Labels indicate the spinnerets (Sp) the previous attachment point of the*

5 *pedicel (image B arrow 1), adipose tissue (image C arrow 2), the Major*

6 *Ampullate glands (images D & E arrows 3 & 4) and the areas of the gland*

responsible for production (Pd), storage (St) and delivery (Dt) of the silk dope to the spinnerets. The scale bar is found in the bottom left of the image and denotes 10 mm.

The dissection process required approximately 40 minutes to complete and broadly occurred in six major steps photographed in Figure 5. These steps are A, isolate abdomen from cephalothorax via the pedicel. B, remove carapace beginning at the opening to the pedicel retaining the spinneret intact. C, opening the adipose tissue to view the glands D, identifying target glands. E, Removing adipose tissue. F, Isolating target gland. This process was designed and iteratively refined to become quicker with a higher success rate over hundreds of hours and hundreds of dissections performed over 18 months. When first attempted this process took more than 90 minutes to complete and would rarely result in a successful dissection. As the process became more practiced the time was reduced and the success rate of dissections increased.

Identifying the opening to the interior of the abdomen where the pedicel previously connected the cephalothorax to the abdomen (proximal to the spinnerets on the ventral side Figure 5A arrow 1). Fine forceps were used to gently open the carapace in a line distally towards the spinnerets (Figure 5B, Sp), carefully skirting the spinnerets ensuring the delivery tubes of the glands were not disturbed. Once the spinnerets had

been separated removal of the remainder of the exoskeleton was carried out. This was done by holding one area of the exoskeleton firmly in place with one pair of forceps whilst pulling the free edge of the exoskeleton gently in an antagonistic direction to the held edge. This was done slowly to avoid the forceps slipping, tearing the free edge off completely or slipping and impaling the organs below. This step was then repeated for each remaining piece or carapace until only the fatty tissue (and organs) remained. It can be helpful during this process to employ a P1000 pipette with a sterile, blunted pipette tip affixed, to gently flow sterile media over any areas where the exoskeleton did not readily come away.

Depending on the species and the time of year it is expected that there would be varying quantities of fatty tissue surrounding the internal organs (Figure 5C, 2). Using a large bore pipette, fresh disinfection media was used to tease apart the fatty tissue to reveal the organs. The flow of sterile media separated the granular nature of the fatty tissue and extended the connective tissue holding the fatty deposit together. A wide bore pipette tip should be used however as a narrow bore pipette produced sufficient fluid movement to damage the underlying glands or even destroy them altogether. Once the fatty tissue had been relaxed or partially dislodged it could then be removed. This was carried out by gripping one end of the dislodged piece of fatty tissue with both pairs of

forceps, whilst holding the pair of forceps closest to the organs firmly and still, pulling the second pair of forceps away from the main body of the fatty tissue. Once separated the fatty tissue was discarded on the far side of the dissection plate so as to prevent it from floating back into view and interfering with the remaining work. This process was repeated until all of the fatty tissue was removed and the silk producing organs were clearly visible (Figure 5 D, E).

The target gland was selected from the main body of the glands by its appearance, size, and position, the Major Ampullate gland pictured above, for example, is by far the largest and sits in plain view in a dorsal position on top of the other glands. The target gland was secured with forceps by gripping the delivery tube as close to the spinnerets as possible. Sterile dissection buffer was applied dropwise in order to isolate and disentangle the production end of the gland from the other glands and organs. This process took considerable time and had to be done slowly and carefully, being too vigorous with the gland at this stage would result in a large tear to the production end of the glands. Once the gland was suitably free (Figure 5F) the delivery tube was separated from the spinnerets using micro scissors. The free gland was then transferred to a Petri dish of disinfection buffer. This was initially achieved by picking up the gland by the delivery tube using a pair of forceps and placing it into

fresh buffer. This process, however, regularly damaged the glands. A more effective method was developed wherein a wide bore pipette of dissection buffer had its plunger partially depressed, this was then held near the gland. By slowly raising the plunger of the pipette a suction force was created pulling the now free gland into the pipette tip through fluid motion. This method proved more effective.

Using this method, Major Ampullate, Minor Ampullate and Tubiform glands were each successfully isolated from *Larinioides sclopetarius* species and from *Zygiella X-notata* species whereas only Tubiform glands were successfully cultured from, *Eratigena atrica.*

Culture and maintenance of the gland

Whilst still in a sterile environment the gland was examined for any damage or leaks. These were apparent due to the viscous silk dope escaping from sites of even minor damage. Glands with observable damage were not used for subsequent culture and were disposed of with the remainder of the spider. The gland was then transferred into a cell culture plate with media (DMEM F12 HAM, pH-7.4, 20°C, 10% FBS, 0.01µg/ml Tetracycline, 0.05µg/ml gentamycin, 100µg/ml Penicillin, 100µg/ml Streptomycin, 0.25µg/ml Amphotericin) and sealed with microporous tape.

When left at ambient conditions the media underwent a gradual increase in pH from approximately 7 to approximately 11, shown by observing the colour change occurring to the phenol red indicator in the media going from clear to pink in the presence of an alkaline pH and comparing this to a phenol red indicator colour chart. Using media without glands in the same plate as control wells, a change in the phenolphthalein indicator present in the media changing colour from clear to pink showed an increase in alkalinity over time.

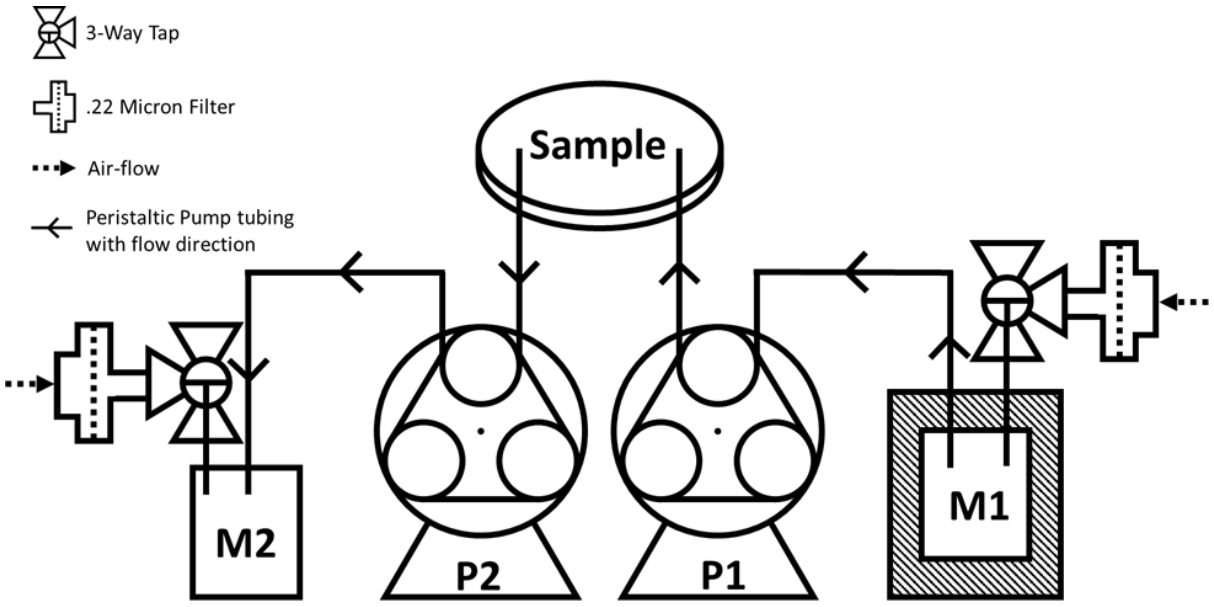

Figure 6 A diagrammatic representation of the peristaltic pumping system built for the safe changing of the media on the cultured glands. P1 and P2 represent the two sterile pumping loops used to independently bring fresh media (M1) to the sample (P1) and remove old media (M2) from the sample (P2). These are kept separate to prevent cross contamination the 22-micron filter was in place to allow the ingress and egress of air to equalise vacuum pressures produced by pumping, whilst limiting the contamination that could enter the closed system.

Figure 6 shows a diagrammatic representation of the peristaltic pumping system that was built by the author from discarded equipment salvaged from old labs, to facilitate the continuous replenishment of fresh media onto and from a dissected sample. Adapted from common practice

int the culturing of primary hepatocyte cultures (Guguen-Guillouzo and Guillouzo, 2010) . M1 and M2 refer to the 1000ml Duran bottles containing the media fortified with antibiotics. P1 and P2 refer to the individual pump tubing loops. The 0.22-micron filters functioned to allow air pressure to normalise within each bottle to prevent the formation of vacuums or undue pressure within the Duran bottles. The grey area indicates an adapted fridge to allow for the fortified media being delivered to remain refrigerated so as to stop the antibiotics from being made inert by the ambient temperatures. This system allowed for the continuous addition and removal of media to and from the plate containing the sample.

Using a Gilson Miniplus 2 peristaltic pump, the tubing used (1m in length 1.5mm internal diameter, 2.5mm external diameter) was found with the pump (unknown origin) and was thoroughly cleaned with sterile distilled water and then ethanol before being autoclaved (124°C 15 minutes). The Duran media bottles were adapted by drilling two holes through the lids using a 1.5mm drill bit. A 3-way stop cock, and the peristaltic pump tubing was placed into the second hole. The top of the bottle lid was then sealed with hot glue. This process was repeated twice. The two sterile loops allowed for the separation of the fresh and contaminated media. The fresh sterile media was brought to the sample

in a self-contained sterile pumping loop. This was kept sperate from the pumping loop that removed the contaminated media. These were separated to ensure that any contaminants that remained from the dissection process could not make their way into the sterile media, rendering it contaminated.

The lid of the Petri dish that contained the samples was made by first bending two 16 gauge (1.6mm diameter) needles by attaching them to the end of a 50ml syringe heating the needle 2/3 of the way down the needle on the blue part of a Bunsen flame until red hot and then bending whilst continuously blowing air through to maintain the internal diameter of the needle. The ends of the needles were then heated gently in a Bunsen flame and pierced through a Petri dish lid; these holes were also then sealed with hot glue. The needle ends (having had their plastic housing removed) were then placed into the internal diameter of the peristaltic pump tubing using an interruption fit. The Petri dish lid along with the attached tubing and the two attached Duran bottle lids were then placed in aluminium foil, sealed with autoclave tape, and then autoclaved (124°C 15 minutes). Once autoclaved the lid apparatus (whilst still sealed) was disinfected with a 70% ethanol solution before being placed into the cell culture hood and exposed to UV for 30 minutes. The lid apparatus was then affixed to the top of two Duran bottles, one

containing the media fortified with antibiotics and the other being empty, whilst two 0.22-micron filters were added to the 3-way tap. A dissected sample was then placed in the Petri dish, then the adapted lid was affixed and sealed in place using microporous tape.

The sealed Petri dish containing the sample was then placed on the microscope stage to be imaged. Whilst the media surrounding the sample was at ambient temperature the bottle containing the media was placed inside a modified fridge (set to 5°C) with a section having been cut from the door to allow for the tubing to emerge. This gap was then plugged using Styrofoam to limit the heat entering the refrigerating area. The pump was then set to deliver 0.25ml of media per minute, allowing for continuous fresh media delivery for 66 hours. Given the extremely slow rate of media delivery, by the time this reached the sample it had come up to ambient temperature.

The pH of the media was monitored using the phenolphthalein indicator in the media. when this started turning pink, indicating a pH of 11 the old media was removed, and fresh pH 7 media was applied. This introduced a problem because every time the plate was opened there was

an increased risk of infection or contamination. This can be mitigated by utilising equipment in the set up shown above in Figure 6.

Observation and recording of glands in culture

The microscopy images were all taken by the author unless otherwise stated. The process of obtaining the images was developed over the first 2 years of study. The camera used was a CMEX5 2F top mounted camera that had been modified with a dark tube to attach the camera to the microscope. The process of learning how to capture the relevant images was an iterative one with each of the (many, many) failed images produced providing an opportunity to further refine the methods. In total approximately 1.7TB of images were collected across the period of study, of which less than 100GB were of a useable quality to be considered for this thesis.

The initial sample prep involved mounting the whole culture plate onto a Nikon Eclipse TS100 and viewing via a CMEX5 top mounted camera set to take an image once every 5 minutes and left over night. This however had the unfortunate side effect of allowing the samples to move whilst being imaged. It was decided to follow the example of (Kaufmann et al., 2012) and attempt to immobilise the glands in agarose gel. This was achieved by forming a 1% agarose gel using the media (without antimycotics) and high-grade agarose (CAS: 9012-36-6). Whilst immobilising the gland was successful; there was however a reduced

production rate of silk dope. It was then decided to use the gel as a blocking structure to reduce the opportunity for movement. This allowed for more stable and precise images to be taken.

Stability was achieved by pouring approximately 750µl of 1% agarose and media into an appropriately sized well and allowing to cool, these gels were then exposed to UV for a minimum of 2 hours to ensure sterility. Once set and sterile a scalpel blade was used to fashion blocks from the gel allowing for a higher level of control over the placement of the gland.

Results

The following results are taken from eight total glands, taken from eight different spiders, across three species of spider, and represent a small subsection of the total over 100 glands successfully cultured from over 60 spiders, utilising the methods described above for these experiments. The glands survived in culture from three to 28 days with the majority surviving for 10 days. The images chosen were done so as they best demonstrated the experimental outcomes from each subsection of the study.

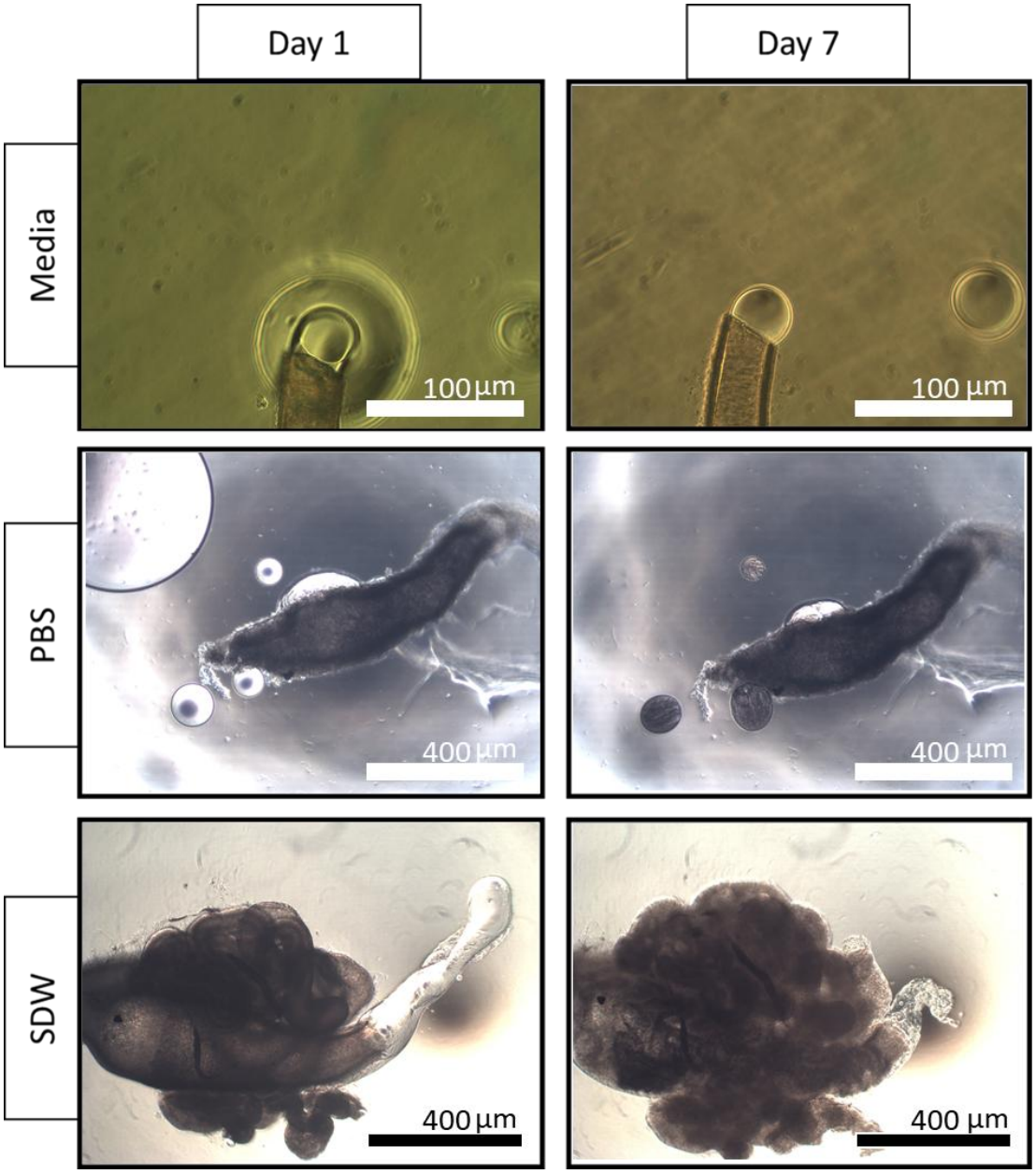

Figure 7 A comparison of the viability of isolated Major Ampullate glands from a Larinioides sclopetarius *cultured in media, phosphate buffered saline (PBS) and sterile distilled water (SDW) shown 1 day and 7 days post dissection*

Figure 7 shows a comparison between the survivability of silk glands in various culture media between day one and day seven post dissection. The different glands are shown in different orientations and as such different light conditions, hence their different appearance from one another. The first row shows the silk gland cultured in phosphate buffered media. This media contains all necessary carbohydrates, proteins, and amino acids necessary for cell culture. It can be seen that an initial large expulsion of dope has begun to occur, in comparison by day 7 the gland shows steady regular production of dope. The first row is shown at a greater magnification to highlight the consistency of silk dope production, whereas the latter two rows are shown at a reduced magnification to highlight the changes along the whole gland. This can be seen as a video by following the link found in Link 1 at the end of the results section.

The second row shows a gland cultured in PBS. As with the first row a large initial expulsion of dope can be seen, however this differs from the first row when looking at the second column which shows no continuing production after 7 days. In the absence of additional protein precursors, production of silk stops.

The third row is in keeping with the first two on day one as a large expulsion of dope can be seen, it however differs from both first rows at 7

days as not only is the gland not producing silk but many cells along its length have lysed resulting in the larger and less clearly defined boundaries of the gland exterior. This is due to the osmotic potential of the cells being lower than that of the pure water surrounding it, causing an influx of water lysing the cells.

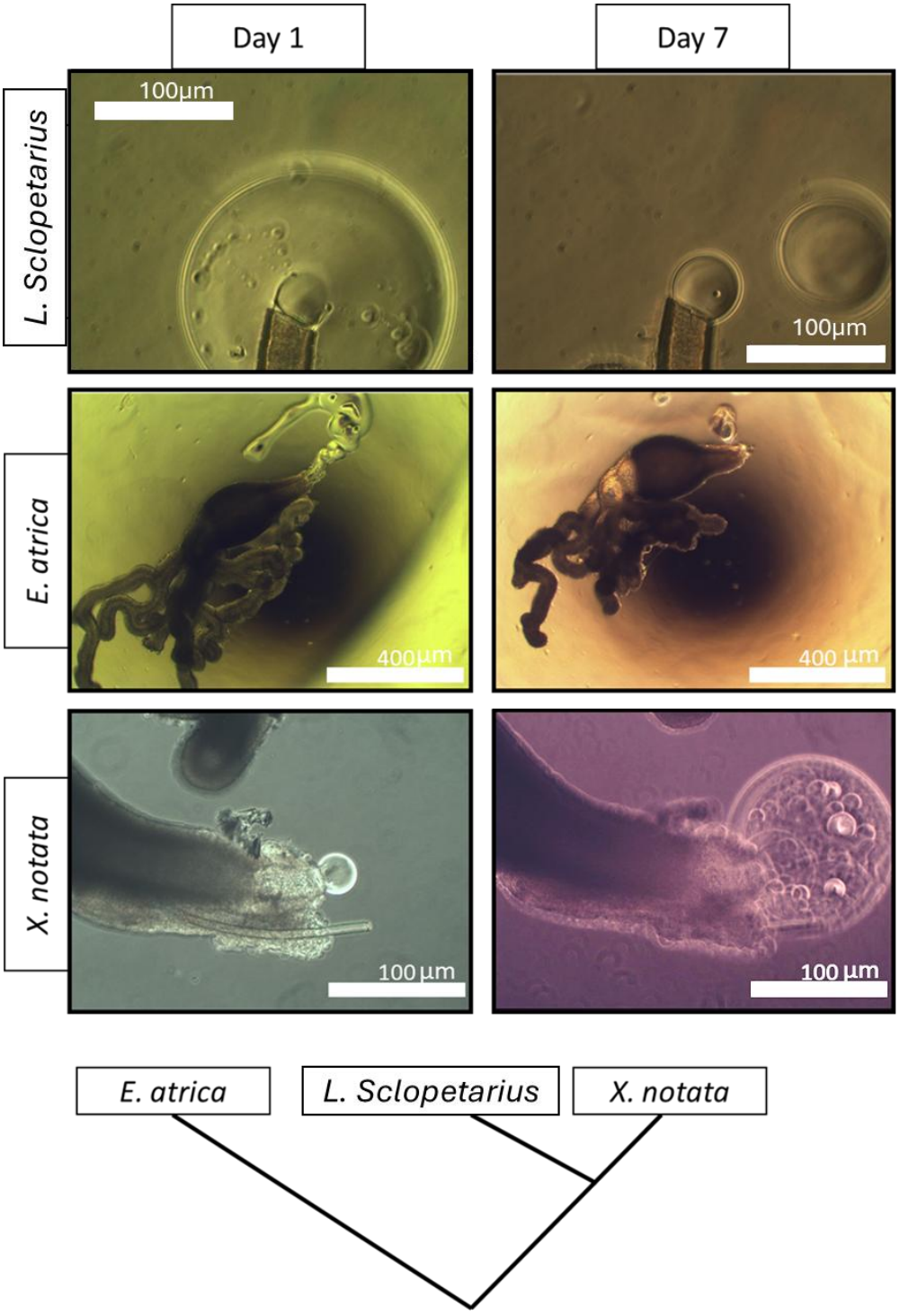

1

2 *Figure 8 A comparison between the viability of glands cultured from*

3 Larinioides sclopetarius, Eratigena atrica *and* Zygiella x-notata *between 1-*

4 *and 7-days post dissection when kept in media.*

Figure 8 shows the comparison between the culture efficacy of an orb weaving species *(Larinioides sclopetarius*), a missing sector orb weaver (*Zygiella x-notata*) and a more distantly related sheet weaving species (*Erigena atrica*). These three species were chosen since of the available species that could be found in the Nottingham area they were abundant and of a size that could be dissected by hand whilst also demonstrating a notable phylogenetic distance from one another (Figure 3). The phylogenetic tree pictured at the bottom of the image is intended to illustrate simply the information showed in Figure 3 where the families of *Larinioides sclopetarius* and *Zygiella x-notata* are highlighted in red, Erigena atrica in green. As can be seen in Figure 6, all of the glands begin on day 1 with a large expulsion of dope which by day 7 has become a much smaller, but consistent, production of silk dope. The differences between glands are found primarily in morphology, which is known to vary greatly between species, and in the rate of production of the silk dope.

Silk glands are well known to vary between different species (Kovoor, 1987). This difference led to the design of this experiment, wherein it was tested whether the culturing methods laid out in this chapter would function on any species other than *Larinioides sclopetarius* on which they were first tested. It can be seen from the figure that all

three species chosen were capable of being cultured and of producing silk dope expulsions whilst in culture.

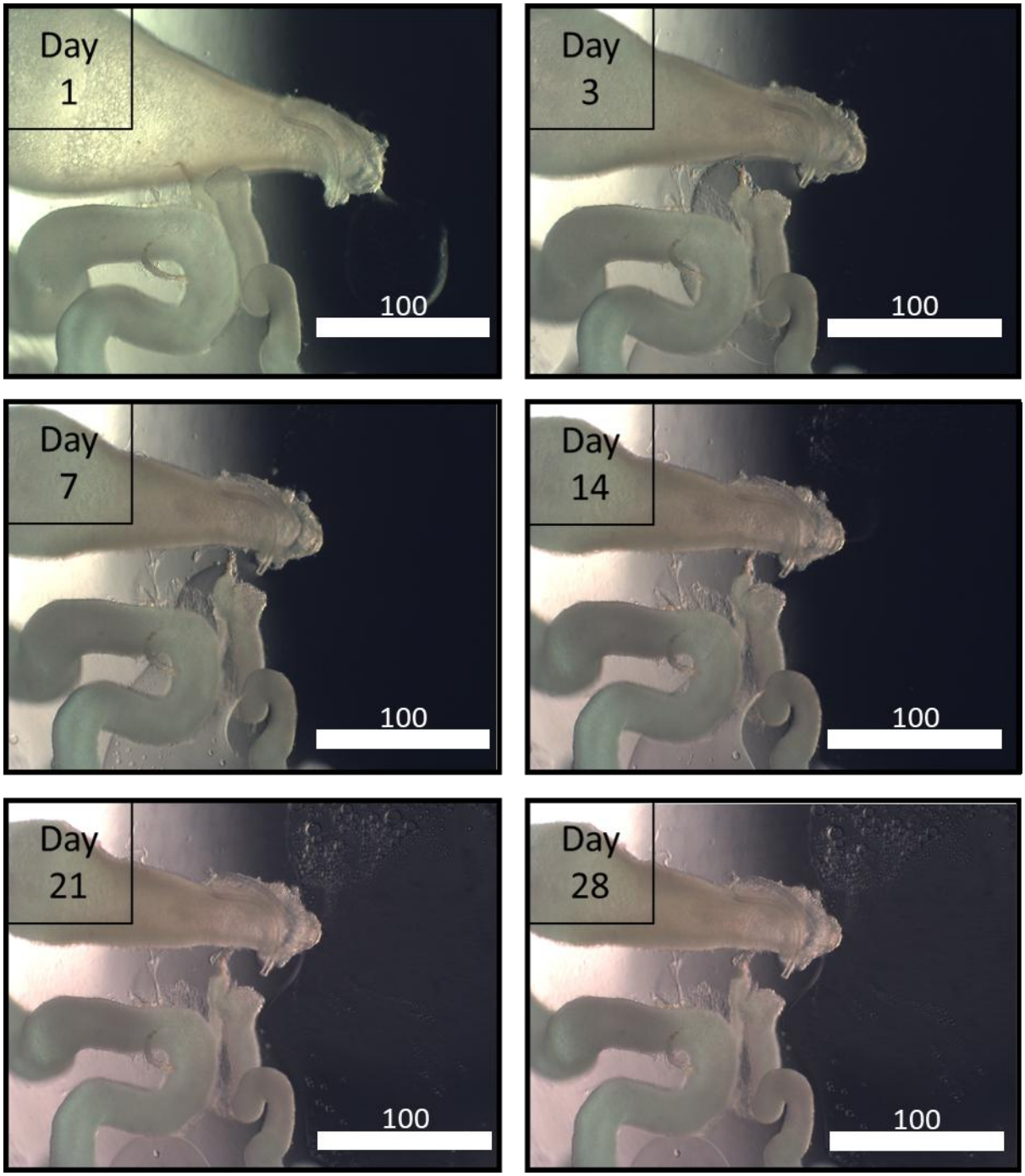

Figure 9 The long-term culture of a Major Ampullate silk gland from a Larinioides sclopetarius *in antibiotic fortified media over 28 days.*

Figure 9 shows the change in morphology of the silk glands over 28 days. The changes are subtle and can primarily be seen in the silk below the gland and the diameter of the lumen of the gland. Importantly the morphology seen on day 1 shows a gland that appears to be "full" which by day 3 appears more deflated. This deflated state appears exacerbated by day 7 but then stabilises from this point onward. Importantly it should be noted that the rate of production from day 3 to day 28 does not appear to change.

Figure 9 shows the long-term culturing of a *Larinioides sclopetarius* Major Ampullate silk gland over the period of a month. After day 3 the morphology of the gland remains consistent, because the gland itself has expelled all its previously stored silk dope and has instead begun expelling only the dope it is currently producing. Using the images of the silk dope being expelled from the gland, a calculation was made assuming a hemispherical droplet size ($\frac{2}{3}\pi r^3$ with r measured from the images present) which led to an estimated total production of 115µl in total, which when divided by the 25 days showed that the silk glands expelled an average of 4.6µl of silk dope every day, Given the initial volume of the silk gland at the beginning of culturing was 4µl (measured by displacement of water) this shows production of the gland's own volume every day of a period of 28 days.

1 Page left intentionally blank

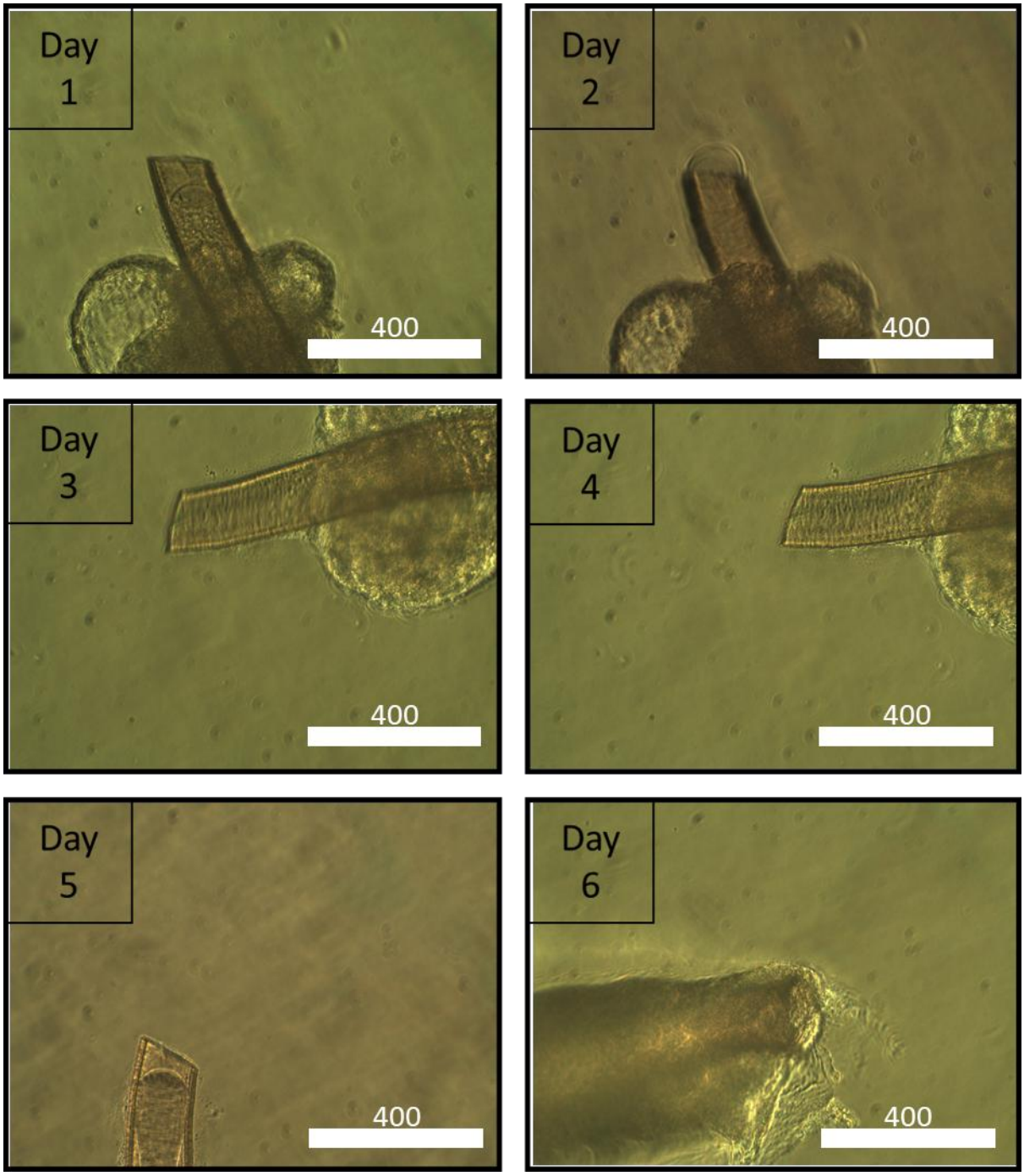

Figure 10 'Cold shock' - Pause in production of a Major Ampullate gland taken from a Larinioides sclopetarius *observed following the addition of fresh refrigerated (4°C) media and antibiotics.*

During the initial attempts at long term culturing, media was made up from 4°C stocks and added directly to the silk gland. This resulted in an observable pause in production that lasted on each occasion between 6 and 8 hours. In the case of day 5, the leading edge of silk dope leaving the gland can be seen retreating up into the gland. This can be seen as a video by following the link below

Link 1. A QR code linking to: https://youtu.be/H4bMtT5UcKE showing a Major Ampullate gland dissected from a Larinioides sclopetarius. The video shows the expulsion of silk dope, the production of silk dope and the production pause seen when cold media is added. Video made up of approximately 7200 images each taken 1 minute apart.

Discussion

In this study, silk glands are shown to produce silk dope in culture in the absence of any cues from surrounding tissues or nervous stimuli. Figure 3 shows the process for removing the target glands from the spider's abdomen and has the fortunate side effect of giving a detailed view of not only the anatomy of the glands but giving us a direct image of how theses glands function *in-vivo*. It can be seen in Figure 3 that the glands are protectively held in place by the fatty tissue surrounding the abdomen. Whilst this tissue has been shown to be used as long term energy storage (Collatz and Mommsen, 1974) the presence surrounding the organs provides a protective layer as an additional benefit. More specifically there is no visible vasculature or nerve structures attaching the glands to the remainder of the spider. These glands receive their nutrition from the haemolymph which is composed primarily from carbohydrates (free and protein bound), lipids, free amino acids and inorganic, and organic ions (Schartau and Leidescher, 1983). The direct control of the production of spider silk comes from the physical pulling of a fibre from the spinnerets by either the spider's hindmost legs or using gravity or wind resistance as a boost. The speed of this "pultrusion" has been shown to fundamentally affect the internal structure of the silk that exits the spinnerets (Young et al., 2021). Orb weaving spiders have direct

neuronal control of the sphincter of muscle found in the spinneret (Herberstein, 2011) which it can employ as a "braking system", allowing the spider to slow its rate of descent or its rate of silk production (Wolff, 2021). This lack of direct control between the spider and its silk gland is likely the reason that the culturing method is able to be successful. Since, as long as the requisite nutrients and pH levels are maintained, the gland "doesn't know" that it is no longer in the spider and will therefore continue to function as if nothing has changed. This allows us to study the gland's functionality as if it were still within the spider, providing a fascinating snapshot into how the glands function physiologically.

Figure 7 tests this idea further, by comparing the viability of glands in culture to those in PBS and in SDW. It has been shown that the content and quantity of a spider's diet can affect the amino acid composition of its silk (Craig et al., 2000). It has also been shown that during periods of starvation spiders can alter their silk composition to be less energetically taxing (Guehrs et al., 2008). The comparison shown in Figure 7 illustrates the effects of nutrient depletion in both PBS and in SDW. This comparison shows that, as can be seen in the first row, the only gland to continue to produce silk dope is the one surrounded by media. This is likely because large scale protein production is highly energetically costly and would likely deplete the gland's stores of amino acids and carbohydrates very

quickly. Therefore, a ready supply of additional metabolic materials is essential for the production of spider silk. This is further backed up by the second row of Figure 7, which shows that in the absence of these precursor metabolic building blocks the protein synthesis stops. The third row of Figure 7 shows very clearly the need for buffered media, because the unbuffered distilled water has such a high osmotic pressure that it begins to lyse cells along the gland along with not producing additional silk. Interestingly though, a comparison between day 7 row 1 and day 7 row 2 shows very little evidence of the cell death that we see in row 3.

Figure 8 shows a comparison between cultured glands from different species of spider. The species were chosen to show a genetic range of species specifically that of a less-specialised sheet weaving spider and two more-specialised orb weavers. The similarities between the glands are predominantly in their function. The expulsion can be seen in both the liquid dope exiting the gland and in the drastic morphological change the glands undergo between the timepoints. These similarities are all the more interesting when compared to the difference between the study organisms. This experiment shows that the method of culturing functions on a minimum of 3 species from 2 different families (Araneidae: *Zygiella x-notata, Larinioides sclopetarius* and Agelenidae *Eratigena atrica)*.

The pause shown in Figure 10 shows a pause in production. There are several possible reasons for the observed pause. The first hypothesis would be that the change in temperature caused a metabolic shock to the cells within the gland causing the production to slow down. This however would not account for the length of time that the pause took to resume, given that the remainder of the media in the well would reach room temperature significantly quicker than the 6-9 hours it took for production to resume. The second more likely explanation is that the cold media caused the shape of the gland to change, this shape change could have increased the internal volume of the gland to increase allowing the silk dope to retract up the gland. This can be seen in row 3, as the silk bolus can be seen physically retreating into the silk gland. This contraction of the dope could be linked to some form of internal pressure sensing mechanism within the gland. A pressure sensing mechanism within the gland would be a simple mechanism for ensuring that the gland never produced so much silk dope that it wound up rupturing the organ. Given the gland's autonomous nature within the spider, it would make sense that the gland would have its own homeostatic mechanisms of regulation. This hypothesis was further supported by the fact that the addition of room temperature media did not cause a similar pause. This was initially tested by chance, where a small quantity (~50ml) of media was left out of the fridge overnight, and given there was no obvious contamination, it

was added to the plates of glands. It was only when comparing the images before and after that this pattern was observed.

The qualitative measurements of increasing pH in the media surrounding the glands from pH 7.4 to pH 8.4 are indicative of a tissue actively respiring and producing metabolic waste products. The change of the colour of the indicator found in the media in the presence of respiring tissues is unsurprising. What is surprising however is the impact that one single gland can have on the pH. The volume of one gland is on average 4µl, and they were cultured in 2ml of media. The fact that a total tissue volume per well of 0.2% could cause such a shift in the pH of the whole well speaks to how much respiration is taking place in the glands. Given the jump in pH from 7.4 to 8.4 over 3 days (samples measured using the colour chart provided with the indicators in the media assumed error rate of 0.1) corresponds to an order of magnitude increase in concentration of OH^- ions, which is significant for something occupying only 1/500th the total volume of the well. To put this into context and to vastly over generalise it is typical to change the media in cell line cultures every 2-3 days (Masters and Stacey, 2007) with the typical cell density being somewhere between 10-20 g/L in exponential growth phase (Eliasson Lantz et al., 2010). These cells required media changes every day with a

cell density of approximately 2mg/L (approximated by volume with an assumed density of water).

Conclusions

The aim of this series of experiments was "to design an ex vivo tissue culture system that allows for the study of silk glands and their production of spider silk." This work demonstrates that spider silk glands can be cultured ex vivo for periods of up to 28 days. This method can be successfully applied to 2 different types of glands (Major Ampullate and Tubuliform), three different species (*Larinioides sclopetarius*, *Zygiella x-notata* and *Eratigena atrica)* across two families (Araneidae and Agelenidae) and marks a step change in what is possible given the lack of any similar reports of success in achieving this aim. Even in other invertebrate species the success is limited to cell lines, smaller less active glands, or parts of glands.

The novelty of the methods and results found in this chapter can be described simply as the first time a silk gland has been successfully cultured ex vivo. Whilst it can be incredibly difficult to prove that something has not been attempted before, especially given the lack of negative results that are published, it can be said that this author failed to find any method or mention of whole silk gland culturing in the literature at large. It can even be said that the broad literature available does not produce many, if any, examples of whole organ culture in insects, let

alone spiders. To determine whether the gland has been successfully cultured, in the absence of better testing criterion, a comparison was made to the previously defined success criteria, namely, the target gland functioning sufficiently to provide the opportunity to observe the production of sufficient material for study.

It has been shown that the dissected and cultured tissue is still active, this has been shown through the metabolic activity of the tissue over days and weeks. This is shown through the change in alkalinity of the culture media possibly because of the cells excreting metabolic waste products, like reactive oxygen species. This is also shown by the absence of successful culturing in the absence of the metabolites found in the media as shown in Figure 7.

The continued production of a liquid dope-like material during the culturing time has been shown through the consistent release of a dope-like material escaping from the end of the gland, even after the initial stored dope has escaped, over periods of up to 28 days, as shown in Figure 9. This behaviour of producing silk dope is consistent with what would be expected of the gland were it still in its native environment.

Both the activity of the tissue and the production of a dope like material indicate a potential usefulness of these culturing methods as an investigative technique. The technique has been shown to work on more than one species and more than one gland type, which could speak to a broader applicability than is demonstrated here, in the future study of factors that affect the production of silk, from a glandular perspective.

Chapter 2. Investigation into the structure and function of the silk glands

Introduction

As stated in the thesis introduction the aim of this chapter is "to investigate what could we learn from these dissected glands?." This chapter will detail how using the method developed in the first chapter the functions of the gland were able to be studied in greater detail, studying at different levels of magnification the structures of the gland and the silks that is produces. In order to investigate this aim, what is currently known about silk glands functionality must first be introduced. Specifically, what is currently known about the anatomy and functionality of the silk glands, as well as what is currently known about damage responses and repair pathways in spiders.

Silk gland anatomy and functionality

The question of how silk glands function has been asked repeatedly, and these studies focus specifically on morphological study and inferences based around what is known about the formation of silk (Yarger et al., 2018, Lewis, 2006, Winkler and Kaplan, 2000). It is challenging to study

these glands without dissection and, without the methodologies mentioned in the previous chapter, it has thus far not been very challenging to view glands as they continue functioning whilst producing silk. It is therefore unsurprising that very little is known about the actual functioning of the glands. How are the cells within the glands specialised to produce silk? How does the spider ensure adequate silk stores to be able to survive? How does a gland, in the absence of vasculature or nervous signals subsequently become repaired? It is upon these questions that this chapter will focus.

Figure 4 shows the variety of silk glands and their corresponding roles within the lifecycle of the species *Araneus diadematus*. As has been previously mentioned, these glands vary between species and have distinct roles for their silks (Tillinghast and Townley, 1993). This chapter will look to expand into the specific structure and function of the Major Ampullate gland found in *Larinioides sclopetarius* an orb-weaving species. The species was chosen for several reasons. The family of orb weavers are the most widely studied and therefore have the largest amount of relevant literature available. They are abundant in the Nottinghamshire area and their relatively large abdomens containing correspondingly large glands allow relative ease of dissection.

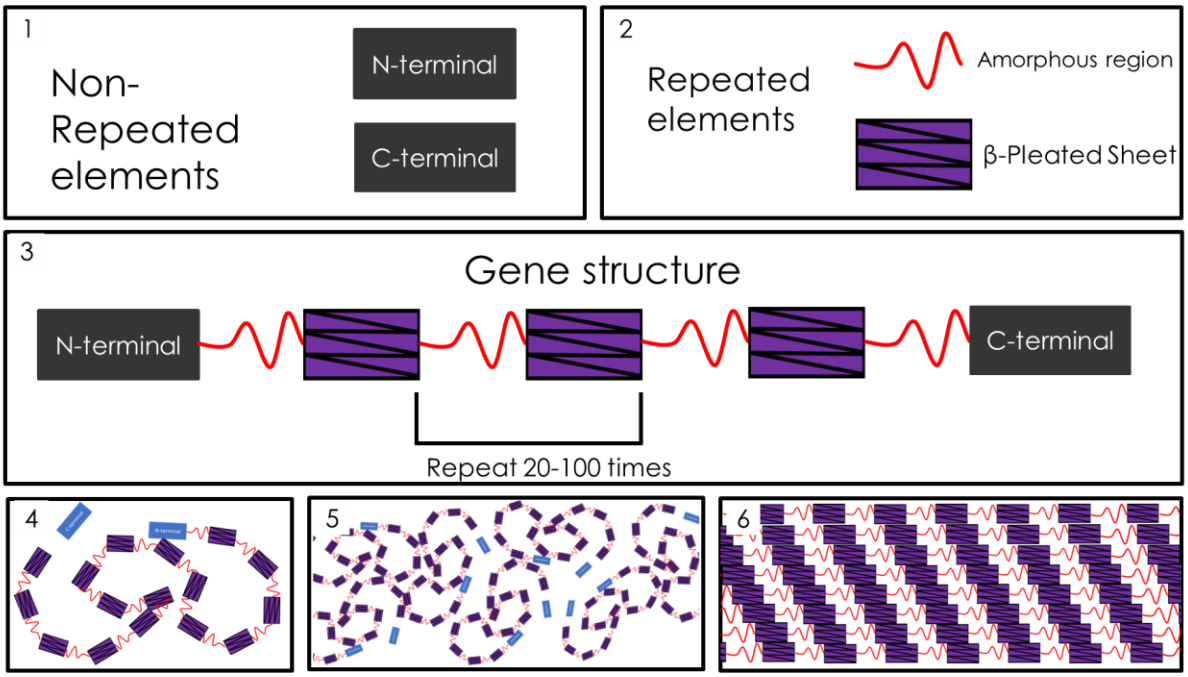

1

2 *Figure 11 Generalised gene structure and protein organisation of the*

3 *Masp1 gene from* Araneus diadematus *and corresponding protein*

4 *complexity found in silk glands (Gosline et al., 1986, Römer and Scheibel,*

5 *2008). The key in box 1 shows the symbols denoting the non-repeating N*

6 *and C-terminal domains of the silk proteins, with box 2 showing the*

7 *repeated amorphous and β-crystalline regions of the silk protein. Box 3*

8 *describes the overall pattern observed in most Major Ampullate silk genes*

9 *and their corresponding proteins, that of 20-100 repeats of the β-*

10 *crystalline and amorphous regions, book ended by the non-repetitive N*

11 *and C-terminal domains. The three boxes at the bottom (4, 5 and 6) show*

12 *the various states of the protein. 4 shows a single protein having been*

13 *transcribed, 5 shows the liquid crystalline silk dope as it begins to form*

dimers by adjoining at the N-terminal domain, before it has been solidified into a solid fibre, and 6 shows the highly regular repeating structure of the silk fibre having been extruded through the spinnerets.

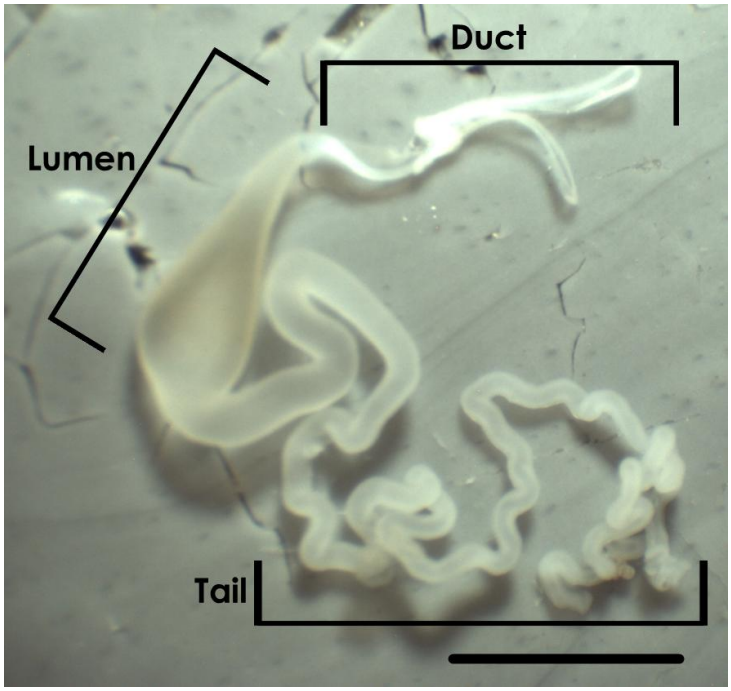

Figure 12 A labelled image of a Major Ampullate gland from Larinioides sclopetarius*. The scale bar in the bottom left of the image denotes 1mm captured using a light microscope under 20X magnification*

Figure 12 shows the labelled Major Ampullate gland from a *Larinioides sclopetarius*. The labelled sections are the duct which solidifies and delivers the silk fibre to the spinnerets, the lumen which stores liquid silk dope within the gland before being used and the tail which produces the liquid silk dope protein and delivers it to the lumen.

Before discussing the intricacies of silk glands, we must first introduce the structure and function of the silk gene and its corresponding protein to fully grasp the specialisation of these glands. Figure 11Figure

11 shows the generalised structure of the silk gene and its corresponding protein. The images at the bottom of the figure show the various states that the liquid silk protein is often found in. They correspond directly to the areas of the gland in which they are found, as in image 4, denoting a single protein, would be found in the tail of the gland (Vollrath and Knight, 2001). Image 5, denoting an irregular amorphous congregation of protein, would be found in the lumen of the gland whilst being stored prior to being utilised. Finally, image 6 shows what the silk proteins look like once they have been collapsed into a regular repeating structure. This repeating structure of β-crystalline and amorphous regions is responsible for the remarkable physical properties that silk possesses.

Figure 12 shows the morphology of a Major Ampullate gland from a *Larinioides sclopetarius* with the functional areas of the gland highlighted and labelled. The duct anatomically connects directly to the spinnerets.

Figure 12 shows the various areas of importance within a silk producing gland. The cells lining the lumen of the tail synthesise and tightly package the silk proteins before excreting them into the lumen of the gland's tail (Andersson et al., 2014). These proteins are then transported to the storage sack of the gland as a mass of disordered protein domains. As the proteins flow toward the tapered domain of the

gland, this allows the proteins to become more ordered as they are forced to adopt a more uniform composition. As the liquid silk dope travels further down the gland the silk proteins become more ordered increasing the number of intermolecular hydrogen bonds within the molecule, this correspondingly increases the mechanical strength of the fibre (Vollrath, Porter and Holland, 2013).

The cells that make up the distinct regions of the silk glands have also been studied in detail using a variety of optical and confocal techniques to make morphological study of these cells. One of the interesting things that has been noted is that these regions and their corresponding cell types vary quite widely between spiders of different species and niches. The 'so-called' simplest make up can be found in Mygalomorph species, with one example being a burrowing spider from the *Antrodiaetus* genus, possessed of multiple copies of only one silk gland type, made up of morphologically indistinct cell types. These cells produce only two silk proteins, one in the distal half of the gland and one in the proximal half of the gland (Palmer et al., 1982). This is compared to the complexity shown in orb weaving species where the secretory regions of the gland are shown to have 2-3 secretory regions each with distinct cell types (Tillinghast and Townley, 1994). Hence it becomes clear that there is a broad variation within the spider family as a whole.

One thorough study into the cellular make-up of the morphologically distinct regions of the silk glands of the *Nephila clavata* was carried out by Moon and Kim, who over 4 papers published between 1988 and 1989 undertook a systematic study of the sections that make up Major Ampullate glands' duct and spigot (Moon et al., 1988a), Major ampullate gland lumen and tail regions (Moon et al., 1988b) and Minor Ampullate silk producing and excretory regions (Moon and Kim, 1989). These detailed morphological studies used light microscopes and stains applied to fixed tissue sections to visualise the cellular differences in the different areas of these glands. It was described that the wall of the lumen was made up of a single layer of columnar epithelial cells, which each contained what is described as "several excretory granules." These granules are described as being structurally distinct from those found in the tail portion. It is stated that the within the glandular epithelial cells of the tail these secretory granules are being directly synthesised and excreted into the inner part of the gland. It is also stated in this particular study no Golgi complexes were found in any of the examined cells (Moon et al., 1988b).

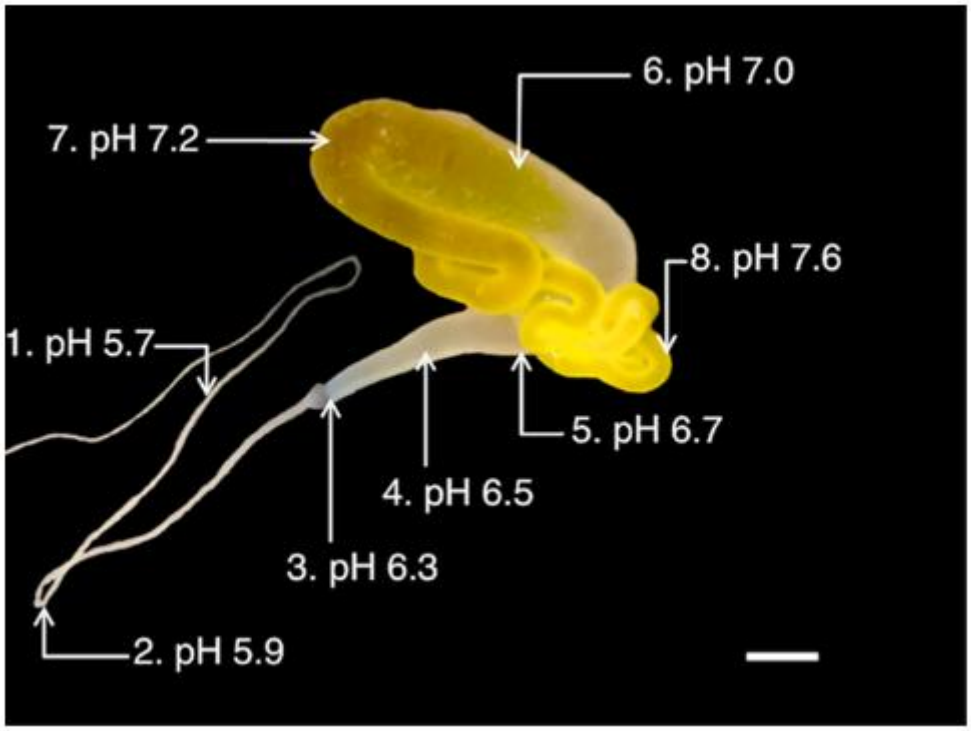

Figure 13 The pH changes that occur along the length of a Major Ampullate gland from a Nephila clavipes*. (scale bar: 1mm) adapted from (Andersson et al., 2014)*

Figure 13 shows the silk gland from a golden orb weaver that has been probed using micro pH probes along its length. Interestingly it shows a gradually descending pH along the length of the gland becoming increasing acidic along the length of the duct (Andersson et al., 2014).

The way in which liquid silk dope becomes a strong, highly insoluble fibre is understood to be due to several factors. The process is understood

to be governed by two main mechanisms: The sheer forces applied to the silk dope as it passes through the narrowing delivery duct, and the drop in pH along the gland caused by the production of carbon dioxide and H^+ in the form of carbonic acid (HCO^{-3} + H^+). These work together to draw water from the liquid silk dope and force the disordered protein into a regular repeating structure as shown in Figure 11 (Andersson et al., 2014, Vollrath et al., 2013).

The drop in pH has an interesting, if slightly paradoxical, effect on the terminal regions of the spider silk protein. Whilst the pH drop causes the N terminal (NT) dimers to become highly stabilised causing them to lock the protein into multimers, the C terminal (CT) domain becomes destabilised and unfolds into β-sheet amyloid fibrils that promote fibre formation. This multimeric faux-fibrous protein aggregate is then forced through an ever-narrowing, duct that is changing direction. The primary motive force in the process is the spider physically pulling the silk fibre from the spinnerets. This pultrusion through the duct and the spinnerets is responsible for the final compact fibre formation (Vollrath et al., 2013).

When considered in the context of varying pH causing N and C terminal changes to the protein, and the role these changed proteins play in the formation of the final silk fibre, it also makes sense that the area

where this is required to take place the most would be the final duct that the silk needs to pass through. This is evidenced by the marked drop in pH from 7 to 5.9 as shown in Figure 13 (Andersson et al., 2014).

Tissue repair and damage response in Spiders

Spiders rely on silk formation heavily for many of their normal functions such as prey capture, prey wrapping, egg sac formation and juvenile dispersion as previously covered. As such damage to these organs would likely be highly detrimental to the spider, it could therefore be expected that natural selection would favour a process that could restore their function. Hence, understanding how these glands may respond to damage became an area of study. A spider's ability to "re-grow" limbs has been the subject of study for centuries. People as early as the 19th century discussed whether this could be applicable to human amputations (Cambridge, 1895). This work is covered in spiders (Wrinn and Uetz, 2007, Vollrath, 1987), harvestmen (Townsend et al., 2017), ticks (Belozerov, 2001) and amblypygids (Igelmund, 1987). The limbs are not however, regenerating in isolation. In each of these studies they focus on the "re-growth" of limbs post moulting. The process of moulting in spiders requires the organism to produce an entire new exoskeleton, into which the spider can then grow (Ramírez and Michalik, 2019). It can therefore be said that whilst a new limb may be formed in this process it has no more regenerated a limb than it has remade its whole self. This narrowing of the literature has left something of a blind spot, given the nature of silk glands as being free floating in haemolymph (although

supported by adipose tissue), and the reliance on silk glands needed for the survival of the spider species, habitat building, prey capture, fall arrest, dispersal , it would stand to reason that any permanently damaged silk gland would cause a serious if not life ending problem. Therefore, the question of how spiders deal with internal injuries has yet to be addressed.

Methods

Transmission Electron microscopy (TEM) Sample Preparation

Transmission Electron Microscopy (TEM) is a technique within the field of microscopy which functions by sending a highly concentrated beam of electrons through a sample and measuring how the electrons interact with each other (Tang and Yang, 2017). This contrasts with the field of Scanning Electron Microscopy (SEM) in which a sample is coated in a very fine layer of a dense reflective material (usually gold), a beam of electrons is fired at the investigated surface and the deflections of the electrons are measured (Abdullah et al., 2014). As an over simplification, SEM is a very powerful tool for studying topology and TEM is a penetrative tool for studying electron density (Eyden, 2002). To better understand the internal structures and functions within the silk glands themselves, samples were analysed using TEM.

Major Ampullate glands were removed from the abdomen of *Larinioides sclopetarius* as described in chapter one. Post dissection (as shown in Figure 5) the glands were washed twice in dissection buffer and rather than being placed into media and antibiotics, they were placed into primary fixation solution made up of 3% glutaraldehyde in 0.1M

cacodylate buffer, overnight at 4◦C. The samples were then washed twice in 0.1M cacodylate buffer for 5 minutes followed by post-fixation with 1% osmium tetroxide in 0.1M cacodylate buffer for 2 hours at room temperature.

Samples were then washed (in distilled water for 2 x 10 minutes). The tissue was dehydrated using graded ethanol, 50% for 2 x 10 minutes, 70% for 2 x 10 minutes, 90% for 2 x10 minutes and 100% ethanol (3 changes, each for 15 minutes) respectively this process was performed at 20°C.

To aid resin infiltration, propylene oxide (100%) was used (3 changes for 15 minutes per change) and followed with the addition of propylene oxide / TAAB Low Viscosity Resin at a 3:1 ratio respectively for 1 hour and a 1:1 ratio overnight. Samples were transferred into vials containing pure resin solution for 2x1 hour prior to selecting the correct orientation and embedding them in BEEM capsules and placing in the embedding oven at 70 °C for 48 hours.

Samples were sectioned with a diamond knife to 80 nm in thickness using Leica EM UC6 (Leica Biosystems, Wetzlar, Germany), placed on 100 mesh carbon support copper grids followed by post-staining which was carried out with saturated uranyl acetate in 50% ethanol and Reynold's lead citrate.

Grids were analysed using a Tecnai Bio-TWIN T12 Biotwin transmission electron microscope (TEM) (FEI Company, Eindhoven, The Netherlands) and run at an accelerated voltage of 100 kV. Images were captured using a MegaView SIS camera.

Polarised light microscopy (PLM)

As a polarised plane of light passes through a crystal structure the light can often be refracted in interesting ways, causing the light to deviate from the initial plane of polarisation. When this resultant light or "extra-ordinary-ray" is passed through a calcite crystal this deviation from the ordinary ray is shown as a variation in colour (Talbot, 1834). This is of particular use due to the highly repetitive nature of the crystal structure in native spun silk being of sufficient crystallinity to elicit a birefringent response.

Samples were prepared for polarised light microscopy by dissection and washing as described in chapter one before being placed onto a clean microscope slide. A cover slip was applied to the gland and the whole system was viewed using an Olympus CH Petrographic polarising light microscope using 4X 10X and 40X lenses viewed through a 10X objective before being imaged in the manner described in chapter one (C1 Methods: Observation and recording of glands in culture)

Imaging of glands and observing response to injury

The glands used in the repair experiments were collected and dissected as stated in chapter one. The glands were left in culture for a minimum of 24 hours before being moved to a testing well and damaged at the distal end of the tail. Glands were damaged by separating a portion of the final third of tail of the gland and removing it with an offset mini spatula, whilst being viewed under a Brunel BMSF adjustable height dissection stereomicroscope. Imaging was performed as previously stated in chapter one, with the exception of Figure 22 where the top-down light for the microscope was forgone in favour of placing a standing lamp next to the sample, shining light at approximately 30° through the sample from top left to bottom right. This allowed for better visualisation of the movement and behaviour of individual cells.

Results

The following TEM results were taken from a single *Larinioides sclopetarius* Major Ampullate gland dissected and cultured following the protocol laid out in the first chapter. The PLM and light microscope images were taken from a pool of over 10,000 images collected from over 20 glands dissected from 13 *Larinioides sclopetarius* specimens. Each figure's images were taken from one gland per figure. The patterns and observations made below were each observed multiple times, and the images selected were chosen as they best demonstrate the events described.

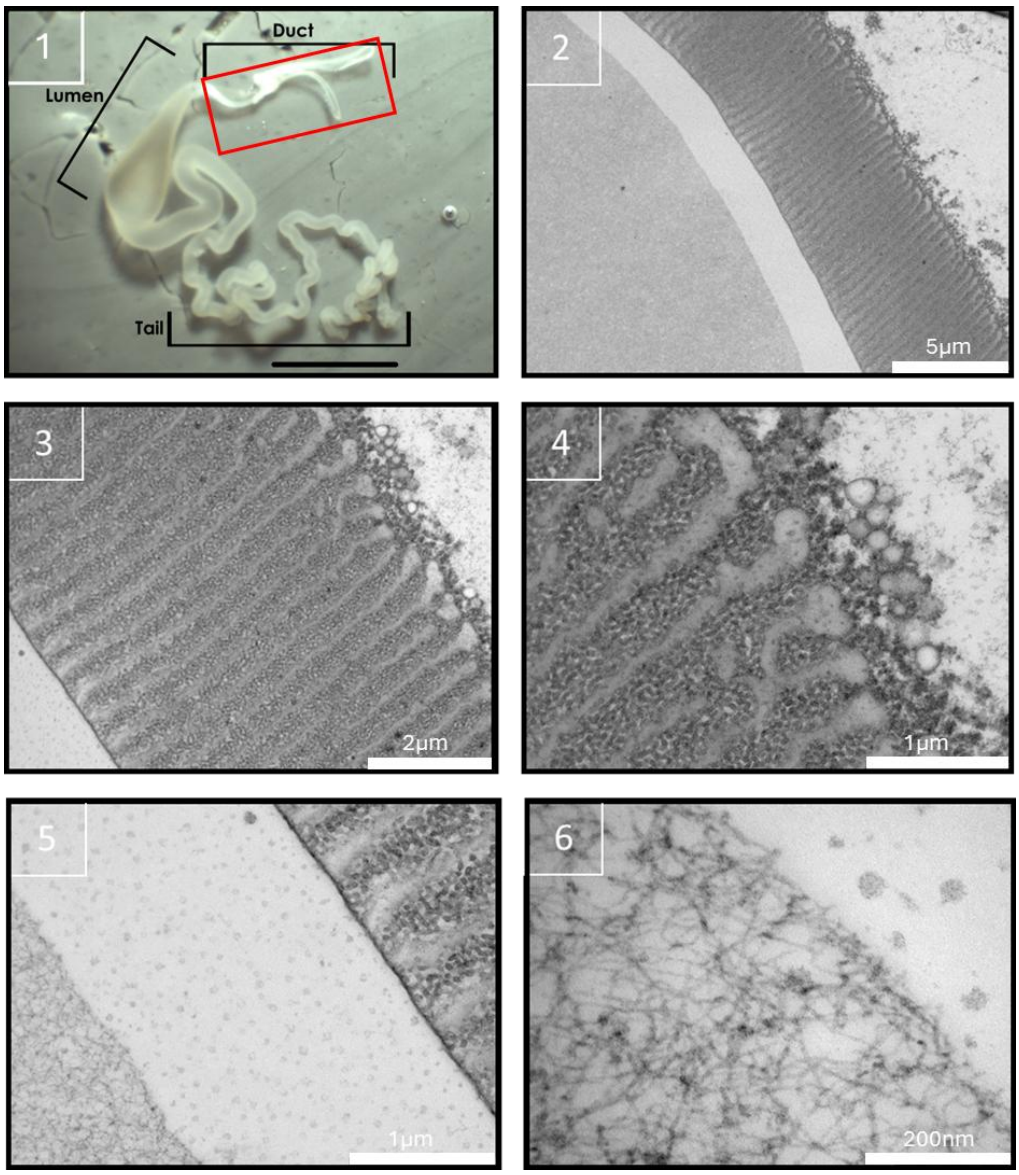

Figure 14. TEM imaging of the duct of a Major Ampullate gland isolated from a Larinioides sclopetarius*. This figure details the TEM performed on a* Larinioides sclopetarius*. The tail of the gland is highlighted by the red box in image 1 (repeated image from Figure 12). The scalebars for each picture can be found in the bottom right.*

The first image of Figure 14 shows an expanded view of the gland with the duct apparatus highlighted. Image 2 shows an expanded view of the duct and silk fibre formed within, a space between the silk and the duct, the physical structure of the duct and finally the outside of the duct wall open to the spider's haemolymph. Images 3 and 4 show a more detailed view of the duct wall. The repeating lateral structure within the duct wall is visually similar to the structures found in *Nephila edulis* G. Davies has shown are made up of chitin and suggested may help avoid unwanted deformations in the duct wall (Davies et al., 2013) .

In image 3 the solid silk fibre formed within the duct in the bottom left of the image will be referred to as interior and the haemolymph facing edge of the duct wall on the top right of the image will be referred to as the exterior edge. The interior edge of the duct can be seen as a well-defined, densely stained edge, while the exterior edge of the duct wall is much more poorly defined, with multiple small spherical bodies surrounding the duct wall.

Image 4 shows in more detail the exterior edge of the duct. The areas of higher and lower electron density within the duct wall do not

show clearly demarcated boundaries. The small spherical bodies surrounding the exterior of the duct appear to be vesicles with clearly defined boundaries.

Image 5 shows a closer look at the interior edge of the duct structure. This shows a highly electron dense area with very clearly defined thin boundaries. The edge of the solid silk fibre is also shown in the bottom left of the image; in this we can begin to see an interlocking structure within the solid fibre. Between the interior edge of the duct and the solid silk fibre we can see a gap. This gap is likely where the fibre is pulling away from the walls of the duct (Vollrath and Knight, 2001) and therefore given us an interesting view of the background non-specific staining artifacts for the preparation methods used. It is worth stating that this area could also be made up of the 5μm layer of glycoprotein and lipid layer that was found to be coating *Nephila inaurata* dragline silk (Stehling et al., 2019).

Image 6 shows a very close up view of the solidified silk fibre found in the duct of the spider. The dense interweaving patterns of what is likely the silk can be seen. This image also provides a detailed look at the small

non-specific staining artifacts. These are the small dots seen between the duct wall and the silk in image 5 and the irregularly shaped artifacts seen next to the silk in image 6.

Page left intentionally blank

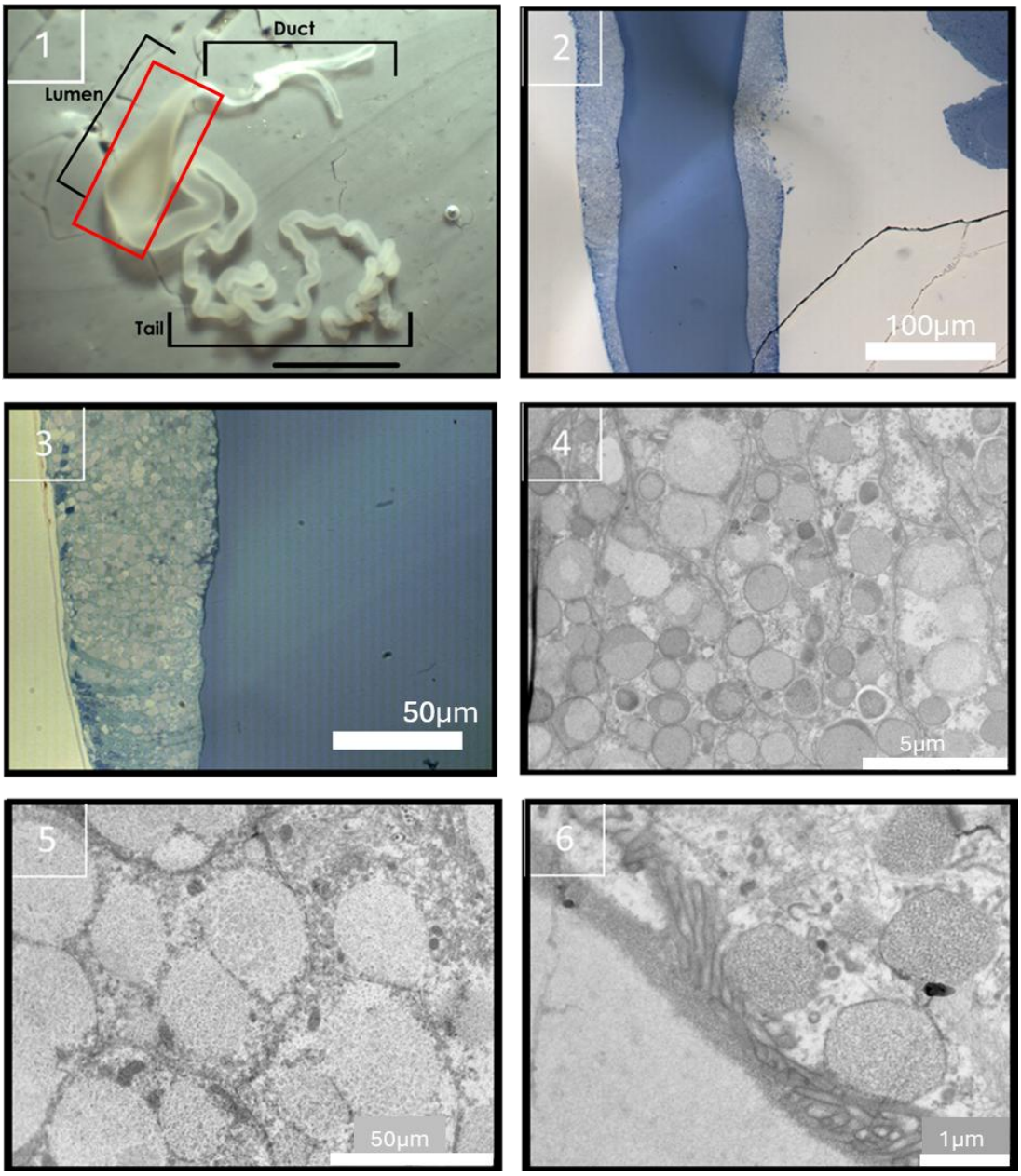

Figure 15. Light microscope (images 1-3) and TEM (images 4-6) imaging of the lumen of a Major Ampullate gland isolated from a Larinioides sclopetarius*. The lumen of the gland is highlighted by the red box in image 1 (repeated image from Figure 12) The scalebars for each picture can be found in the bottom right*

The first image of Figure 15 shows an expanded view of the whole gland with a red box highlighting the lumen. The lumen is thought to function only to store dope prior to its being needed.

Image 2 shows a light microscope view at 20X magnification of a cross section through the whole gland stained with a simple Coomassie protein stain. The right-hand edge of this section shows a large crack in the resin in which the gland is immobilised. It can also be seen that the right hand of the lumen appears to be damaged, whether this happened as a result of the dissection process or the fixation and staining procedure is unknown, what can be seen however, is very dense staining of the protein in the central lumen, the liquid silk dope.

Image 3 is a closer look at this same Coomassie stained lumen, this time at 40X, highlighting specifically the left-hand wall of the lumen with the silk directly to its right. The image shows a very clearly defined interior edge to the lumen, much thicker than that shown in Figure 14.

The image also shows an interesting patchwork pattern within the wall of the lumen. Images 4 and 5 show this patchwork pattern in closer detail. This patchwork is made up of vesicles with the same internal patterning that is present in the liquid silk found within the gland’s tail,

shown in Figure 16 images 5 and 6, suggesting that this extensive number of vesicles are all filled with additional silk dope. Similar "excretory vesicles" were also found in the Lumen walls of Major Ampullate glands in *Nephila edulis* (Knight and Vollrath, 1999), although these vesicles showed a distinctive repeating pattern that is absent here.

Image 6 shows the interior edge of the lumen. This interior edge looks as though it is made up of multiple vesicles that have relinquished their cargo and are enroute to be recycled. This likely, given the patterning within the collapsed and partially collapsed vesicles, matches both that of the vesicles within the cells in Figure 15 and that of the pattern observed in the fibre in Figure 14 images 5 and 6.

Page left intentionally blank

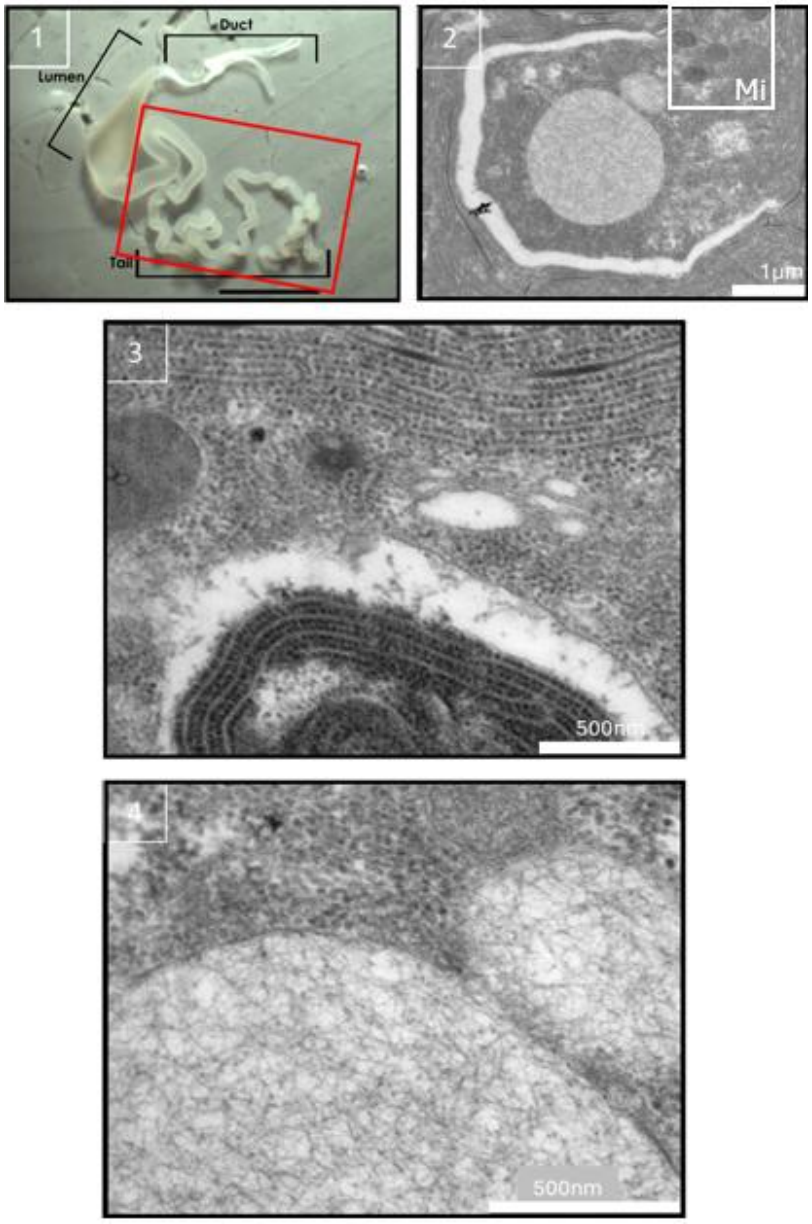

Figure 16. TEM imaging of the tail of a Major Ampullate gland isolated from a Larinioides sclopetarius*. The duct of the gland is highlighted by the red box in image 1 (repeated image from Figure 12 with a 1mm scale bar). All other scale bars are labelled Mitochondria in image 2 labelled (Mi).*

The tail is known to be the area of the gland that produces much of the silk dope, and as can be seen from image 1, highlighted at the bottom of the image by the red box, is longer than the other 2 areas of the gland combined. Image 2 shows an overview of a typical cell found in the tail of the gland. In the top left hand of the image, multiple mitochondria can be seen (labelled Mi), which given the cell's role in protein production is unsurprising. The nucleus can be seen in the left of the image next to the very large vesicle in the centre of the image, surrounded by what appears to be a very heavily electron dense substance found within the cytoplasm of the cell. The central vesicle when compared to the vesicles seen in in Figure 15 and the silk fibre seen in Figure 14 appears to be filled with silk dope.

Image 3 shows at the top and bottom some very dense endoplasmic reticula with a small collection of ovals seen between them. Given the proximity of these to the endoplasmic reticula, it is likely that these function to produce the vesicles shown in the earlier image which store the silk being produced. It can also be seen from image 3 that the electron dense substance filling the cell seen in image 2 is made up of thousands of individual ribosomes.

Image 4 shows a close-up on the edge of the vesicles found in the centre of the cell. It can be seen from image 4 that the edge of these vesicles is very thin and surrounded by ribosomes right up to the edge of the vesicle. The interior of the vesicles can also be seen to be filled with, visually, the same silk found in the previous Figures.

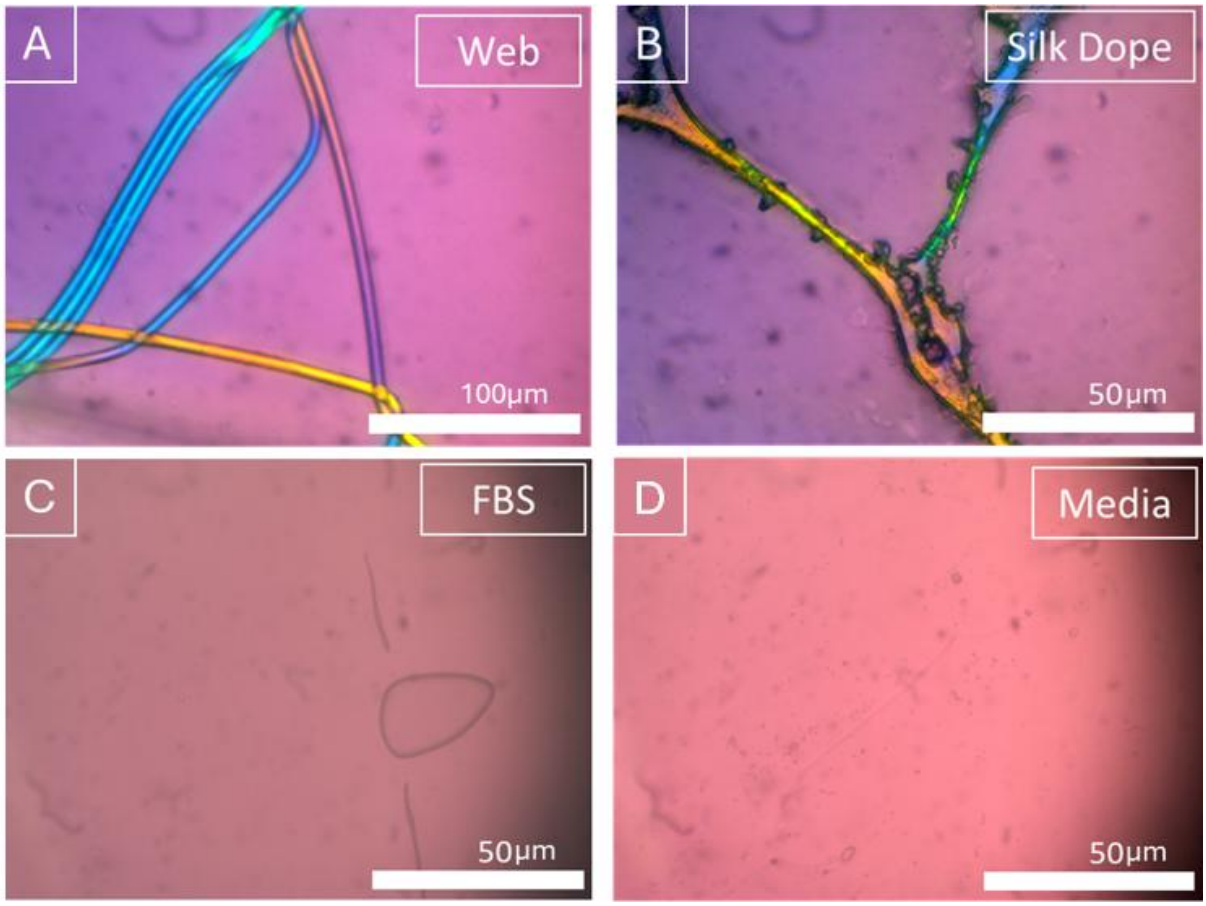

Figure 17. A comparison between the birefringence of native spun silk and silk allowed to solidify in culture media, as described in chapter one methods (P49-54). These are compared to a high protein substrate of foetal bovine serum (FBS) that has been allowed to solidify in the same way and to the culture media, without silk, which has also been allowed to dehydrate in the same way. Scale bars are found in the bottom right hand of the image.

Figure 17A shows the patterns of birefringence seen in in native spun spider silk collected directly from the pot the spider was kept in. The

clearly visible and demarcated colours are formed by the polarised light interacting with the molecular orientation of the repeating crystalline structure being found along a preferential direction (Ward, 2012). The change in colour is caused by the relative orientation of the crystal structure in relation to the incoming polarised light from the microscope.

Figure 17B shows the silk that had been allowed to solidify in culture. It can be seen from the image that areas of the solidified silk share colours in common with that of the native spun silk, especially those that are shown in similar orientations to that shown in the native spun silk. It can also be seen that there are a variety of other colours likely caused by overlapping or non-uniform crystal structures being present, due to the less controlled nature of the fibre formation.

The bottom left image is intended as a control, to show what happens when a high protein substrate, foetal bovine serum (FBS), is left to dry in the same way the liquid silk was allowed to dry. It can be seen from the image that no form of regular repeating structure can be seen within the protein, and moreover no form of fibre has formed.

Similarly, Figure 17D was intended as a control to show what happens when just the gland's media is left to solidify in the same way. The media alone shows no form of fibre formation and specifically no form of birefringence, which shows that the effects seen in image B are due only to the liquid silk being present and solidifying.

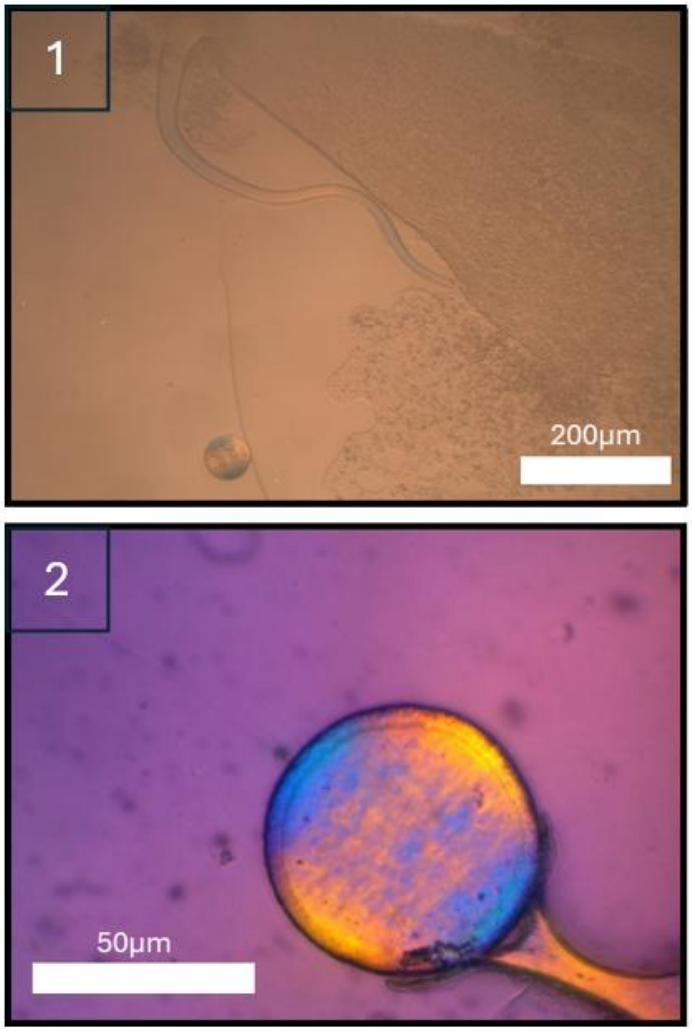

*Figure 18. Polarised light microscopy of a whole gland, with a solidified silk droplet. A whole Major Ampullate silk gland (*Larinioides Sclopetarius*) was removed from dissection buffer and placed onto a microscope slide with a coverslip over the top of it. The weight of the coverslip burst the gland, thus causing liquid silk dope to spill from it. The dope can be seen on the well. Image 1 was taken using a variable magnification dissection microscope and therefore the scale is calculated from by image 2 containing the same droplet of solidified silk as seen in image 1.*

Image 1 shows the ruptured gland with the liquid silk spilling out onto the middle of the slide. In the bottom left of the screen a single droplet of solidified silk can be seen showing a birefringence of blue and yellow. The same birefringence can be seen in the duct leading away from the lumen of the gland. This is likely due to the duct beginning to solidify the liquid silk from the lumen. As the silk becomes ordered during its passage through the duct it begins to have a regular repeating crystal structure which in turn interacts with the polarised light and thus shows birefringence. Interestingly the same birefringence shown in Figure 17 cannot be seen in the liquid silk. This is likely due to the disordered nature of the silk proteins found in the lumen as described in Figure 11. Without the regular repeating structure of solidified silk, a birefringent response would not be elicited.

Images 1 and 2 show the same solidified silk droplet, before and after allowing the liquid silk surrounding it to solidify. This leads to image 2 having a connecting arm of solidified silk showing birefringent properties that image 1 does not have.

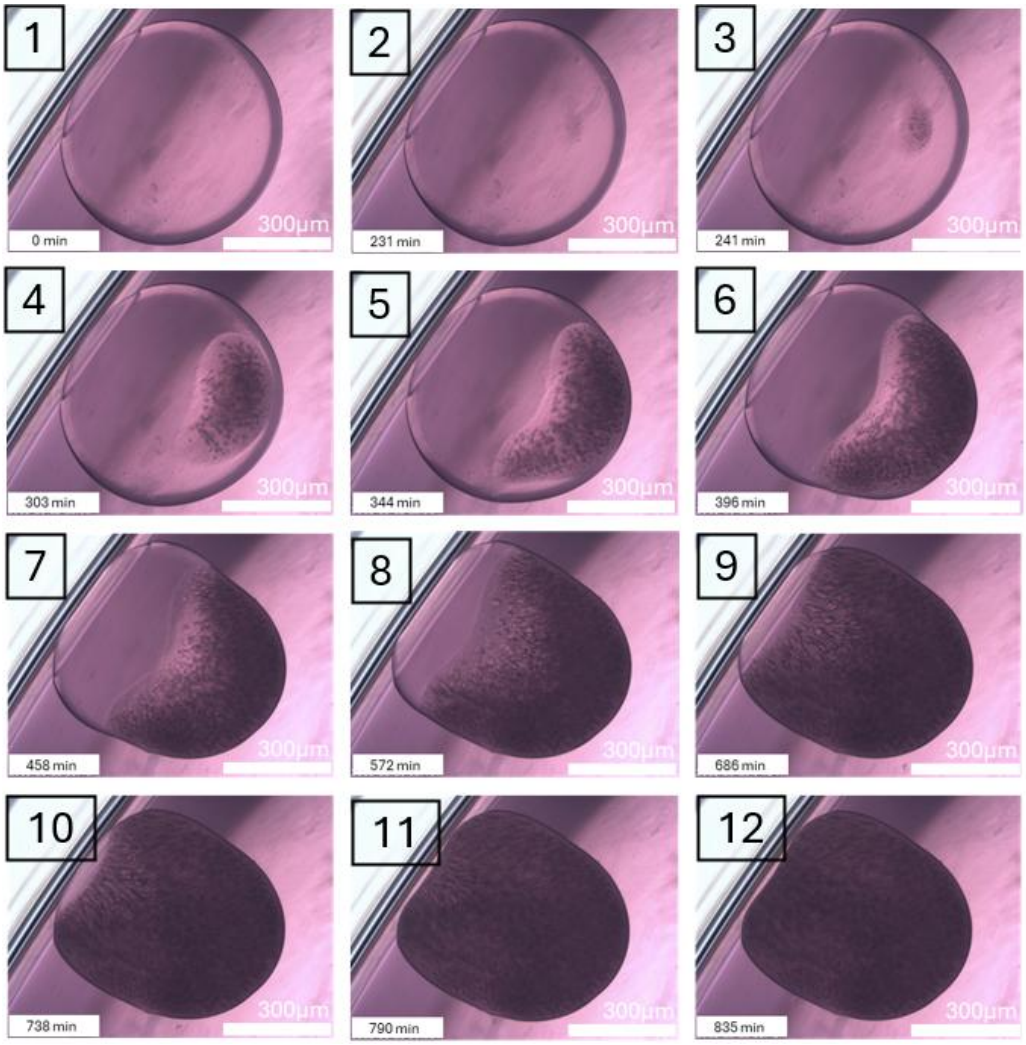

Figure 19. Solidification of silk dope expelled from a Major Ampullate gland from Larinioides sclopetarius over 9 hours at pH 11. Scale bars shown in the bottom right of the image and time elapsed in minutes bottom left. The silk droplet measures approximately 500 µm across and has an approximate volume of 0.0325µl assuming a hemispherical volume. Solidification can be seen beginning at 231 minutes and ending at 790 minutes the following day. A video of this can be seen by following Link 2 below.

As can be seen by images 2 and 3 of Figure 19, the droplet seems to begin to solidify from a point roughly centre right on the droplet, resulting in a slightly darker area of partially solidified silk.

The second and third rows (images 4-9) show the continuation of the silk solidification from a single point, as well as the formation of small inclusion bodies of what seems to be clear liquid. There seems to be a clear front preceding the area of solidification, which looks similar to a meniscus. As this front of solidification passes through the silk droplet the previously circular shape appears to become deformed due to internal stresses. The final row (images 10-12) shows the solidification front finally completing, having moved throughout the entire droplet. Interestingly the uneven movement of the solidification has resulted in a final solidified shape that appears significantly smaller that the initial droplet and very irregular in shape.

Link 2 A large bolus of silk dope from a Major Ampullate gland from a Larinioides sclopetarius *solidifying in culture. Each frame taken 2 minutes apart. Video made using Fiji. Made up of 490 images.*

Hyperlink: https://youtu.be/J3uiiE8wTmE

Page left intentionally blank.

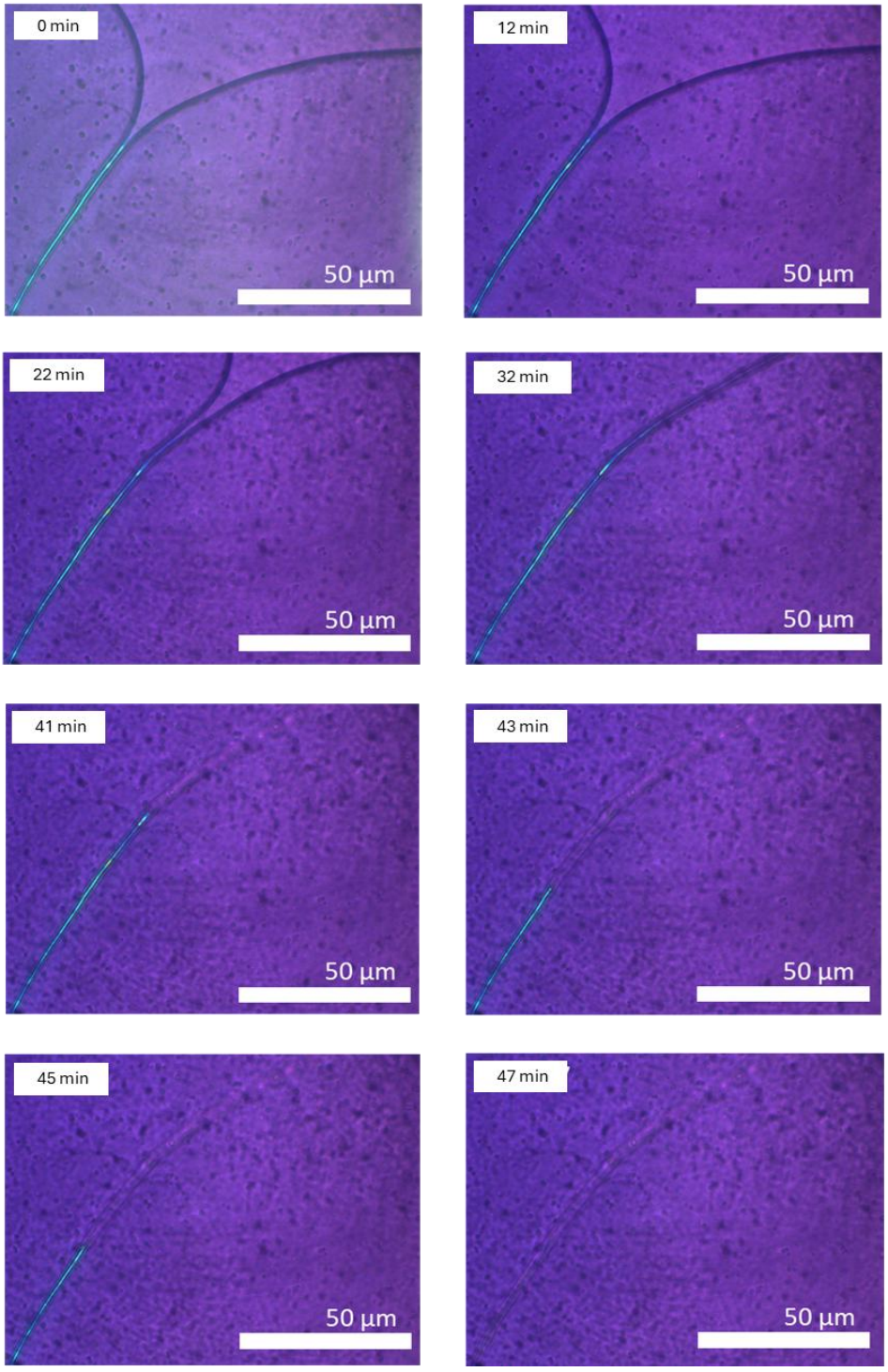

Figure 20. Formation of a silk thread and its subsequent internal elasticity over a time period of 47 minutes, viewed using polarising light microscopy. Scale bars are found in the bottom right of each image.

As in Figure 18, a whole gland was placed on a slide, broken with the weight of a cover slip and not sealed, to allow the silk dope to “dry”. In Figure 20 however, the focus was placed on the outer edge of the escaped silk dope. After extending to its limit the front of silk dope began retreating, and upon closer inspection, fibre formation was observed.

The first two rows show the initial formation of the fibre by the retreating front of silk, in 10-minute increments from 0 to 32 minutes. The retreating front of silk dope shows no birefringence, whilst the fibre that is left behind shows very striking birefringence, similar to that of native spun silk shown in Figure 17. the last image shown in the second row shows the front of silk dope finally leaving behind the deposited fibre.

The second two rows show the solidified fibre seeming to retract back out of the aperture of the microscope. This takes 6 minutes (from 41-47 minutes) from the fibre being totally left by the silk dope to the fibre being completely unseen on the aperture. This seems to happen in two stages, the first row shows the initial retraction with the second row showing the final shift off screen. A video of the whole process can be seen by following link 3 below.

Link 3 Silk from a Major Ampullate gland from a Larinioides sclopetarius *solidifying under polarised light microscopy. Video made using Fiji, made up of approximately 70 images taken 1 minute apart.*

Hyperlink: https://youtu.be/1VDzDGrF5uY

1 *Page left intentionaly blank*

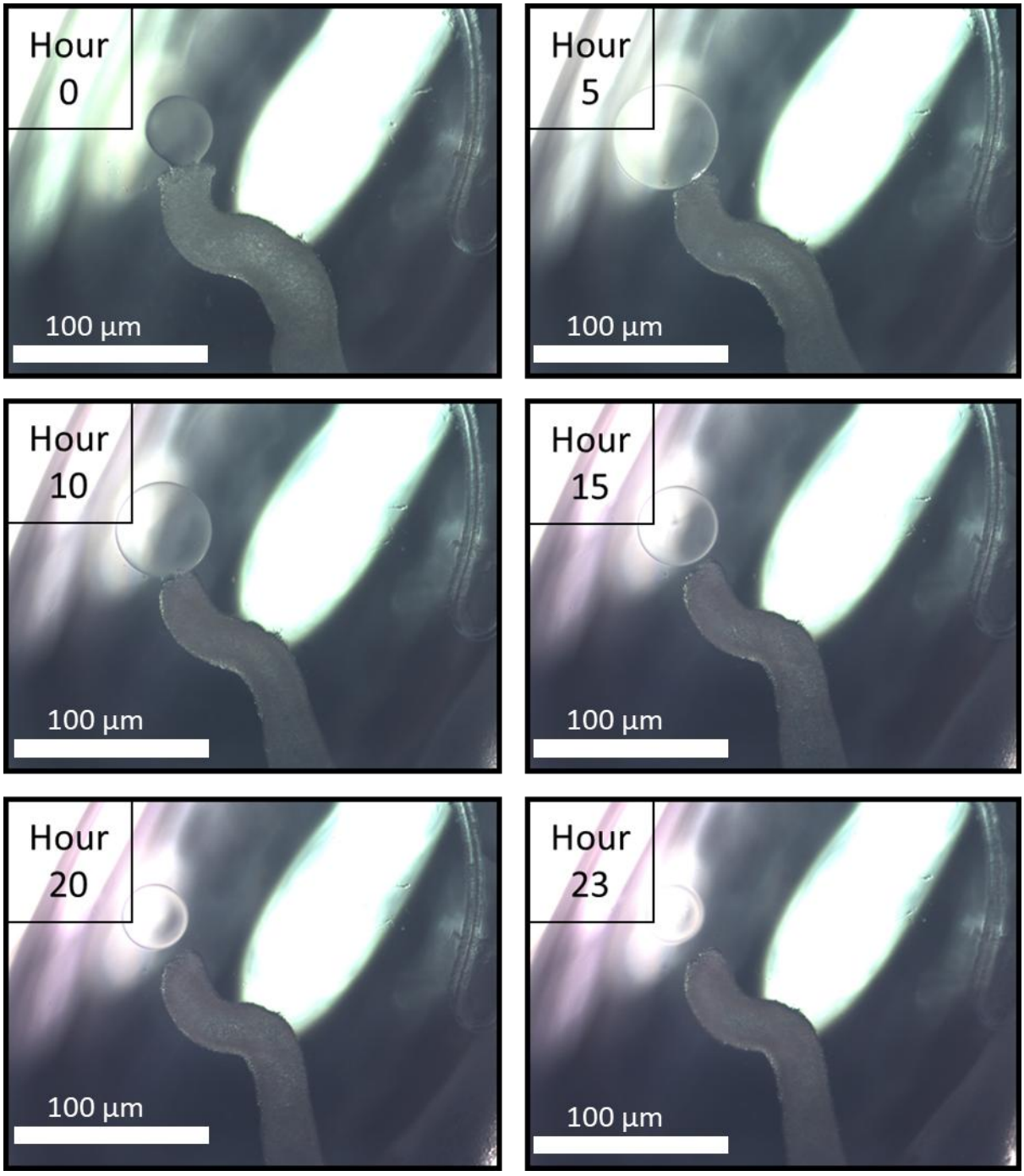

Figure 21. The complete repair of the tail of an isolated Larinioides sclopetarius *Major Ampullate gland in culture over 23 hours. Scale bars can be found in the bottom left of each image.*

A gland was removed from the abdomen of a specimen, washed and cultured, before beginning the experiment as stated in the methods (Chapter one, Methods, dissection, and maintenance of glands in culture p49-54). Silk dope begins to escape from this damaged site, the opposite end from where the silk should normally be coming from. The edges of the tail can be seen to be rough and flared out slightly at the site of damage. The diameter of the rest to the tail remains unaltered.

At hour 5 there is still escaping silk dope from the site of damage, however the ends of the tail are beginning to round over and become less ragged. The diameter of the tail also remains consistent. At hour 10 the rate of escape of dope from the sight of damage has begun to slow down considerably. The site of damage appears to be almost completely rounded over with only a very small opening left. The diameter of the tail appears to be reduced both at the cut site and below it.

At hour 15 there is no longer silk escaping from the damage site at the tail. The cut site has completely smoothed over leaving behind contiguous, if asymmetric, edges. The diameter of the whole tail is reduced. Interestingly the silk droplet appears to be shrinking, however, this is not the case. Once the silk droplet has separated from the stream of silk dope escaping the tail, its own surface tension pulls the droplet into

a more spherical shape, thus reducing its footprint on the base of the well.

At hour 20 the asymmetry in the damage site is reducing, as the diameter of the tail begins to increase once more. At hour 23 the damage site is now symmetrical, and the tail diameter has returned to pre-damage levels. The symmetry and diameter of the repairing tail of the gland are functioning as a rough indicator of the stage of repair, with the return to pre damage size functioning as a visual indicator that the repair has completed. A video of the whole process can be seen by following Link 4.

Link 4 Major Ampullate gland from a Larinioides sclopetarius *repairing intentional damage in culture. Video made using Fiji, made up of 1380 images taken 1 minute apart.*

Hyperlink: https://youtu.be/vDfpI-Ugq6I

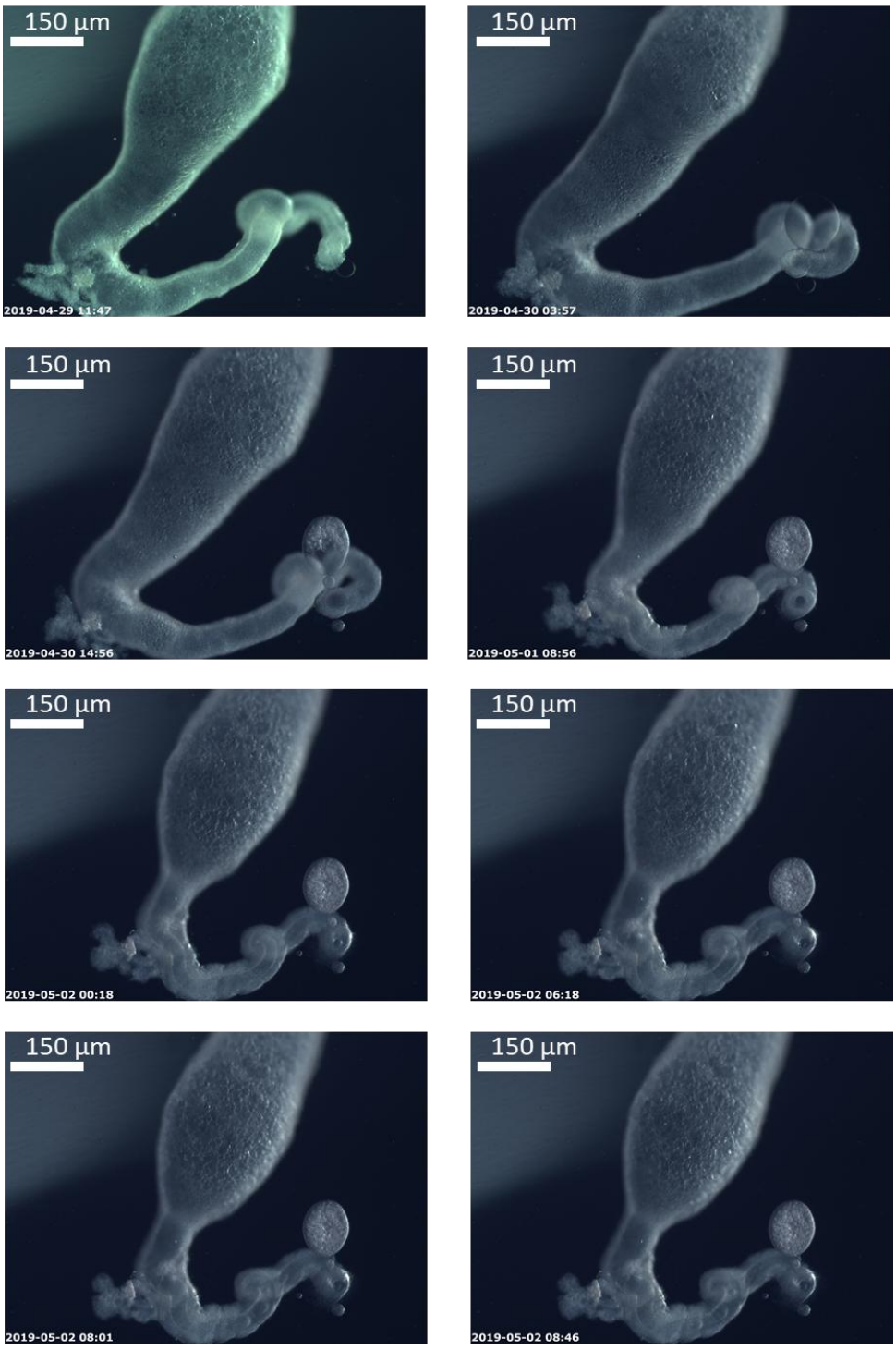

Figure 22. Whole Major Ampullate gland view of repair in culture from a Larinioides sclopetarius. *Scale bars found in the top left of each image and a time and date stamp in the bottom left.*

This figure shows a whole gland view of a *Larinioides sclopetarius* gland repairing in culture over 70 hours. The gland was removed and cultured as described in the methods (chapter one, Methods, dissection and maintenance of glands in culture p49-54) although this gland was not placed in fresh media, but was instead, after being intentionally damaged, placed back into the media that it had occupied for 3 days prior. The images were taken in a similar way to that previously described although in place of using the 'microscopes top-down lamp, a standing lamp was utilised, with light shone in an angle of 30° from top right to bottom left, to give greater contrast of the cell surface. The first two images (hours 0-16) show the damaged gland leaking dope both from the tail and from the duct (unseen, off screen). This leads to, in the second image, the lumen of the gland having visibly reduced in volume. The surface of the lumen appears consistent with what appears to be large vesicles as were shown in Figure 15.

The second row (hours 27-45) shows what appears to be the lumen regaining volume whilst the surface of the lumen appears to be changing shape, likely due to the emptying of vesicles of silk dope into the lumen of the gland. In the first image we can see the silk escaping from the tail is not only slowing down in its rate of escape, but is also beginning to solidify in a similar manner to that shown in Figure 19. By the second

image the escaped silk has completely solidified, and no more fresh dope appears to be escaping form the tail of the gland. It also shows what appears to be the damaged end of the tail beginning to heal to the bottom of the well.

The third row (hours 60-66) shows the lumen of the gland beginning to gradually fill up as the movement of the vesicles, seen in the previous four images, begins to slow down. The second image also shows the beginnings of silk dope production, beginning again in the tail. The final row (hours 67-68) shows the stabilisation of the size of the lumen and the production of additional silk coming from the tail of the gland. A video showing the full process can be found by following Appendix Link 5.

Appendix Link 5 Major Ampullate gland from a Larinioides sclopetarius repairing intentional damage in culture. video made using Fiji, made up of 4061 images taken 1 minute apart. Hyperlink:

https://youtu.be/G0vOY6E1gdQ

Discussion

In this study it is shown that we can visualise the solidification of spider silk dope, both as a large mass and as an individual fibre being formed on a slide. It has been shown that spider silk glands can repair themselves autonomously. It has also been shown that the different areas of the silk glands are cellularly specialised to perform different roles, though the presence of varying structures and organelles appearing in different densities in different areas of the glands. Figure 16 shows the cells in the tail which are specialised for producing protein. The cells are almost completely full of protein manufacturing machinery, with a very high number of ribosomes surrounding the rough endoplasmic reticulum. Given the abundance and proximity of these ribosomes it seems possible that the very large silk gene mRNA would be being passed from ribosome to ribosome for the most efficient production of protein. This would however need to be investigated further. This ribosomal density combined with the presence of many mitochondria make these cells powerhouses of protein production. Their vesical transport of the silk protein is also interesting given their ability to move large quantities of hydrophobic protein from their protein replication machinery to the lumen of the glands. The large size of the silk gene when produced in *E. coli* caused truncates synthesis roughly every 1000 codons of the gene. These

truncations were problematic for the cells. This was because in the absence of a His tag they could not be exported, resulting in un-exported aggregates and leading to cell death(Fahnestock et al., 2000). Therefore, immediately storing the hydrophobic silk dope in this way negates the possibility of protein aggregates forming and disrupting cell function. It is worth mentioning however that these hydrophobic protein production problems noticed in the *E. coli* are unlikely to be seen within normal eukaryotic cells producing their native proteins likely due to similar vesicular transport or other methods to prevent this aggregate problem.

When viewing the cellular structures of the gland through the lens of not just production, but also of survival, then the structures seen in Figure 15 begin to take on a new light. The large vesicles apparent in the cells surrounding the lumen were initially believed to be just additional production taking place (Moon et al., 1988b) but are more likely to be a secondary storage mechanism. This function can be seen in Figure 22, where the damaged gland, having lost much of its silk dope, begins to refill before the damage is healed sufficiently to prevent further leaking of the silk dope. Additionally, the first three rows of Figure 22 show a distinct change in both the width of the lumen and in the overall shape of the lumen. This combined with the changing topology of the lumen indicate that the vesicles being stored in the cells surrounding the lumen

are being deposited into the main storage lumen to maintain the necessary stocks of silk needed for the survival of the spider.

When looking at Figure 16 in the context of the dehydration necessary for silk formation (Figure 13, Figure 19, Figure 20) and in the context of the ordering of the silk protein into the regular repeating β-sheet crystalline structure (Figure 13, Figure 18, Figure 20) (Knight et al., 2000) we can start to understand the nature of the unknown structure that makes up the duct of the gland is likely to be the chitinous structures described by Davies (Davies et al., 2013) (expanded upon below). The long nature of the duct with many sharp turns could very well act to increase pressure within the duct, in an attempt to force excess water from the silk fibre. This would require the duct itself to have additional structural support, to ensure that the duct would stand up to the stresses placed upon it. This mechanism is similar to the function of the loops of Henle found within nephrons in mammalian kidneys, where a sharp turn in the kidney vesicle causes a dramatic localised increase in blood pressure, forcing water, and metabolic waste products, from the bloodstream, whilst retaining the larger blood cells that cannot escape (Greger, 1985). In a similar vein, these large turns could be functioning to force water from the protein whilst keeping the larger silk proteins from being able to escape, thus dehydrating the protein fibre. These loops

could also be functioning to increase the sheer forces within the duct and force the silk fibre into the regular repeating structure that affords silk its remarkable properties (Dicko et al., 2004). The interesting internal structures that makes up the walls of the duct are likely intended to allow for the egress of water whilst maintaining the strength necessary to withstand high shear forces in the turns within the gland (Davies et al., 2013). These shear forces that are present have a huge impact on the formation of the final silk fibre, in fact it has been shown that the fibre, whilst forming, pulls away from the duct wall in the distal end of the duct (Knight et al., 2000).This is further confirmed by the observations made in Figure 14, which shows what appears to be this mechanism taking place. This shrinking of the fibre is where the final formation of the repeating β-pleated sheets structure occurs. What is also interesting about this structure and the pulling away from the walls of the duct itself, is that it gave rise to an alternative hypothesis of silk formation, moving away from extrusion and towards pultrusion. The work by G. Davies that originally identified the presence of chitin in spider silk gland ducts also noted similar chitinous structures present in the ducts of silkworm glands (Davies et al., 2013). This structural similarity between spiders and silkworms lead to the testing of the pultrusion hypothesis utilising silkworm silk as an analogous organism. It was found, by comparing the force necessary to produce silk fibres using pushing or pulling forces, that it was more biomechanically capable of producing silk by utilising the

lower force required through the application of pultrusional forces (Sparkes and Holland, 2017).

The benefits of comparative polarised light microscopy (PLM) should be addressed. In this study the patterns of birefringence between native spun silks and silks solidified ex-vivo have been compared. This comparison uses the colours shown in silks moving in a distinct direction as a proxy for demonstrating the presence of a repeating crystal structure existing in the same plane. The nature of PLM, a tool used often in the analysis of geological samples, makes it suited to the study of spider silk. Historically PLM particularly and birefringence have been used to elucidate the effects of wetting on the strains within a silk fibre (Work, 1977), the order of macromolecular formation (Viney et al., 1991) and, in concert with tensile strength testing, the relationship between silk draw speed and the material properties demonstrated (Holland et al., 2012). It is also worth mentioning that it has been shown that increasing strain on silk fibres increases their birefringence (Glišović et al., 2008). Given the broad investigative uses of PLM, it is important to narrow the case for use in this investigation. The visualisation of comparative shifting of polarised light when interacting with a regular crystal structure will act as a detector of the necessary regular repeating structure that is seen in native spun silk. Given the width of the average β-pleated sheet is 2.1nm (Arnott et al.,

1967) and the wavelength of visible light is 380-700nm, a single β-pleated sheet will not interact with polarised light for the purposes of microscopy. Given this is the case, for there to be any observable interaction between the β-pleated sheets and the polarised light there must be a minimum of several hundred β-pleated sheets adjacent to and aligned with one another. Then the only method by which an observable effect could come about is if the β-pleated sheets from multiple silk proteins were aligned. Creating a region with enough regularity to interact observably with the polarised light and create a colour difference. It can therefore be stated with confidence that the only way for an observable colour shift from no observable difference from the background, to an observable difference from the background to be recorded from the polarised light microscopy study of solid silk fibres, is if there are multiple β-pleated sheet regions from multiple different silk proteins aligned in the same plane, as is known to be the case in native spun silk..

Having discussed the importance of the structure of the silk glands in allowing the silk to solidify and form fibres, it is important to state, these conditions are, evidently, not necessary for the formation of solid silk. Figure 19 demonstrates this quite well, as it shows silk solidifying in a culture media (not a specialised duct), surrounded by water (not haemolymph), at a basic pH (not an acidic one), without any shear forces

being applied to it. Whilst the silk has certainly solidified, it is in no way in a fibrous conformation. Having said that, under similar conditions when shear forces are applied to the solidifying silk through the medium of a retracting front of silk dope (Figure 20) a thread with a regular repeating structure is formed. The thread that is formed in Figure 20 shows a visually similar pattern of birefringence as seen in native spun silk, as shown in Figure 17, as well as an ability to retract under its own elasticity. When discussed within the context of the pultrusion works performed on silkworms by (Sparkes and Holland, 2017), the discovery of chitin in the duct of spider silk gland by (Davies et al., 2013), the identification of the gaps surrounding the spider silk fibre within the duct of the gland by (Knight et al., 2000) and its conformation in Figure 14, it can start to be seen that the theory of pultrusion in spiders is likely true as well. The appearance of a birefringent fibre being formed as a non-birefringent liquid dope moves away from the fibre (Figure 20), may be the first visual proof of this hypothesis.

The comparison of native spun silk, to the solidified silks seen in Figure 17, Figure 18, Figure 19 and Figure 20 allows for the examination of an important question: How is the silk produced from the dissected glands different from that of native spun silk? Figure 17 shows closely the patterns of birefringence that can be seen within the native spun silk. The

colours shown are consistent along areas showing the same orientation. Changing this orientation changes the colour of the birefringence being shown. The fibres look distinct and uniform. When this is compared to the solid droplets of the silk shown in Figure 18 and Figure 19, the difference is clear. The disordered droplets of silk are capable of forming the regular repeating crystal structure necessary to produce birefringence, but these areas of structure are not ordered. The birefringence is made up of many colours and there are only very small areas of homology within the droplet. In short, whilst this silk has some similarities with native spun silk, it is demonstrably not the same. This, however, becomes less true when the silk dope is subjected to more of the mechanical forces that are usual in the formation of native spun silks. The pultrusion effect discussed in the previous chapter clearly has an ordering effect on the solidification of silk. The fibre formed in Figure 20 shows a uniform birefringence along the entire length, moreover this colour continues to appear as more of the fibre is deposited by the retreating edge of the liquid silk dope. When this silk is compared to the native spun silks it becomes clear that they are in fact very similar in structure but differ greatly in fibre diameter.

An important distinction to make with regards to the claim that neither a low pH nor sheer forces are required for the solidification of silk is this, they certainly help. When comparing the rate at which a falling

spider can produce and utilise large quantities of silk to, for example, arrest a fall, with the rate of solidification shown in Figure 19 and Figure 20 (9 hours and 50 minutes respectively) the difference is dramatic. When comparing the instantaneous solidification in native spun silk to the 9 hours it takes to solidify in culture and with the 50 minutes it takes to solidify in a relatively low moisture environment, we begin to see a pattern forming with regards to the mechanisms which underpin the solidification of silk. A key additional point to include when comparing the solidification of native silk fibres and dissected silk dopes is the removal of the glands duct in the latter. When native silk is produced a pultrusional force is applied from the spinneret, this force is applied directly to the solidified silk fibre as it is pulled through the duct of the gland (Vollrath et al., 2013). When the silk is solidifying in culture it is doing so in the absence of this pultrusional force and in the absence of the duct and the specialised structures within that aid in the dehydration of the silks and aid in the application of the shear forces to the silk (Davies et al., 2013).

The solidified form of silk is the energetically favourable state for the protein to be in. Were this not the case then silk would not independently solidify. Secondly, the energetic difference between these two states of relative disorder is small. Were the solidified state significantly more energetically favourable than the liquid state, then the

reaction shown in Figure 19 would have been significantly quicker, not only to begin, but to complete once begun. From the silk being initially expelled from the gland to the first noticeable beginnings of solidification took 4 hours of the silk being entirely undisturbed. From the start to finish the solidification takes over 9 hours, and spreads from a single point. This implies the need for a nucleation point onto which the rest of the proteins can bind and begin to polymerise. Were this not the case we would likely have seen the reaction begin over multiple points or occur to the entire droplet at once.

When comparing the rate of solidification in Figure 19 to that of Figure 20 we can see an almost 10 times quicker solidification. This is likely due to several factors. Firstly volume, the volume of silk dope polymerising and solidifying in Figure 19 is significantly larger than that shown in Figure 20. This will clearly affect the rate of reaction, as less protein would obviously take less time to solidify. The second factor at play is the environment in which the solidification is taking place. Figure 19 shows silk solidifying in culture media surrounded by water, whereas Figure 20 shows the silk solidifying in air. This leads to the third obvious difference, that of the application of some form of pultrusion force being applied to the silk as it is being solidified. This is exemplified, not only in the way in which the front of liquid dope “pulls” the newly formed fibre,

but also in the way that once this force is absent the fibre retracts under its own elasticity. This can lead to several assumptions. Firstly, the ability for the silk to dehydrate is vital to its speed of formation. Secondly a pultrusion force being applied to the fibre, not only allows the fibre to form more readily, but also allows the repeating structure of silk to be more easily formed. When considered with the data from Figure 19, it would seem that a pultrusion force coupled with a nucleation point onto which the proteins can bind and become ordered, is vital to the formation of silk threads.

When taking these factors into account with the findings shown in Figure 13 (Andersson et al., 2014) and taking a further look at not only the structure of the duct (Figure 16) but also the length and turns found in the whole duct (Figure 16) it seems more than likely that the low pH exhibited along the duct functions primarily to create a high osmotic pressure to draw moisture from the fibre formation whilst allowing the energetically favourable repeating nature of the silk fibre to drive formation.

Given the necessity of silk for all aspects of a spider's life cycle, egg casing, prey capture, habitat building, and prey wrapping, it is unsurprising that there exists a mechanism for the repair of silk glands. It

is worth stating that what has been observed in culture may not necessarily reflect what would occur within the whole organism. However, given the lack of other works on the same subject available the results shown in Figure 22 do provide the first glimpse into glandular repair in spiders. Given any damage to the carapace from attempted predation could damage these vital organs and given the free-floating nature of the glands in haemolymph, it is also unsurprising that this repair pathway functions in culture, given that the gland itself has no direct feedback mechanism to the larger organism. This is shown in Figure 21 and Figure 22. Figure 22 shows a view of the whole gland whilst repairing itself. This is interesting, as previously mentioned in Figure 15, as it shows the utilisation of the vesicles of silk found in the cells surrounding the lumen of the gland (Figure 15) but also because of the evidence of the movement within the full length of the gland. It should be restated that the gland is stationary in media. The plate containing the media is not moving or changing. Therefore, the movement of the gland can only be due to the changes happening within the gland. Another important distinction to make is that no musculature exists on the gland. This is interesting in the context of the movement of the gland because it implies that this movement likely occurs because of changes within the gland. There are several possible explanations for this movement. Firstly, considering the movement of vesicles from within cells into the lumen of the gland, this “emptying” of the cells would inherently cause the volume

of the cells to decrease, thus changing their shape relative to that of the neighbouring cells, and resulting in movement. The second possible explanation of this is that of cellular replication within the gland. If upon encountering damage the gland seeks to repair this damage with new cells, these would have to be reproduced from somewhere. This increase in cell copy numbers would also result in movement. The third possible explanation for the movement would be the physical movement of new cells to the site of damage to plug the site of damage. The most likely explanation, however, would be that of a combination of all three. We can see from Figure 21 that whilst repairing damage, the hole at the damage site is closed against the force of silk attempting to escape. This implies that cells ae either being recruited to the site of damage or are being replicated at the damage site, to close the damage site. Given the nature of the changing topography of the lumen shown in Figure 22, it is likely that vesicular transport is also occurring.

Conclusions

In conclusion, the spider's dependence on silk and an ability to produce and store the silk has led to the evolution of a highly specialised organ capable of producing vast quantities of liquid silk, also capable of preventing this dope from solidifying within the gland. This independently functioning organ capable of self-repair still holds many secrets yet to be elucidated.

Appendix Link 6 (not linked to a figure, for interest only) Major Ampullate gland from a Larinioides sclopetarius repairing intentional damage in culture. video made using Fiji, made up of 9944 images taken 1 minute apart.

Hyperlink: https://youtu.be/8_5NgJkymTA

Chapter 3 The formation of a novel spider silk ionic liquid biomaterial and it's use in understanding the formation and solidification of spider silk

Introduction

To address the third aim of "to investigate what could be done with dissected silk glands" the primary focus of the chapter will be the development of a novel methodology to dissolve full length, solidified spidroin proteins from a solid, native spun fibre into an ionic liquid solvent creating a novel biomaterial, coupled with a novel methodology for then re-solidifying the silk proteins from solution into a solid protein once again. This will be done allowing for a cell-free view of the process of silk solidification that takes place within the gland. The work will be further augmented by the addition of tests carried out on native full length silk protein dope, prior to being solidified within the gland. Until now it has not been possible to collect this material. However, thanks to the methods set out in chapter one these material tests will shed new light on the processes believed to be integral to the solidification of spider silk. It is

hoped that these insights into the production of spider silk, full-length, native form, could inform attempts to produce silk synthetically.

When the genes that make up spider silk proteins have been studied, it has been found that the amino acid structure varies greatly between species, however the N and C terminals of these disparate genes are highly conserved, even among species that diverged 240 million years ago (Strickland et al., 2018). Interestingly, whilst variation between species was shown between the amino acid sequences, a discernible pattern of regular repeating regions within the proteins was also found (Ayoub et al., 2007) This genetic homology between the structure of the genes themselves and the specific structure of the C terminal regions suggests that these structures are important for the function of the molecule. This is shown to be the case when solid fibres are studied using X-ray crystallography and NMR, showing that the regular repeating regions within the gene correspond to areas of high strength β crystalline regions and smaller less regular “molecular spring-like" areas (Bram et al., 1997, Jenkins et al., 2010, Strickland et al., 2018)

The exact nature of the transition from disordered silk dope into a regularly ordered fibre is not as well understood. The generally accepted hypothesis is that as the gel-like silk dope enters the duct it begins to be

acted upon by shear forces, whilst being passed through increasingly acidic regions of the gland, before finally reaching the spinneret as a solid fibre that the spider can pull out and utilise (Vollrath and Knight, 2001). Interestingly an *in-silico* study from Giesa et al (2016) found, using 3D molecular modelling, that shear forces of 300-700MPa were required to produce a silk-like fibre and that the shear forces were vital to the alignment of the β-helix regions of the silk fibre. The particularly interesting part of this is that β-pleated sheet regions of proteins gain their high tensile strength from the formation of large numbers of hydrogen bonds between the strands of the protein. Another interesting advancement to this theory was a study into why silk does not solidify whilst being stored in the lumen. Eisoldt et al. (2010) found that the concentration of aqueous salt ions in the lumen played a significant role in stopping the protein from solidifying in the gland. The study also showed that when transitioning from the lumen into the duct and whilst passing through the duct, the aqueous Na^+ ions are displaced and forced out by an influx of K^+ ions promoting the solidification of the fibre (Eisoldt et al., 2010). This is also supported by the molecular analysis of the C-terminal domain that showed that two of the only polar amino acids within the domain form a salt bridge between arms of the protein. When this salt bridge is interrupted electrostatically, fibre formation is promoted. Whilst these studies are invaluable to attempting to understand the precise nature of what occurs within the gland, they were unable to use direct

examination techniques as they did not have access to the initial starting materials, namely the full-length natively produced liquid silk dope. Given the exact nature of the solidification of silk is yet to be understood, it is unsurprising that the dissolution of silk is also yet to be understood.

The desire to understand the formation of silk comes from a need to understand exactly how silk's material properties come about. The hypothesis being, if one can replicate the spinning process with artificial fibres, one might be able to make an artificial silk substitute. Two of spider silk's properties are its biocompatibility and the antimicrobial nature of some silks. The antimicrobial nature of silks has been at least partially known about for hundreds of years, with the 13th century Welsh herbalists, the physicians of Myddfai, describing silk's benefit as "styptic for cuts" (Williams, 1928). Historically, spider silk has been used for wound bindings and coverings to stave-off infection (Holland et al., 2019). Whilst it can be assumed the ancient peoples utilising these methodologies did not understand the biochemical underpinnings of their methods, their prevalence is worth noting. There have been several studies into the prevalence and ability of spider silks to have bactericidal and fungicidal properties. Most seem to agree that sheet weaving species such as house spiders and wolf spiders show the most antimicrobial properties. The antimicrobial nature appears to be primarily through the

inability of bacteria to bind to the silk, and therefore not being able to form colonies (Phartale et al., 2019, Wright and Goodacre, 2012).

Biocompatibility in the context of spider silk refers to the ability of silk to produce a specific biological function without causing off-target effects or inflammation (Widhe et al., 2012). Using this working definition, several studies have found spider silk to be an incredibly useful and biocompatible material for medical uses. Silk has been used as a material for stabilising injured bladders (Steins et al., 2015) or as a binding scaffold to facilitate the healing of severed nerve endings (Allmeling et al., 2008). There have been many studies that have shown silk's efficacy as a biomaterial both in facilitating the growth of host cells and in its ability not to cause inflammation of the tissues that it is in close proximity to (Holland et al., 2019). The success of spider silk as a biomaterial is likely due to the molecules' "low visibility." Silk is made up of approximately 60% small nonpolar amino acids with the fibre itself having a very low immunological profile. This is due to the majority small nonpolar amino acids. Silk is, therefore unlikely to promote an immune reaction as it is highly unlikely ever to be identified as foreign by the immune system (Ayoub et al., 2007).

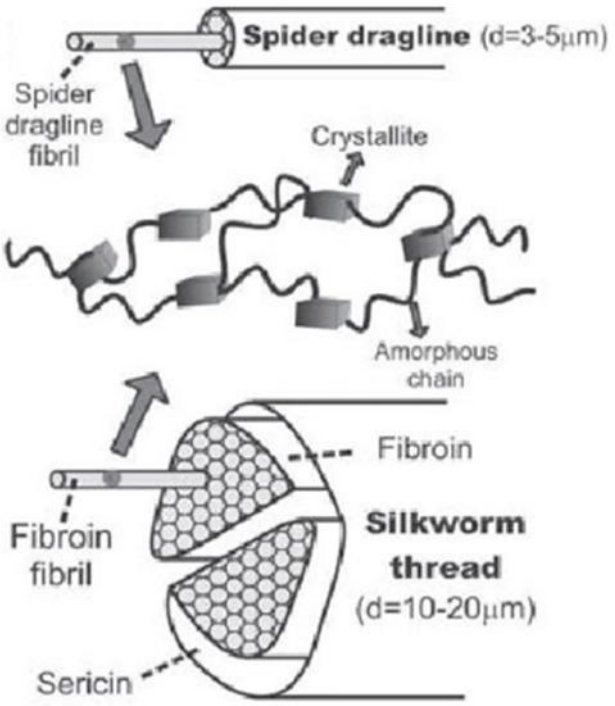

Figure 23 A structural comparison between spider silk fibres and the fibres produced by the silkworm Bombyx mori *taken from Liu & Zhang (2014).*

One of the commonly referred to analogues of spider silk is the silk gathered from the domesticated silkworm *Bombyx mori*. The silk harvested from silkworm cocoons has been being used in textile manufacturing for over 4000 years (Ude et al., 2014) and macroscopically bears a resemblance to spider silk, in that it is a naturally occurring protein fibre produced by a specialised gland in an arthropod. Figure 23 shows a comparison between the morphological structure of silkworm silk and spider silk. Both fibres are made up of smaller subunits. Spider silk

has repeating, flexible, amorphous regions interspersed with crystalline regions. Silkworm silk is made up of two larger, crystalline, fibroin regions surrounded by an amorphous, flexible, sericin layer to confer flexibility to the fibre (Liu and Zhang, 2014). When discussing the mechanical properties of *Bombyx* silk versus that of spider silk we see comparable properties. Both have a density of $1.3KgM^{-3}$, both are extensible, elastic, and strong, although spider silk is the higher performing fibre, being roughly twice as strong and elastic, and capable of extending one third more (Craven et al., 2000, Pérez-Rigueiro et al., 2000). One of the major reasons that *Bombyx* silk is so widely researched is the ease of its farming. Many individual silkworms can be monitored and farmed side by side, producing high silk yields per unit area, a boast that cannot be made by spider silk. The cannibalistic nature of spiders makes their farming unsuccessful. Many silk researchers have opted to work on the abundant, if slightly less mechanically remarkable, *Bombyx* silk, rather than focus on the more mechanically remarkable, but more difficult to obtain, spider silk (Koeppel and Holland, 2017). The structural similarities between *Bombyx* silk and spider silks, as protein fibres made up of strong crystalline regions and amorphous flexible regions, makes silkworm silk a valid control material when studying spider silk, as well as being an interesting subject matter in and of itself.

One of the benefits of comparing the two silks is the ability to compare their respective literature. For example, a study undertaken in 2004 concerning the dissolution and regeneration of *Bombyx mori* silks using ionic liquids (Phillips et al., 2004a) found that with extensive preparation, silkworm silks could be dissolved in ionic liquids. This finding was interesting as many of the previous methods for the dissolution of silkworm silk resulted in problems. One method, for example, required high concentrations of aqueous lithium salts or calcium chloride, resulting in a solution that would only remain shelf-stable for periods of up to a week (Yamada et al., 2001). Another method relied on the degumming, freeze drying, enzymatic cleavage, dialysis and dissolution in 1,1,1,3,3,3-hexafluoro-2-propanol (HFIP) (Ha et al., 2006). In both of these examples broad methods had to be utilised to dissolve any of the silk proteins. The use of ionic liquids simplified this issue.

The term "Ionic Liquid" refers to a group of organic solvents. They are particularly interesting as they are, in fact, salts, whose large structure makes their melting point below 100°C (Wilkes, 2002). The first ionic liquids were discovered towards the end of the 19th century (Gabriel and Weiner, 1888) and have since become a vital part of modern chemistry (Wilkes, 2002).

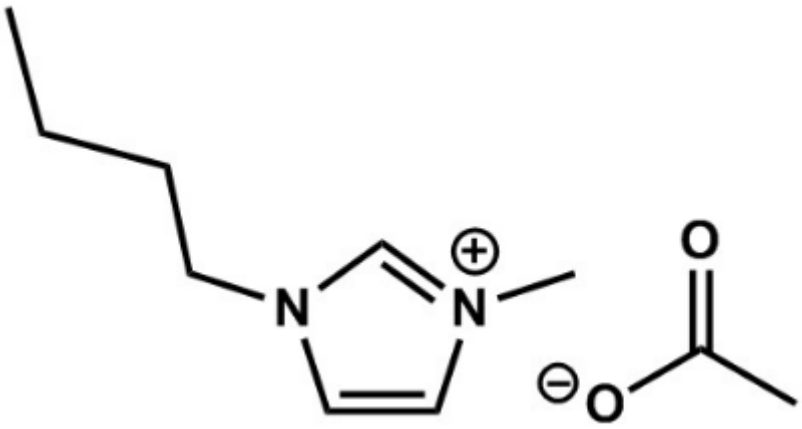

Figure 24 Chemical structure of the ionic liquid 1-Butyl-3-methylimidazolium acetate (BMIM-OAc)

Figure 24 shows the chemical structure of the ionic liquid BMIM-OAc. The Cation can be seen to have much larger structure when compared to a metal salt (NaCl for example) with the anion being a significantly smaller structure. The large and irregular shape of this salt prevents the formation of a regular ionic lattice structure, preventing the salt from forming a solid structure, therefore keeping it liquid at room temperature.

Liquid salt solvents are an exceptionally useful tool in that, unlike many other solvents, they do not evaporate. This means that once the solvent has been used it can be recovered, leading to them often being referred to as green solvents (Teixeira, 2012). It is worth mentioning,

however, that the toxicity of ionic liquids, combined with their often non-environmentally friendly manufacturing processes, has led many to avoid using the term (Swatloski et al., 2003). Their strength as solvents derives from their extremely polar nature. This highly polar nature allows ionic liquids to heavily disrupt hydrogen bonding without degrading the primary protein structure. This allows large, complex, water insoluble molecules to be solubilised (Teixeira, 2012). This large-scale disruption of hydrogen bonding was precisely what allowed for the success of the Mantz group in 2004 in their attempts to dissolve and regenerate *Bombyx* silks using ionic liquids (Phillips et al., 2004b). More interestingly, upon removal of the ionic liquid, the *Bombyx* silk was able to re-solidify, likely re-forming many hydrogen bonds in the process (Phillips et al., 2004a). Imidazolium based ionic liquids were chosen for this study due to their relative ease of accessibility and their well-established uses in the wider literature (Gonfa et al., 2011). The four specific ionic liquids that were studied in this chapter were 1-Butyl-3-methylimidazolium chloride (BMIM Cl), 1-Butyl-3-methylimidazolium acetate (BMIM OAc), 1-Ethyl-3-methylimidazolium acetate (EMIM OAc) and 1-Ethyl-3-methylimidazolium chloride (EMIM Cl). Given that the prior literature showed the success of ionic liquid dissolution of silkworm silk, these four ionic liquids were chosen to investigate if the size of the cation or anion of the ionic liquid had any effect of the success of the dissolution.

In this chapter, a novel method for the dissolution and precipitation of spider silk will be laid out. The further study, utilising both precipitated silks and solidified silk dope to shed light on the process of silk solidification, will also be presented. This further study was facilitated by allowing for a more controlled environment in which the specific aspects of silk solidification can be viewed without biological interference. The potential avenues for further study brought about by the investigations previously discussed in this thesis will also be laid out, Further works were planned to be carried out but were unfortunately abandoned due to the covid-19 pandemic Appendix 1 contains a description of the experiments designed, but that unfortunately could not be performed.

Methods

Dissolution of silk

Samples of silk were collected from the lab culture of a *Larinioides sclopetarius*, weighed and separated into samples of equal weight. Silk was shown to be resilient to dissolution in ethanol, methanol, concentrated sulphuric acid (1M), concentrated sodium hypochlorite (2M), dilute nitric acid (0.1M) and dilute sodium hypochlorite (0.1M) or sodium hypochlorite (2M) and hydrogen peroxide (5%). In each attempt samples were left overnight at room temperature. The only exception is the incubation with sulphuric acid, where this was repeated and the sample was held at 96°C overnight. The resilience to dissolution by submerging the silk, agitating, and incubating overnight at room temperature, before being neutralised and passed through a cellulose filter. The filters were then flooded with Coomassie blue protein stain and washed three times each with glacial acetic acid and methanol, until the filter had returned to its original colour. The filters were then observed under a dissecting microscope at X8 magnification. In all test large lengths of blue-stained silk were clearly visible on the filter, showing silk's resistance to dissolution. It is worth caveating, however, that it is unknown if this remaining section of silk was made up of both the outer and inner core of

the fibre, or if the outer core had dissolved away leaving only the inner core.

Silk samples were collected from spider pots taken from the lab spider culture, labelled as either spun web (SW likely made up of Major Ampullate, Minor Ampullate and Piriform silks (Vollrath, 1994) or egg Sac (ES made up of Tubiform and Acneiform silks (Vollrath, 1994) or collected from the field work site where the spiders were initially harvested (labelled as environmentally collected web, ECW, a combination of all collected webs and likely made up of all silk types). These samples were chosen to showcase the efficacy of the methodology across multiple silk types and with a large collection of different silk types ubiquitously. The multiple silk types of the ECW were particularly useful in the initial development of the methods as ECW was relatively easy to come by. This allowed for a plentiful and easily replenished stock for testing. Once a method had been shown to work on the ECW it could then be tested on the much smaller quantities of specific silks collected in the lab. These samples were compared with a positive control silk taken from *Bombyx mori (+Ve). Bombyx* silk functions well as a positive control because it was used as the subject of the seminal study into the dissolution of silks (Phillips et al., 2004b) and therefore, is known to both dissolve in ionic liquids and to re-solidify. A negative control of just ionic liquid (-Ve) was

also used. Both controls were treated in the same way as the test silk samples to show that any observed results come from the dissolved silk and not the solvent. Silk was cleaned by removing, with forceps, any obvious contaminant, uneaten flies, or spider malts. The samples were washed to remove as much of the non-web material as could be realistically achieved. The was started with 100% ethanol and detergent, until the wash solution reached a consistent clarity, finishing with three wash steps in sterile distilled water to remove any remaining detergent. Although this wash step removed large quantities of debris, small or particularly difficult to remove debris remained. Samples were then dried in a 36°C oven for one hour until a consistent weight had been reached. 100mg samples were then weighed and mixed with either 1-Butyl-3-methylimidazolium chloride (BMIM-Cl), 1-Butyl-3-methylimidazolium acetate (BMIM-OAc), or 1-Ethyl-3-methylimidazolium chloride (EMIM-Cl), or 1-Ethyl-3-methylimidazolium acetate (EMIM OAc) forming a 10% weight / volume solution. The acetate and chloride cations were chosen as they showed variable viscosity at room temperature. The resultant solution was then incubated overnight in a 60°C, in a 240-rpm shaking incubator, to dissolve. Following the heat aided dissolution, samples were centrifuged at 14000rpm for 15 minutes causing any remaining web contaminates and undissolved silk to pellet the bottom of the vessel which allowed for the clarified ionic liquid and silk solution to be removed to a separate clean vessel.

Precipitation of silk

Dissolved samples were precipitated by utilising the natural immiscibility of silk proteins in EtOH, combined with the affinity of ionic liquids to readily dilute in EtOH. This confluence of properties allows dissolved 100µl 10% W/V silk samples to be pipetted onto microscope slides, submerged in an excess of 100% EtOH and gently agitated for 1 hour before discarding the EtOH and repeating twice more. This serial dilution of the ionic liquid caused the silk proteins to precipitate out of solution onto the microscope slide. Precipitated silk was visualised using a polarised light microscope as previously described (chapter 2, methods, P100).

Spin-coating

Spin-coating is a material testing method that relies on loading a sample onto a small glass plate and spinning at high revolutions per minute to deposit a thin even layer of the substance onto the plate. Initially used in the late 1950's (Emslie et al., 1958), spin-coating provides an opportunity to study very thin layers of viscous solutions and has become a common tool in the world of material sciences (Cohen and Lightfoot, 2011). Spin-coating plates were first cut to an appropriate size

(2.5x2.5cm), then cut sample plates were placed into a sonicating water bath for 5 minutes. Sample plates were then dried using compressed N_2, before being washed in ethyl lactate, acetone, methanol, and isopropanol, with sonication and drying with N_2 being applied between each wash step. Sample plates were loaded into the spin-coater and held in place with suction. The plates were then loaded with 500µl of EtOH and spun as a final cleaning step. 200µl of dissolved silk was applied to the spin-coating plate before being spun at 4000 rpm for 30 seconds on max acceleration (0-4000rpm in 3 seconds). 500µl of EtOH was then applied and spun to remove any residual ionic liquid left on the plate, repeating if the silk sample on the spin-coating plate had not yet solidified. Samples were then viewed using polarised light microscopy as previously described in chapter two (chapter two, Methods, Polarised light microscopy p100). The same protocol was followed when spin-coating liquid dope with the exception that once the sample was loaded onto the spin-coating plate, no additional ethanol was applied.

Results

The following figures are taken from a series of experiments into attempts to dissolve spider silk and from attempts to solidify spider silk, either raw silk dope, or dissolved solid silks, from a liquid medium. The development of the methods included attempting seven unsuccessful methods before a successful one was found. Once a successful method was found it had a 100% success rate in both ionic liquids. The images chosen in the figures are taken from a pool of over 1300 images. The images chosen where selected as they best portray the experimental outcome being shown.

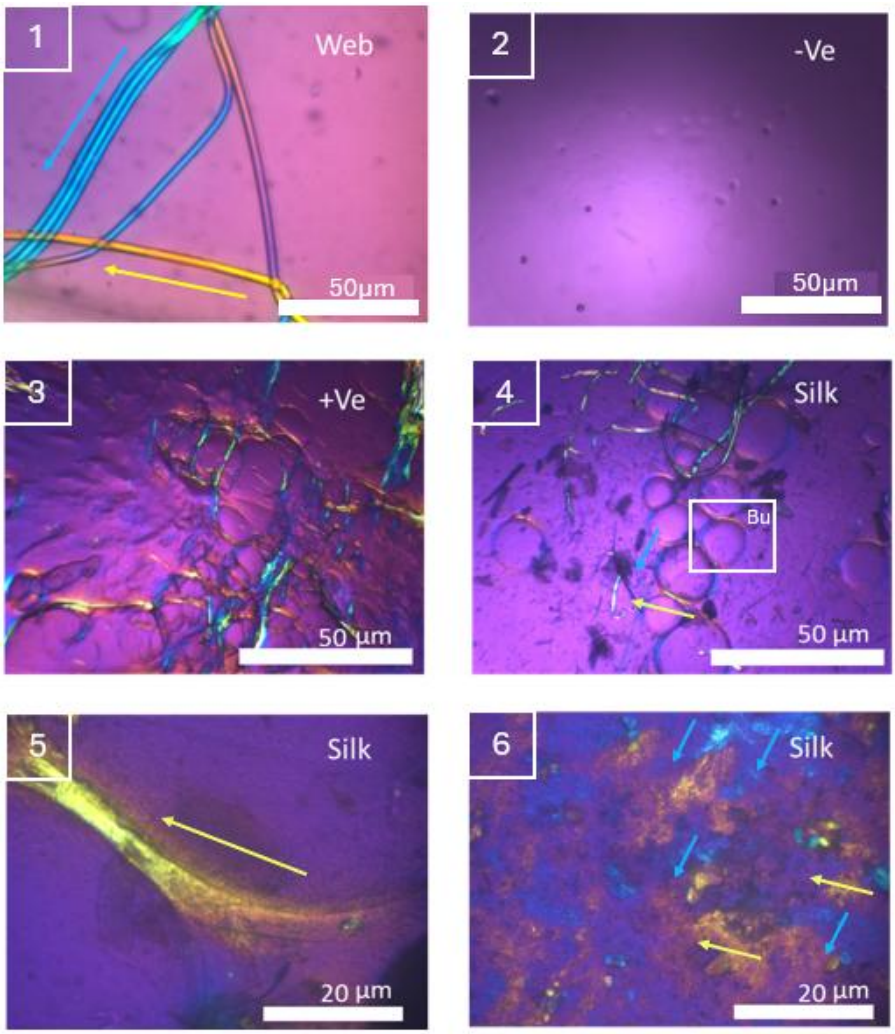

Figure 25 Birefringence comparison between native spun silk (Web)(1), ionic liquids only (-Ve)(2) dissolved and precipitated Bombyx mori *silk (+Ve)(3), dissolved (10% w/v silk in BMIB-Cl) and precipitated spider silk (Silk)(4-6) viewed through an Olympus CH Petrographic polarising light microscope using 10X and 40X lenses. Scale bars are found in the bottom right of each image, annotated with coloured arrows showing the orientation of the crystal structure. The box labelled Bu denotes a bubble formed during the solidification process.*

Figure 25 shows, using polarised light microscopy, a comparison between native spun silk (web), ionic liquids only (-Ve), *Bombyx mori* silk (+Ve) and dissolved and precipitated spider silk (Silk). All samples, except the native spun web, were dissolved in BMIM-Cl before being pipetted onto a glass slide. All samples were then washed in ethanol and dried until a constant weight had been achieved. Whilst being washed the silk and ionic liquid solution appeared to gain height and formed what looked like a three-dimensional, gel type structure, with what looked like bubbles forming in the solution. As successive washes were applied the height of this structure diminished until it appeared to be a very thin film on the slide. What is thought to be one of these bubbles is highlighted in image 4 with the label "Bu"

In Figure 25 the native spun web provides context for the native birefringence shown through polarised light microscopy (PLM). The coloured arrows on image 1 of Figure 25 show the birefringent colours of native spun spider silk in two different orientations. The negative control (-Ve), unaltered ionic liquid treated in the same way as the samples, shows that any birefringence seen in the other samples is due to the silk present within the ionic liquid. This control shows that the birefringence

seen is not a product of either the ionic liquid itself or the washing and drying process. As shown in the previous chapters, when in their liquid form, silks do not show birefringence due to their lack of a refined, repeating crystal structure. Therefore, the presence of birefringence in the *Bombyx* sample shows the efficacy of the methods. Image 4 of Figure 25 shows that the dissolution from solid spun fibres and subsequent precipitation onto the slide was successful, as it shows the same colours seen in image 1 and 3. Image 4 also shows a highlighted structure labelled "Bu" this is believed to be one of the bubble like structures that may have formed during the wash step of the re-solidification process.

The latter 3 images of Figure 25 show precipitated spider silk at varying magnifications. These images have been annotated with coloured arrows corresponding to the same colours seen in image 1.T, he colour of the birefringence corresponds to the orientation of the crystal structure as discussed in chapter two (chapter 2, Image 4 shows the precipitated silk showing the same patterns and colours of birefringence shown in the *Bombyx* silk in image 3 and in the native spun web in image 1. This image also shows the presence of a large amount of debris. This debris is small parts of invertebrates previously caught in the web prior to dissolving, and which could not be removed through washing or centrifugation. The bottom two images of the figure show higher

magnification view of the precipitated silk. Image 5 shows an area where the forces applied to the silk whilst drying have caused a pseudo fibre to have formed. This pseudo fibre shows a very high degree of birefringence. Image 6 shows a higher magnification view of what initially appeared to be a smooth section of precipitated web. Upon closer examination, the silk forms areas of homogeneity, with the silk proteins forming in similar directions to that of their neighbours, highlighted with arrows corresponding with the direction of organisation seen in the other images of the figure, with each of these areas of homogeneity seeming to blend into a more disordered array of proteins.

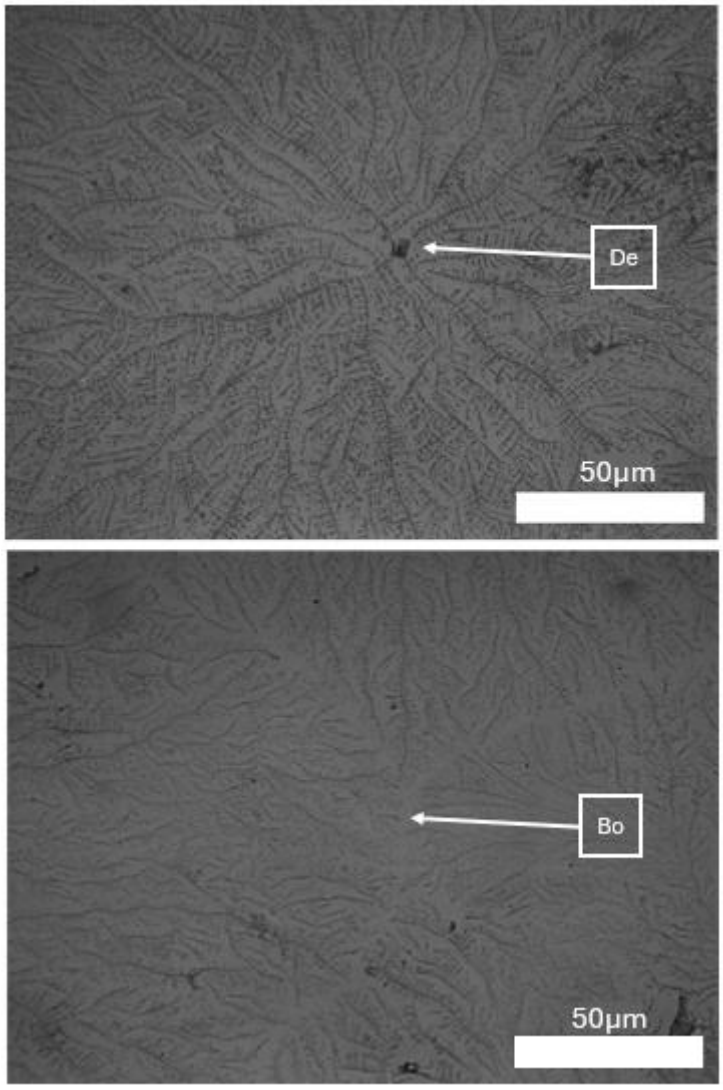

Figure 26 Spin-coating of native silk dope imaged using a light microscope. Samples spun at 4000rpm for 45 seconds, imaged using a Nikon Eclipse TS100 and viewing via a CMEX5 top mounted camera. "De" denotes debris found in the centre of the plate and "Bo" denotes the boundary between two phases

Figure 26 shows the results from performing spin-coating using native spider silk dope. Three individual glands were macerated on a

clean spin-coating plate before being allowed to sit for one minute. Samples were then spin-coated at 4000 rpm for 45 seconds until dry. The central points of the crystallisation structures are most likely damaged fragments of gland epithelium acting as nucleation points. An example of this is highlighted by the label De in Figure 26.

There have been attempts to form *Bombyx* or spider silk from regenerated or recombinant silks (Liu et al., 2019) and even a study using native liquid dope from *Bombyx mori* silk (Greving et al., 2012). Figure 26 represents the first attempts made to categorise the fibre formation from native liquid spider silk dope in laboratory conditions. It can be seen from the figure that the silk is crystalising in web-like patterns, spreading radially from a single point. This radial spread is made up of principal limbs which branch and go on to form multiple smaller limbs. Interestingly this can be seen happening multiple times across the spin-coating plate. The lower image of Figure 26 shows the point of confluence of three such crystallisation structures. It can be noted that whilst the spreading continues until all available space is occupied within the web-like structure, the limbs do not seem capable of joining end on end. This can be seen in the clear boundaries occurring between the crystallisation points.

Discussion

As previously stated, there are many problems with the immiscible nature of spider silk, which limits the ease of characterising the composition of these proteins. As listed in the failed attempts to dissolve silk methods, the resistance of silk to being solubilised by alcohols (ethanol, methanol, propanol) and the resistance of the core fibre to being broken down by strong acids (sulfuric and nitric acids) or strong bases (sodium hypochlorite, sodium hydroxide) or even the presence of oxygen radicals (sodium hypochlorite and hydrogen peroxide) make studying the biochemical makeup of the silk difficult. Whilst it has been shown to be possible to dissolve *Bombyx* silks in HFIP, the preceding processes inherently modify the fibre (Ha et al., 2006). One of the principle problems is its difficulty in being dissolved by the most frequently used solvents, which in turn limits the ability to utilise many forms of investigative techniques. This precludes any form of gel electrophoresis, any form of Western blotting and any of the various advanced chromatography techniques that have made modern proteomics such a diverse field. Whilst genomic tools have allowed the observation of the liquid protein in silico and the solid protein in material research, the lack of access to the litany of commonly used analytical techniques limits the work that can be undertaken on the liquid silks themselves. This

promoted the development of the methods to dissolve and precipitate silks using ionic liquids, as it allowed access to more investigative techniques that, in conjunction with polarised light microscopy, were not previously available. In addition, without these methods, the only avenue for study is the mechanical properties of spun silks, or the genetic makeup of the silk protein genes combined with observations of the gland itself. This difficulty of studying the folding behaviours of spun silks in real time has led to a potential blind spot in the research, as until now, it could not be shown for certain what specifically is happening within the gland and to the silk proteins themselves.

Figure 25 shows the first successful attempt to dissolve full-length spider silk proteins, as well as the first successful attempt to precipitate full-length spider silk proteins in a non-native conformation. This can be seen from the birefringence patterns shown in the native fibres being present in the final precipitated layer. As expected, these patterns can only be seen when polarised light is passing through a regular repeating structure. As previously stated in chapter two (chapter two, Discussion P141-142) the presence of any areas of consistent colour change in polarised light microscopy represents the presence of a minimum of hundreds of silk proteins all aligned with one another, a pattern that cannot be observed in the dissolved silk solution.

What is of particular interest is that, whilst under the same conditions, there can be a large variety of structures formed. Interestingly, whilst the ionic liquid and silk solution is submerged in ethanol, it was observed that a quasi-gel-like structure forms. Given that, when separate, the miscible solutions are 100% pure ethanol and 100% pure ionic liquid, when mixed, the forces of diffusion will tend towards a macroscopically even mixture of the two liquids. This means that in the solution of ionic liquid and spider silk, the ionic liquid will be washed away by the ethanol. Given this is happening in a three-dimensional structure, the forces of diffusion will not be occurring evenly across the whole structure, as the external surfaces will be more accessible to the ethanol wash. It could therefore be hypothesised that this might create a situation whereby silk no longer in solution will be surrounded by areas where the silk still is in solution. Given the dissolved silk is more mobile than the now solidified silk, this could create small holes in the 3D silk ionic-liquid-ethanol quasi-gel. These areas of differing properties might allow for the formation of a sponge-like structure and therefore, at distinct stages of the precipitation, the silk will be acted on by differing forces. If this were true these areas of differing forces would likely cause a birefringent pattern, such as the one observed in the latter three images of Figure 25.

The birefringent pattern can be seen in the bottom of images 3 and 4 of Figure 25, where the round, bubble-like structures show a higher degree of birefringence around their edges, where they were likely acted upon by more shear forces. The last two images of Figure 25 show this in more detail. The image on the left shows what appears to be a region where the presence of a directional force applied to the silk whilst "drying" has aligned the proteins into a small fibre-like area. This is highlighted in image 5 by an arrow of a corresponding colour. This arrow is similar in colour and orientation to one of the arrows also shown in image 1 of Figure 25. The similarity of the direction and colour between the two silks shows a regular repeating structure in the same orientation. However, in image 6 of Figure 25, not only will the proteins still solidify in the absence of a directional force, but when they do, they form small regions of homology, where the proteins will align with each other. This is highlighted by small arrows showing the areas of the sample with the same colours, and therefore the same orientation, as seen in image 1 of Figure 25.

Imidazolium based ionic liquids were chosen for this study due to their relative ease of accessibility and their well-established uses in the wider literature (Gonfa et al., 2011). The four specific ionic liquids that were chosen all showed similar results to those displayed in Figure 24. The

scope of the experiment was to determine the possibility of dissolving and precipitating spider silks, rather than to show the efficacy or advantages of a single ionic liquid type over another. The acetate cationic variants were chosen, to provide potential substrates for the electroporation of a silk ionic liquid solution, as electroporation of chloride cations would produce chlorine gas, which would be a health hazard. The success of the methodology is likely due to the highly polar nature of the ionic liquids themselves. This highly polar environment very effectively interrupts already formed hydrogen bonds and prevents them re-forming. Given that β-pleated sheets hydrogen-bonding to adjacent β-pleated sheet regions in separate proteins is what binds the silk fibre together and gives rise to the strength and resilience of the fibre, interrupting these bonds interrupts the structure of the whole fibre. This separation of the proteins from one another is what allows for the dissolution to occur. Given it is the highly polar nature of the ionic liquid that allows for dissolution of silk it should be possible to perform the same or similar methods using a wide variety of ionic liquids. Specifically, it has been shown that cellulose based hydrogels can be formed by dissolution in a solution of BMIM OAc and DMSO (Satani et al., 2020) as can spider silk. Imidazolium based ionic liquids in general and BMIM OAc specifically however are considered highly toxic to people and the environment (Leitch et al., 2020) meaning this specific protocol is not fit for medical investigation. There is however an avenue for future work in that cellulose has also been shown to

dissolve in tris(2-hydroxyethyl)methylammonium methylsulfate which is considered a minimally toxic ionic liquid, both to organisms and to the environment (Markiewicz et al., 2016). It is not guaranteed that because two molecules share a solvent in common, they will behave similarly in solvents shown to work on one of the two. It is, however, a worthwhile future study, as dissolution of silks in biocompatible ionic liquids would open the door for a potential use case within medical device manufacturing.

Figure 26 represents the first attempt to categorise the formation of silk from native spider silk dope. Whilst previous models have gained evidence using *in-silico* models based on genomic data, or physical observations made on spun silk fibres, or a combination of both, this experiment represents the first time native, full-length, spider silk proteins have been solidified due to *in-vitro* interventions. The rationale behind using a spin-coater was that it was the simplest method of introducing large shear forces into a several-microlitre quantity of silk dope in a uniform manner. Figure 26 shows what seems to be a nucleating agent in the centre of the web-like structures which supports the findings shown in Figure 25. Also shown in Figure 26, the radial limbs of these structures seem incapable of meeting and joining with another radial limb when travelling in opposite directions. This is shown in the

distinct gaps surrounding each web-like structure. When taken into account with the findings of the Buehler lab which states the shear forces required to form spider silk into fibres is 300-700MPa (Giesa et al., 2016), these findings are particularly interesting within this context of the direction of the forces applied to a plate. On any spinning surface the direction of the force applied is radially outwards from the centre of the plate, therefore the assumed results for this work would be that one would see a single web-like pattern radiating outwards from the central axis of movement. The fact that this is not the case is interesting. Consider a single point of nucleation as imaged in Figure 26, only one of the limbs of the crystallisation pattern can be in the direction of the radial force applied. Every other radial limb is either working slightly or totally against the plane of the force being applied. Furthermore, the observation that the radial limbs seem incapable of joining with another limb moving in the opposite direction, raises interesting questions about the polarisation of the protein fibres and their inability to form in non-native conformations. Elucidating the mechanisms causing this effect is an avenue for further study.

When we observe the solidification of silks shown in Figure 25 and Figure 26, it is important to consider the environments that have led to this solidification. According to the literature there must be a movement of

sodium ions as well as a strong acidification coupled with strong shear forces for a silk fibre to be formed. These assumptions have been made based on anatomical study of the silk glands, study of the haemolymph surrounding the glands and computer modelling of the proteins themselves. This is interesting, however, as at no point during the solidification of either the dissolved silks, or the solidification of the native spider dope, under spin-coating, was there either a strong acid or shear force (in the order of several hundred million Newtons per square meter) present. This therefore begs the question: if silk could form without these things present, then how vital are they? It has already been shown that silk, when left undisturbed externally to the gland, will preferentially solidify on a plate from a single point of nucleation as shown in Figure 19 and, whilst this formed neither fibres nor fibre-like structures, it does show the solidification in a heavily alkaline solution.

A recombinant simplified silk protein coupled with a soluble protein partner was able to self-assemble into fibres following proteolytic separation of the solubility partner (Stark et al., 2007). This example also shows the formation of solid fibres in the absence of shear forces or a low pH. When Yin et al. (2017) were able to successfully isolate the hydrophilic areas of spider silk fibroins, they found that these areas spontaneously arranged themselves into complex hierarchical structures

in aqueous conditions, completely in the absence of shear forces or extremes of pH (Yin et al., 2017).

Figure 25 and Figure 26 show the formation of both pseudo fibres and solid silk in the absence of both a low pH and considerable shear forces. An interesting potential explanation for these disparities is that the descending pH reportedly measured in the glands and their surrounding haemolymph, could be due to an excess of sodium ion hydrate structures interfering with the proper functioning of pH readers and not an excess of hydrogen ions. The positive nature of the sodium ion in aqueous solutions has a tendency to attract the lone electron pairs of the water molecules, leaving the positive dipole of the hydrogen atom exposed, and creating a weak electrostatic force that would create a falsely inflated number of positive dipoles on a small scale (Wang et al., 2019b).

PH meters imply the concentration of hydrogen ions in a solution (pH) by measuring the potential difference between two terminals. One terminal in the test solution and one in a small quantity of liquid of controlled a pH. The electrical difference between the two terminals is then used to calculate the pH. Rather than by calculating the actual concentration of hydrogen ions in the solution. This could cause erroneous readings when in the presence of a large quantity of sodium hydrate ions,

as it is possible that a sharp local increase in the concentration of sodium ions could create sufficient sodium hydrate ions to give a false reading on a pH meter. This would be supported by the fact that the β-pleated sheet regions of the silk protein, which are so vital to silk fibre structure, are held together by hydrogen bonds, which can be stopped from forming by the presence of an acidic pH. When taking all of this into consideration, a possible new hypothesis for the formation of a solid silk fibre can be postulated. Namely, that the principal driver of the formation of silk is a directional polymerisation brought on by nucleation. This nucleation driven polymerisation may require refinement. It is likely that this is where the importance of the shear forces in the duct of the gland comes in. The most efficient method of testing this would be by viewing a whole silk producing gland under an ultrasound microscope such as the one developed by Salvatore La Cavera in the University of Nottingham. Using this technique, which relies on the relative difference in the acoustic properties of different substances, it may be possible to determine exactly where within the gland a silk thread solidifies and furthermore, if the density of the newly solid fibre, then continues to solidify along the length of the duct.

Conclusions

In conclusion, the ability to study the liquid protein silk dope that is produced in the silk gland allows for an opportunity that has hitherto not been available. Whilst the material itself is by no means novel, the ability to isolate and study the highly concentrated native silk proteins is. This allows for the in-depth study of the specificity of silk solidification. As this chapter shows, it is possible that the previously assumed vital processes that occur within the silk gland of descending pH and shear forces, may not be as vital to the process of producing solid silk as previously assumed. Additionally, the ability to dissolve and re-precipitate native spun silk proteins allow for many different diagnostic tests to be performed. Specifically, the previous inability to utilise any solvent based analytical chemistry techniques need not be such an impediment. Now that silk can be formed both from, and without the actions of, a silk gland, comparative enthalpy change of formation calculations could be made to determine the precise level to which the actions within the gland improve the molecular strength of the protein, giving rise to potential insights for industrially produced biomaterials hoping to mimic the material properties of spider silk.

Aside from the benefits that can be gained in the academic study of silks, the ability to dissolve silks into a stable, highly polar solvent could open the door to industrial applications. For example, if a high current were to be passed over a thin layer of silk dissolved in ionic liquids, then it would be possible to separate the anion and cation of the ionic liquid thus removing the solvent and depositing the silk. With work this could quickly become a method for 3D printing with spider silk proteins. The ability to create a porous gel from spider silk impregnated with ethanol, could open the possibilities for modifying native full-length, silk proteins with additional materials, for use as medicinal hydrogels or films. Similarly, using this methodology, medical implants could be coated in biocompatible, antimicrobial, biodegradable coatings that promote cell adhesion whilst inhibiting bacterial growth.

Thesis Discussion and Conclusions

Discussion

The importance of silk to the life cycle of spiders cannot be overstated. From egg sac to prey capture, habitat building to courtship rituals (Ghislandi et al., 2017), without silk most spiders would not survive. The ability to study the glands that produce that silk as they function therefore, provides a valuable tool for the study of silks and spiders. The development of a methodology for the dissection and culturing of silk glands provides the first opportunity to study the silk glands whilst still functioning in an *ex-vivo* system. The glands, when situated normally within the spider, are free floating in a nutrient rich haemolymph. Whilst they are commonly surrounded by adipose tissue, they are neither controlled by, nor directly attached to, muscle or nerve cells. When viewed from the gland's perspective, there is little mechanical difference between functioning within the spider and continuing to function in culture. This not only allows for the study of the whole gland undergoing vital metabolic functions but has the distinct advantage over any form of immortalised cell line work, that the work did not require major structural changes to the genome before the cells could be studied.

The importance of silk to biomaterial research should not be overlooked. An antimicrobial, biocompatible fibre that is cryogenically and rotationally stable, roughly as strong as high-grade steel and capable of dissipating 70% of energy imparted to it as heat, could have many uses. Despite multiple attempts to produce spider silk on an industrial scale, the resultant proteins, whilst impressive, cannot boast all the material properties that native full length spider silk fibres can. The ability to study the gland and the liquid silk dope in a controlled environment could provide industrial insights that would make the industrial production of spider silk a reality.

The key findings from chapter one are that it is not only possible to dissect out intact glands from distinct species and keep them alive in culture, but that whilst in culture the gland behaves as it would when still situated within the spider. The processes of nutrition and excretion within the silk gland can now be studied in a controlled environment. This would open the door to future works, building a far deeper understanding of the specific cellular mechanisms that lead to the production of spider silk.

Chapter two serves to demonstrate the investigative techniques that can be applied to this system and the novel findings that can be obtained through the study of cultured glands. Firstly, the detailed view of

the distinct cellular specialisations that occur along the length of the gland, shows the vital nature of each part of the gland working in concert. Secondly, the ability to view the solidification of silk dope from outside the gland over time, provides the first look at an investigative novel material, allowing for more in-depth work into the precise nature of silk as it solidifies, both into an aggregate and into a fibre. Finally, the gland repair pathway. The discovery of a self-contained, autonomous repair pathway in an organ, vital to the survival of the organism, is both surprising and obviously necessary. Were a spider to sustain damage to their silk glands, then not only would there not be available silk where needed, but the constantly escaping and solidifying silk would probably cause the organism to die. In this respect, the existence of a repair mechanism is unsurprising. What is surprising is that this repair pathway is initiated, carried out and terminated entirely by the gland, without the assistance of external damage reporting molecules. The discovery of this repair pathway could not have been possible without the development of the dissection and culturing techniques presented and could pave the way to fascinating work on the cell-cell interactions and repair pathways in spiders. Not only this, but once the mechanisms underpinning the repair pathway are elucidated it could lead to the development of novel methodologies for large scale culturing of silk producing cells.

The third chapter focused on the development of a novel method for the dissolution of native spun, full length, silk proteins, as well as a complementary method for the precipitation of spider silk onto a substrate. The chapter also focuses on studying the solidification of spider silk from liquid silk dope, in a gland-free environment, for the first time. When viewed separately these results are both novel and interesting. The ability to dissolve and re-precipitate spider silk could open the door to multiple biomaterial applications, from 3D printing to medical implant coatings. Whilst the ability to perform investigative techniques on liquid silk dope provides an opportunity to further study and better understand the solidification of spider silk. When used in conjunction, however, these techniques provide an interesting opportunity to study the solidification of silk in the absence of factors deemed to be vital for its solidification. Factors such as shear forces and descending pH have long been thought to be fundamental to the formation of silk. The ability to remove or control for these factors could provide insights into the formation of spider silk. These insights could be vital to biomaterial researchers unlocking the full potential of synthetic or artificial silks. Chapter Three also details experiments designed to form the next phase of this research, specifically how to begin adapting this novel system for biomaterial research that could have industrial applications.

Thesis Conclusions

The three aims stated in the beginning of this thesis were:

1. To design an ex vivo tissue culture system that allows for the study of silk glands and their production of spider silk.

In investigating this aim it has been shown firstly that silk glands from multiple species can be dissected and cultured, providing a novel and widely applicable new investigative technique for the study of spider silk.

To investigate what could we learn from these dissected glands.

Through investigating this aim it has been shown that silk glands are capable of autonomous glandular repair, elucidating not only how internal damage could be fixed in spiders at large, but providing an avenue for future research.

To investigate what could be done with dissected silk glands.

In investigating this it has been shown that native spider silk can solidify, not only into aggregates, but also into fibres, in the absence of factors thought necessary for their formation. In addition, that spider silks can be dissolved and resolidified, opening up an interesting avenue for potential medical applications.

The work described in this thesis is not a finite avenue of investigation with a predefined outcome that is being targeted. The "research journey" embarked on is not one with a final or simple conclusion, instead it is one of discovery. This work could best be described as a good start. The chapters describe the discovery and development of a novel technique, and the attempts made to leverage this new technique into better understanding the fundamental aspects of spider silk. This work could well have industrial applications, or academic ones, ideally the works would be applied in both fields simultaneously. What can be said with certainty is that it is possible to culture spider silk glands. Those glands continue to produce native spider silk long after the original host has died and that the opportunity to study these glands provides an opportunity that has only just begun to be explored.

Appendix 1. The designed experimental works abandoned due to Covid 19

In this section, experiments that were designed but never able to be implemented will be laid out. Specifically, due to the pandemic and the corresponding inability to access lab spaces, many of the experiments that were planned and organised could not be attempted. This section should therefore be viewed as an extensive future work section. Whilst predictions made as to the results of these investigations are based in the context of experiments previously carried out and the wider literature, they should be used to demonstrate the intended outcomes and any speculation based on those results should be viewed as such.

Experimental Design

Cell Death Assay

To test the potential biocompatibility of precipitated silk, two tandem cell survival assays will be performed using prokaryotic pathogen analogues and eukaryotic human analogue cells. For each experiment: dissolved silk will be pipetted in each well of a 96-well plate, *Bombyx* silk will be pipetted in each well of a 96-well plate as a positive control, unaltered ionic liquid will be pipetted into each well of a 96-well plate as an experimental control and finally an untreated 96-well plate will all be washed repeatedly in ethanol and dried until a constant weight is achieved, as described above (chapter three, Methods, Disoloution of silk P162-164). To four of the eight prepared plates a controlled volume of *Escherichia coli* will be added, and to the other four a controlled volume of human analogue cell type will be added, most likely HeLa or CHO cells, depending on availability.

The spider silk coated wells are the test sample to show how both bacterial and human analogue cells behave when in contact with spider silk. This can then be used to test whether the biocompatibility shown in

native spun silks is also present in silks that have been dissolved and precipitated.

The *Bombyx* coated wells will act as a material control, as *Bombyx* silk can be dissolved using the same methods as spider silk but is not reported to show the same biocompatibility.

The ionic liquid plate will act as a methods control. By treating the plates in the same way as the test plates, as in washing in ethanol and drying until consistent weight is achieved, it can be shown that either there is no remaining ionic liquid present on the plates, or that the residual ionic liquid that may be present is not affecting the growth of the cells.

The empty plate will provide the baseline measurements against which the experimental plates can be compared. Using this empty plate to show how a normal growth curve would behave under the same treatments, allows for a strong comparison to native growth rates.

Plates will then be incubated in a plate reader to monitor the growth, for 12 hours, to allow the cell culture to reach a stable population. Optical density measurements will be analysed by calculating

an average increase or decrease in optical density for each time point, as well as a final measurement showing the total difference in optical density across the experiment. This will be analysed using the equation $\frac{(\Sigma(ODtime - OD\ initial))}{96}$ providing a good number of samples from which to take an average. Whilst these methods are crude they will function to show a strong initial indicator of the survivability of the materials,(Postgate, 1967). A positive result in this experimental work would indicate the worthwhile progression onto more in-depth study into the viability of this silk material as a medical implantable.

A secondary, more detailed study would be undertaken. This follow up study would be determined by the results of the previous work. As such the strict structure of the scheme of work cannot be determined. Having said this, the broad structure would likely lead from microscope-based, cell death assays as set out in the NIH Assay GMguidance manual (Riss et al., 2004). The aim of this program of research would be to begin to attempt to follow the guidance laid out in the International Standard for Biological Evaluation of medical devices — Part 5: Tests for *in-vitro* cytotoxicity. This would mark the first steps into "true" functionalisation, as it would indicate the actual viability of a spider silk based medical device.

Designing and producing a plasmid for the production of transgenic silks

To attempt to functionalise the gland's enormous protein making capabilities, a transgenic silk gland will be created. This will be done in three phases: Designing and producing the plasmid, transfecting the gland, and confirmatory PCRs.

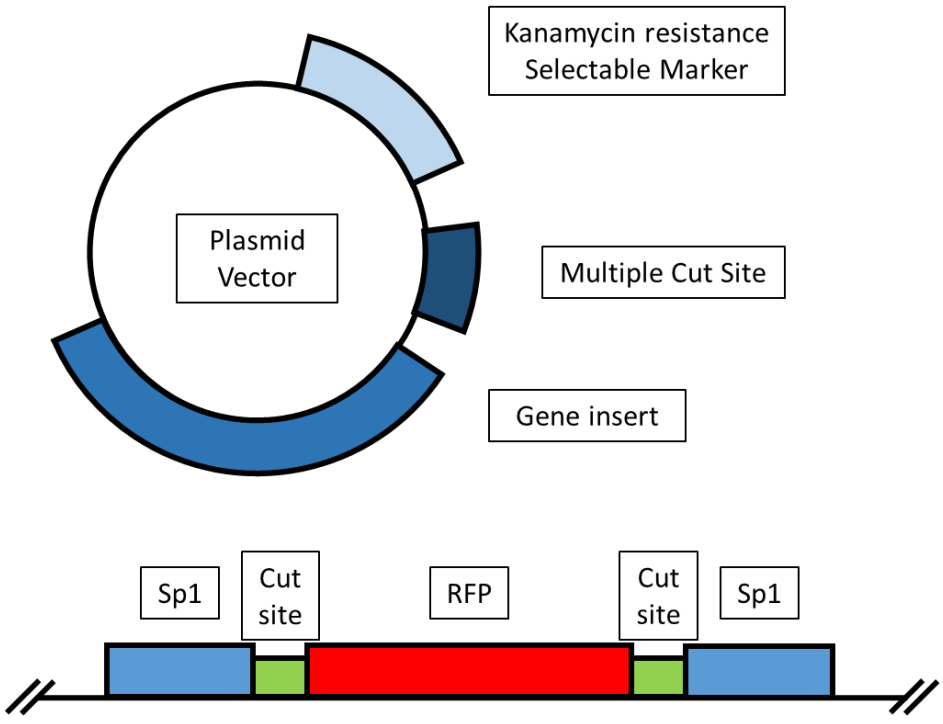

Figure 27 A diagrammatic representation of an idealised gene integration plasmid and corresponding gene insert. The key features are the 200bp flanking regions of MaSp1 gene, flanking the red fluorescent Protein (RFP) gene insert. This will be placed on a simple amplification plasmid with a selectable antibiotic resistance marker.

Using a model species with a known genome (*Nephila clavipes*), primers will be designed to PCR out 200bp sections of genomic MaSp1 gene, as shown in Figure 27. To be able to produce these gene fragments, first DNA extraction of whole glands must be performed to collect the necessary template DNA. Following this, the template DNA will be used in a PCR reaction to amplify specifically the 200bp gene fragment. This specific size of gene fragment will be selected for from any other potential gene fragments through gel electrophoresis purification.

Once the gene fragments have been produced and purified, they can then be ligated into an amplification plasmid so that they are flanking either side of an RFP gene. RFP was chosen to provide the clearest possible positive signal if successful, as silk glands show minor auto fluorescence in the green channel (Palmer, 1985a). Once the plasmid has been successfully ligated it can then be transfected into *Escherichia coli* and subsequently cultured in kanamycin containing media, to select for successfully transfected cells. To confirm successful transfection a miniprep followed by confirmatory PCR will be performed using primers designed to cover both the gene insert and the plasmid itself. Once successful amplification is shown, several litres of transfected *Escherichia coli* will be produced and allowed to grow before being collected and the plasmids removed and purified using a MaxiPrep kit and gel

electrophoresis purification. The plasmid stock will then be frozen to ensure continued stock availability.

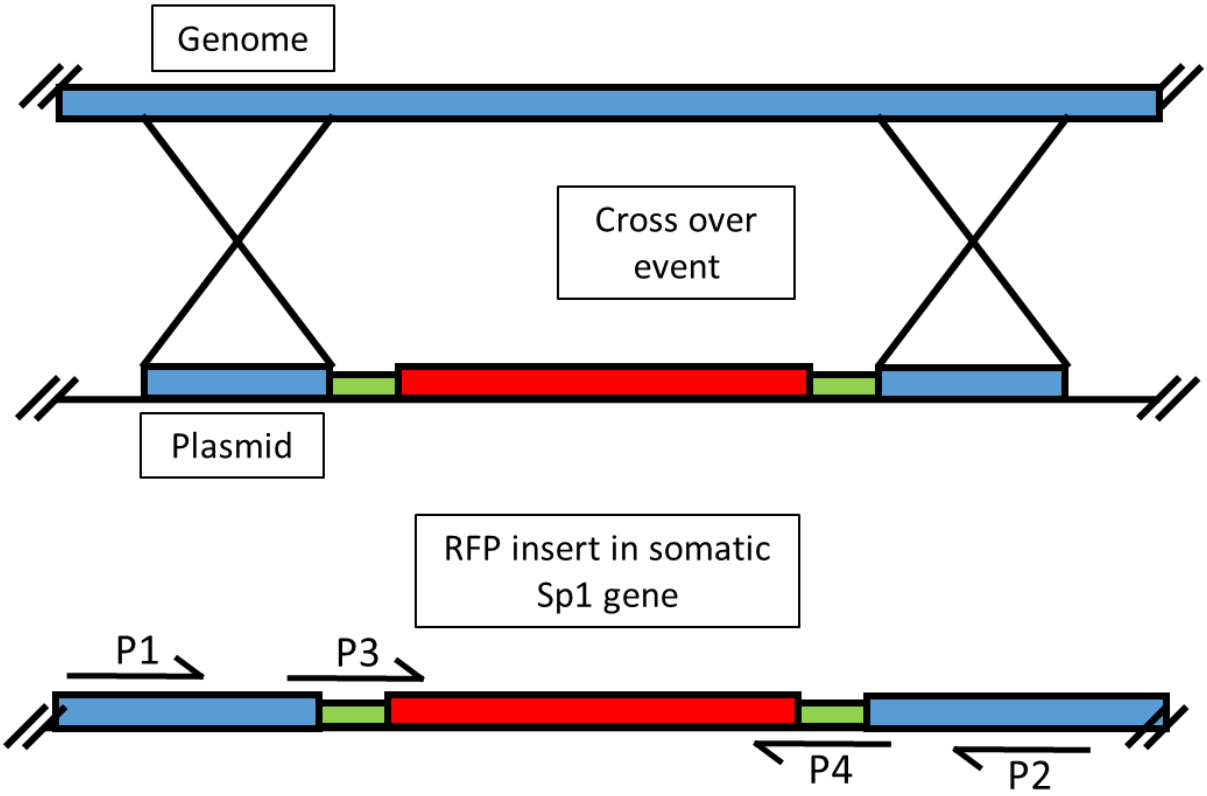

Figure 28 A diagrammatic representation of a double strand crossover event that could integrate the transgenic gene into the host genome.

A diagrammatic representation of the ideal double strand crossover event that could be utilised to incorporate the transgenic gene into the genome of the host organism (Figure 28). The lower part of Figure 28 shows a representation of the transgenic genomic gene with the confirmatory PCR primer sites highlighted. The confirmatory primers will function to demonstrate the successful integration of the plasmid into the genome. Confirmatory primers 1 and confirmatory primer 2 will cover an area of the genomic Sp1 gene is not present in the insert and an area of

the Sp1 gene present on the insert. These will show proper integration of the insert into the genome. Primers 3 and 4 will cover areas of the Sp1 insert and the RFP gene to show proper integration of the RFP insert. These primer pairs will function as follows P1&P2- will show the full Sp1 Gene is still present. P1&P4 will show successful integration at the start of the Sp1 gene. P2&P3 will show successful integration with the end of the Sp1 Gene. P3&P4 will show that the RFP insert is integrated and intact.

Through exploitation of the DNA repair mechanism that governs double strand breaks and non-homologous end joining, it should be possible to integrate the modified gene into the silk gland. This will rely heavily on the homologous regions of the gene insert being recognised as a "damaged gene" and then being subsequently re-incorporated into the genome. This process could be aided by intentionally damaging the gland to promote the repair pathway and its involved cell replication.

Plasmid DNA will then be digested to remove and linearise the specific target fragment. The gene insert will then be introduced to the gland in a minimal amount media using the lipofectamine gene delivery system. This will deliver the gene directly to the cells of the gland where either the gene will become incorporated into the genome of the gland through non-homologous end joining, or the gene insert will interact with

the protein manufacturing machinery of the cell directly and begin producing transgenic silks from there. To determine which of these outcomes has occurred, confirmatory PCRs will be performed.

Cell repair pathway

To elucidate the nature of the whole gland autonomous repair pathway a large-scale transcriptomic screen will be performed. This will be done using a model organism such as *Nephila clavipes* with a sequenced and annotated genome.

100 glands from culture will be damaged at incremental time points throughout the repair process, with each batch then being flash frozen in liquid nitrogen to preserve the RNA, before being processed and the RNA purified and stabilised. This RNA will then be sent off for RNA sequencing. This sequence will be used to create a transcriptomic clock detailing the genomic events underpinning the repair pathway.

Using this transcriptomic clock to determine the baseline housekeeping genes being consistently transcribed, it will then be possible to identify any genes that have been up or down regulated outside baseline housekeeping levels. Using this data in conjunction with

database searching to determine homologues in more highly studied systems, it should be possible to compile a list of genes most likely to be involved in the repair pathway. Then using rtPCR a more detailed and in-depth study can be undertaken to show precisely when and how each gene is active in the system.

Conditionally on the success of all previous steps, a final possible experiment would be undertaken. If a single or group of genes was found to be highly active at the start of the repair process then those genes would be integrated individually onto an expression plasmid to then be cultured, expressed, and purified. These selected repair markers could then be introduced to undamaged glands in an attempt to promote the repair pathway, with effects observed using microscopy.

Discussion of predicted results and future work

Once the process for the dissolution and precipitation of spider silk had been developed, it fortunately opened a door to further study of silks that had up until that point not been possible. Unfortunately, the global COVID 19 pandemic made further exploration of this work impossible. Due to this shift in ability to perform novel works, the predicted results about to be discussed will be hypothetical. Their hypothetical nature will hopefully be viewed as reasonable possibilities. It is also hoped that the hypothetical nature of the methods discussed will be viewed as achievable and logical steps towards determining the possible outcomes. It must however be stated directly that the works about to be discussed were not undertaken, but where the planned next steps and any hypothetical results discussed from this point onward will be clearly marked as such.

The ability to produce an even layer of silk proteins would allow for the study of the claims that silk is antimicrobial and biocompatible; that is that silk prevents bacteria from binding and multiplying but still allows for, or does not interfere with, the growth of human analogue cells. The next step would be to test the silk surface with human cells, specifically those of a periosteal cell line, in order to test the silk's compatibility with the cell type most likely to be encountered in skeletal implants

(Matsushima et al., 2011). If silk allows for the growth of periosteal cells, then there could be huge potential for promoting actual bio-incorporation of medical implants, whilst preventing the formation of biofilms that are so problematic in modern medicine.

The production of transgenic silk glands could have enormous potential benefits in the production of pharmaceutical proteins. It has been shown in previous chapters (chapter 2, Figure 16 P112-114) that the cells in a gland's tail are densely packed with protein-making machinery. Not only do glands produce an enormous quantity of protein in comparison to their size, but they also excrete the protein in an immiscible viscous liquid. Further, having the ability to tag or alter silk proteins *in-vivo* would open avenues for research into the real-time production of silk and reveal much about the inner workings of silk glands.

It is extremely difficult to predict with any accuracy what the results from the gland repair pathway screen would be. Firstly, the results would have to be compiled into a transcriptome before the gland could even begin to be examined. The process of actively mining the data for relevant up or down regulated genes could take anywhere from several weeks to several years. Furthermore, the process of creating and using a large-scale, genetic screen to determine which gene is responsible for the

cell division observed in the previous chapter (Chapter 2 Figure 22 P133-135), could also be very time consuming. With that said, the glandular repair pathway is wholly contained within the gland. The lack of external repair mediation pathways affecting the process would indicate a simple system where a stimulus leads to action. The stimulus could be the sudden loss of pressure within the gland, a chemotactic signal from the media/ haemolymph or a cell-cell-signalling pathway being interrupted. The simpler the system underpinning the repair pathway the easier it should be to elucidate. Once the genetic underpinnings of the repair pathway are better understood, it should be possible to utilise this pathway to stimulate the production of large numbers of silk gland cells, specifically adapted to produce large quantities of silk.

This methodology for producing large quantities of silk producing cells has a notable advantage over traditional methods for producing immortalised cell lines. It does not require large-scale genetic alteration. As previously mentioned, (P42-43), when producing an immortalised cell line, the aim is to induce a cancer-like state, where the somatic, differentiated cells regain the ability to divide and reproduce. Often this will involve subjecting the cell types to chemical or physical mutagens or specifically targeting and activating somatically silenced oncogenes. Regardless of the methodology, this process often results in truncated or

deleted genes, whole genome duplications and loss of function mutations, and often the first genes to suffer are the ones being actively transcribed at the time. Given that damaging the DNA repair pathways tends to lead to more gene mutations, doing this in a tissue whose sole responsibility is the production of vast quantities of a single protein, would likely be counterproductive.

The ultimate outcome from this research would have been the ability to combine all the previous work into an ability to produce large quantities of transgenic cells. If a large amount of silk producing cells could be altered to produce a transgenic protein containing a target pharmaceutical protein, then the protein could be delivered uncontaminated into pure water, where cleavage of the silk proteins would deliver pure, contaminant-free product which could be collected. This effectively reduces an often-costly purification process down to simply centrifuging out a solid mass of aggregated silk proteins. More promising still would be combining the production of transgenic silks with the ability to coat medical implants. It could be possible to produce an antimicrobial, biocompatible layer impregnated with growth factors, to promote cell adhesion or facilitate new cell growth or faster healing.

Thesis References

ABDULLAH, S. Z., BÉRUBÉ, P. R. & HORNE, D. J. 2014. SEM imaging of membranes: Importance of sample preparation and imaging parameters. *Journal of Membrane Science,* 463**,** 113-125.

AFFATATO, S., COLIC, K., HUT, I., MIRJANIĆ, D., PELEMIŠ, S. & MITROVIC, A. 2018. Short History of Biomaterials Used in Hip Arthroplasty and Their Modern Evolution. *In:* ZIVIC, F., AFFATATO, S., TRAJANOVIC, M., SCHNABELRAUCH, M., GRUJOVIC, N. & CHOY, K. L. (eds.) *Biomaterials in Clinical Practice : Advances in Clinical Research and Medical Devices.* Cham: Springer International Publishing.

ALLMELING, C., JOKUSZIES, A., REIMERS, K., KALL, S., CHOI, C. Y., BRANDES, G., KASPER, C., SCHEPER, T., GUGGENHEIM, M. & VOGT, P. M. 2008. Spider silk fibres in artificial nerve constructs promote peripheral nerve regeneration. *Cell Proliferation,* 41**,** 408-420.

ANDERSSON, M., CHEN, G., OTIKOVS, M., LANDREH, M., NORDLING, K., KRONQVIST, N., WESTERMARK, P., JÖRNVALL, H., KNIGHT, S., RIDDERSTRÅLE, Y., HOLM, L., MENG, Q., JAUDZEMS, K., CHESLER, M., JOHANSSON, J. & RISING, A. 2014. Carbonic Anhydrase Generates CO2 and H+ That Drive Spider Silk Formation Via Opposite Effects on the Terminal Domains. *PLoS Biology,* 12**,** e1001921.

APSTEIN, C. 1889. *Bau und Function der Spinndrüsen der Araneida*, Nicolaische Verlags-Buchhandlung.

ARNOTT, S., DOVER, S. D. & ELLIOTT, A. 1967. Structure of β-poly-l-alanine: Refined atomic co-ordinates for an anti-parallel beta-pleated sheet. *Journal of Molecular Biology,* 30**,** 201-208.

ARUNKARTHICK, S., ASOKAN, R., ARAVINTHARAJ, R., NIVEDITHA, M. & KUMAR, N. K. K. 2017. A Review of Insect Cell Culture: Establishment, Maintenance and Applications in Entomological Research. *Journal of Entomological Science,* 52**,** 261-273.

ASKARIEH, G., HEDHAMMAR, M., NORDLING, K., SAENZ, A., CASALS, C., RISING, A., JOHANSSON, J. & KNIGHT, S. D. 2010. Self-assembly of spider silk proteins is controlled by a pH-sensitive relay. *Nature,* 465**,** 236-238.

AYOUB, N. A., GARB, J. E., TINGHITELLA, R. M., COLLIN, M. A. & HAYASHI, C. Y. 2007. Blueprint for a High-Performance Biomaterial: Full-Length Spider Dragline Silk Genes. *PLoS ONE,* 2**,** e514.

BEE, L., OXFORD, G. & SMITH, H. 2017. *Britain's Spiders*

A Field Guide, Princeton University Press.

BELOZEROV, V. N. 2001. *Russian Journal of Developmental Biology,* 32**,** 129-142.

BENTON, J. R. 1907. Strength and elasticity of spider thread. *American Journal of Science,* s4-24**,** 75-78.

BLACKLEDGE, T. A., SUMMERS, A. P. & HAYASHI, C. Y. 2005. Gumfooted lines in black widow cobwebs and the mechanical properties of spider capture silk. *Zoology,* 108**,** 41-46.

BRAM, A., BRÄNDÉN, C. I., CRAIG, C., SNIGIREVA, I. & RIEKEL, C. 1997. X-ray diffraction from single fibres of spider silk. *Journal of Applied Crystallography,* 30**,** 390-392.

BRITISH-ARACHNOLOGICAL-SOCIETY, T. 2022. *Summary for Larinioides sclopetarius (Araneae)* [Online]. https://srs.britishspiders.org.uk/portal.php/p/Summary/s/Larinioides+sclopetarius: The British arachnological society [Accessed 05/02/2022 2022].

CAMBRIDGE, O. P. 1895. American Spiders and their Spinning Work; a Natural History of the Orb-weaving Spiders of the United States, with Special Regard to their Industry and Habits. *Nature,* 51**,** 505-507.

CARREL, A. 1910. CULTIVATION OF ADULT TISSUES AND ORGANS OUTSIDE OF THE BODY. *JAMA: The Journal of the American Medical Association,* 55**,** 1379.

CARREL, A. 1924. Tissue culture and cell physiology. *Physiological Reviews,* 4**,** 1-20.

CARTER, H. 1923. *The Tomb of Tutankhamun: Volume 2: The Burial Chamber,* London, Bloomsbury.

CHALLIS, R. J., GOODACRE, S. L. & HEWITT, G. M. 2006. Evolution of spider silks: conservation and diversification of the C-terminus. *Insect Molecular Biology,* 15**,** 45-56.

CHAW, R. C. & HAYASHI, C. Y. 2018. Dissection of silk glands in the Western black widow Latrodectus hesperus. *The Journal of Arachnology,* 46**,** 159-161, 3.

CHUNG, H., KIM, T. Y. & LEE, S. Y. 2012. Recent advances in production of recombinant spider silk proteins. *Current Opinion in Biotechnology,* 23**,** 957-964.

COHEN, E. & LIGHTFOOT, E. J. 2011. Coating Processes. *Kirk-Othmer Encyclopedia of Chemical Technology.*

COLLATZ, K. G. & MOMMSEN, T. 1974. Lebensweise und jahreszyklische Veränderungen des Stoffbestandes der SpinneTegenaria atrica C. L. Koch (Agelenidae). *J. comp. Physiol.,* 91.

COYLE, F. A., GREENSTONE, M. H., HULTSCH, A.-L. & MORGAN, C. E. 1985. Ballooning Mygalomorphs: Estimates of the Masses of Sphodros and Ummidia Ballooners (Araneae: Atypidae, Ctenizidae). *The Journal of Arachnology,* 13**,** 291-296.

CRAIG, C. L., RIEKEL, C., HERBERSTEIN, M. E., WEBER, R. S., KAPLAN, D. & PIERCE, N. E. 2000. Evidence for Diet Effects on the Composition of Silk Proteins Produced by Spiders. *Molecular Biology and Evolution,* 17**,** 1904-1913.

CRAVEN, J. P., CRIPPS, R. & VINEY, C. 2000. Evaluating the silk/epoxy interface by means of the Microbond Test. *Composites Part A: Applied Science and Manufacturing,* 31**,** 653-660.

CUMBERS, J. 2019. *New This Ski Season: A Jacket Brewed Like Spider's Silk* [Online]. Forbes. Available:

https://www.forbes.com/sites/johncumbers/2019/08/28/new-this-ski-season-a-jacket-brewed-from-spider-silk/?sh=71129bd9561e [Accessed 16/02 2021].

DAVIES, G. J. G., KNIGHT, D. P. & VOLLRATH, F. 2013. Chitin in the Silk Gland Ducts of the Spider Nephila edulis and the Silkworm Bombyx mori. *PLOS ONE,* 8**,** e73225.

DAY, M. F. & GRACE, T. D. C. 1959. Culture of Insect Tissues. *Annual Review of Entomology,* 4**,** 17-38.

DICKO, C., VOLLRATH, F. & KENNEY, J. M. 2004. Spider Silk Protein Refolding Is Controlled by Changing pH. *Biomacromolecules,* 5**,** 704-710.

DIMITROV, D. & HORMIGA, G. 2021. Spider Diversification Through Space and Time. *Annual Review of Entomology,* 66**,** 225-241.

EISOLDT, L., HARDY, J. G., HEIM, M. & SCHEIBEL, T. R. 2010. The role of salt and shear on the storage and assembly of spider silk proteins. *Journal of Structural Biology,* 170**,** 413-419.

ELIASSON LANTZ, A., GERNAEY, K. V., FRANZÉN, C. J. & OLSSON, L. 2010. 12 - Online monitoring of fermentation processes in lignocelluloses-to-bioalcohol production. *In:* WALDRON, K. (ed.) *Bioalcohol Production.* Woodhead Publishing.

EMILE, O., FLOCH, A. L. & VOLLRATH, F. 2007. Time-Resolved Torsional Relaxation of Spider Draglines by an Optical Technique. *Physical Review Letters,* 98.

EMSLIE, A. G., BONNER, F. T. & PECK, L. G. 1958. Flow of a Viscous Liquid on a Rotating Disk. *Journal of Applied Physics,* 29**,** 858-862.

EYDEN, B. 2002. Electron microscopy in the diagnosis of tumours. *Current Diagnostic Pathology,* 8**,** 216-224.

FAHNESTOCK, S. R. & IRWIN, S. L. 1997. Synthetic spider dragline silk proteins and their production in Escherichia coli. *Applied Microbiology and Biotechnology,* 47**,** 23-32.

1 FAHNESTOCK, S. R., YAO, Z. & BEDZYK, L. A. 2000. Microbial production of
2 spider silk proteins. *Reviews in Molecular Biotechnology,* 74**,** 105-119.

3 FOELIX, R. 2007. *Biology of spiders,* New York, Oxford University Press.

4 GABRIEL, S. & WEINER, J. 1888. Ueber einige Abkömmlinge des Propylamins.
5 *Berichte der deutschen chemischen Gesellschaft,* 21**,** 2669-2679.

6 GARRISON, N. L., RODRIGUEZ, J., AGNARSSON, I., CODDINGTON, J. A.,
7 GRISWOLD, C. E., HAMILTON, C. A., HEDIN, M., KOCOT, K. M., LEDFORD,
8 J. M. & BOND, J. E. 2016. Spider phylogenomics: untangling the Spider
9 Tree of Life. *PeerJ,* 4**,** e1719.

10 GHISLANDI, P. G., BEYER, M., VELADO, P. & TUNI, C. 2017. Silk wrapping of
11 nuptial gifts aids cheating behaviour in male spiders. *Behavioral Ecology,*
12 28**,** 744-749.

13 GIBSON, A. L. F., CARNEY, B. C., CUTTLE, L., ANDREWS, C. J.,
14 KOWALCZEWSKI, C. J., LIU, A., POWELL, H. M., STONE, R., II, SUPP, D.
15 M., SINGER, A. J., SHUPP, J. W., STALTER, L. & MOFFATT, L. T. 2020.
16 Coming to Consensus: What Defines Deep Partial Thickness Burn Injuries
17 in Porcine Models? *Journal of Burn Care & Research,* 42**,** 98-109.

18 GIESA, T., ARSLAN, M., PUGNO, N. & BUEHLER, M. 2011. Nanoconfinement of
19 spider silk fibrils begets superior strength, extensibility and toughness.
20 *Nature Precedings***,** 1-1.

21 GIESA, T., PERRY, C. C. & BUEHLER, M. J. 2016. Secondary Structure Transition
22 and Critical Stress for a Model of Spider Silk Assembly.
23 *Biomacromolecules,* 17**,** 427-436.

24 GLIŠOVIĆ, A., VEHOFF, T., DAVIES, R. J. & SALDITT, T. 2008. Strain Dependent
25 Structural Changes of Spider Dragline Silk. *Macromolecules,* 41**,** 390-398.

26 GONFA, G., BUSTAM, M., MAN, Z. & MUTALIB, M. A. 2011. Unique structure and
27 solute–solvent interaction in imidazolium based ionic liquids: a review.
28 *Asian Trans. Eng,* 1.

29 GOOGLE-BOOKS n.d. *"Biomaterial",* Google Books.

GOSLINE, J. M., DEMONT, M. E. & DENNY, M. W. 1986. The structure and properties of spider silk. *Endeavour,* 10**,** 37-43.

GOSLINE, J. M., DENNY, M. W. & DEMONT, M. E. 1984. Spider silk as rubber. *Nature,* 309**,** 551-552.

GRACE, T. D. C. 1969. Insect Tissue Culture and Its Use in Virus Research. *In:* SMITH, K. M. & LAUFFER, M. A. (eds.) *Advances in Virus Research.* Academic Press.

GREGER, R. 1985. Ion transport mechanisms in thick ascending limb of Henle's loop of mammalian nephron. *Physiological Reviews - American Journal of Physiology,* 65**,** 760-97.

GREVING, I., CAI, M., VOLLRATH, F. & SCHNIEPP, H. C. 2012. Shear-Induced Self-Assembly of Native Silk Proteins into Fibrils Studied by Atomic Force Microscopy. *Biomacromolecules,* 13**,** 676-682.

GUEHRS, K. H., SCHLOTT, B., GROSSE, F. & WEISSHART, K. 2008. Environmental conditions impinge on dragline silk protein composition. *Insect Molecular Biology,* 17**,** 553-564.

GUGUEN-GUILLOUZO, C. & GUILLOUZO, A. 2010. General Review on In Vitro Hepatocyte Models and Their Applications. *In:* MAUREL, P. (ed.) *Hepatocytes: Methods and Protocols.* Totowa, NJ: Humana Press.

HA, S.-W., ASAKURA, T. & KISHORE, R. 2006. Distinctive Influence of Two Hexafluoro Solvents on the Structural Stabilization of Bombyx mori Silk Fibroin Protein and Its Derived Peptides: 13C NMR and CD Studies. *Biomacromolecules,* 7**,** 18-23.

HARVEY, D., BARDELANG, P., GOODACRE, S. L., COCKAYNE, A. & THOMAS, N. R. 2017. Antibiotic Spider Silk: Site-Specific Functionalization of Recombinant Spider Silk Using "Click" Chemistry. *Advanced Materials,* 29**,** 1604245.

HEIM, M., RÖMER, L. & SCHEIBEL, T. 2010. Hierarchical structures made of proteins. The complex architecture of spider webs and their constituent silk proteins. *Chemical Society Reviews,* 39**,** 156-164.

HEIN, C. 2010. Shaping Tokyo: Land Development and Planning Practice in the Early Modern Japanese Metropolis. *Journal of Urban History,* 36**,** 447-484.

HERBERSTEIN, M. E. 2011. *Spider behaviour: flexibility and versatility*, Cambridge University Press.

HOLLAND, C., NUMATA, K., RNJAK-KOVACINA, J. & SEIB, F. P. 2019. The Biomedical Use of Silk: Past, Present, Future. *Advanced Healthcare Materials,* 8**,** 1800465.

HOLLAND, C., O'NEIL, K., VOLLRATH, F. & DICKO, C. 2012. Distinct structural and optical regimes in natural silk spinning. *Biopolymers,* 97**,** 368-373.

HORMIGA, G. 2002. Orsonwelles, a new genus of giant linyphiid spiders (Araneae) from the Hawaiian Islands. *Invertebrate Systematics,* 16**,** 369.

HOWAT, W. J. & WILSON, B. A. 2014. Tissue fixation and the effect of molecular fixatives on downstream staining procedures. *Methods,* 70**,** 12-19.

HUEMMERICH, D., SCHEIBEL, T., VOLLRATH, F., COHEN, S., GAT, U. & ITTAH, S. 2004. Novel Assembly Properties of Recombinant Spider Dragline Silk Proteins. *Current Biology,* 14**,** 2070-2074.

IBRAHIM, A., SOLIMAN, M., KOTB, S. & ALI, M. M. 2020. Evaluation of fish skin as a biological dressing for metacarpal wounds in donkeys. *BMC Veterinary Research,* 16.

IGELMUND, P. 1987. Morphology, sense organs, and regeneration of the forelegs (whips) of the whip spiderHeterophrynus elaphus (Arachnida, Amblypygi). *Journal of Morphology,* 193**,** 75-89.

JENKINS, J. E., CREAGER, M. S., BUTLER, E. B., LEWIS, R. V., YARGER, J. L. & HOLLAND, G. P. 2010. Solid-state NMR evidence for elastin-like β-turn structure in spider dragline silk. *Chemical Communications,* 46**,** 6714-6716.

KASTON, B. J. 1964. The Evolution of Spider Webs. *American Zoologist,* 4**,** 191-207.

KAUFMANN, A., MICKOLEIT, M., WEBER, M. & HUISKEN, J. 2012. Multilayer mounting enables long-term imaging of zebrafish development in a light sheet microscope. *Development,* 139**,** 3242-3247.

KNIGHT, D. & VOLLRATH, F. 1999. Hexagonal columnar liquid crystal in the cells secreting spider silk. *Tissue and Cell,* 31**,** 617-620.

KNIGHT, D. P., KNIGHT, M. M. & VOLLRATH, F. 2000. Beta transition and stress-induced phase separation in the spinning of spider dragline silk. *International Journal of Biological Macromolecules,* 27**,** 205-210.

KOEPPEL, A. & HOLLAND, C. 2017. Progress and Trends in Artificial Silk Spinning: A Systematic Review. *ACS Biomaterials Science & Engineering,* 3**,** 226-237.

KOVOOR, J. 1987. Comparative Structure and Histochemistry of Silk-Producing Organs in Arachnids. *In:* NENTWIG, W. (ed.) *Ecophysiology of Spiders.* Berlin, Heidelberg: Springer Berlin Heidelberg.

LAWLOR, K. T., VANSLAMBROUCK, J. M., HIGGINS, J. W., CHAMBON, A., BISHARD, K., ARNDT, D., ER, P. X., WILSON, S. B., HOWDEN, S. E., TAN, K. S., LI, F., HALE, L. J., SHEPHERD, B., PENTONEY, S., PRESNELL, S. C., CHEN, A. E. & LITTLE, M. H. 2021. Cellular extrusion bioprinting improves kidney organoid reproducibility and conformation. *Nature Materials,* 20**,** 260-271.

LAZARIS, A. 2002. Spider Silk Fibers Spun from Soluble Recombinant Silk Produced in Mammalian Cells. *Science,* 295**,** 472-476.

LEITCH, A. C., ABDELGHANY, T. M., PROBERT, P. M., DUNN, M. P., MEYER, S. K., PALMER, J. M., COOKE, M. P., BLAKE, L. I., MORSE, K., ROSENMAI, A. K., OSKARSSON, A., BATES, L., FIGUEIREDO, R. S., IBRAHIM, I., WILSON, C., ABDELKADER, N. F., JONES, D. E., BLAIN, P. G. & WRIGHT, M. C. 2020. The toxicity of the methylimidazolium ionic liquids, with a focus on M8OI and hepatic effects. *Food and Chemical Toxicology,* 136**,** 111069.

LEWIS, N. E., LIU, X., LI, Y., NAGARAJAN, H., YERGANIAN, G., O'BRIEN, E., BORDBAR, A., ROTH, A. M., ROSENBLOOM, J., BIAN, C., XIE, M., CHEN, W., LI, N., BAYCIN-HIZAL, D., LATIF, H., FORSTER, J., BETENBAUGH, M. J., FAMILI, I., XU, X., WANG, J. & PALSSON, B. O. 2013. Genomic landscapes of Chinese hamster ovary cell lines as revealed by the Cricetulus griseus draft genome. *Nature Biotechnology,* 31**,** 759-765.

LEWIS, R. V. 2006. Spider Silk: Ancient Ideas for New Biomaterials. *Chemical Reviews,* 106**,** 3762-3774.

LIU, X. & ZHANG, K.-Q. 2014. Silk Fiber — Molecular Formation Mechanism, Structure- Property Relationship and Advanced Applications. InTech.

LIU, Y., REN, J. & LING, S. 2019. Bioinspired and biomimetic silk spinning. *Composites Communications,* 13**,** 85-96.

LOEB, M. J. & SCHNEIDERMAN, H. A. 1956. Prolonged Survival of Insect Tissues in Vitro1. *Annals of the Entomological Society of America,* 49**,** 493-494.

LOYOLA-VARGAS, V. M. & OCHOA-ALEJO, N. 2024. An Introduction to Plant Cell, Tissue, and Organ Culture: Current Status and Perspectives. *In:* LOYOLA-VARGAS, V. & OCHOA-ALEJO, N. (eds.) *Plant Cell Culture Protocols.* New York, NY: Springer US.

MADSEN, B., SHAO, Z. Z. & VOLLRATH, F. 1999. Variability in the mechanical properties of spider silks on three levels: interspecific, intraspecific and intraindividual. *International Journal of Biological Macromolecules,* 24**,** 301-306.

MARKIEWICZ, M., MASZKOWSKA, J., NARDELLO-RATAJ, V. & STOLTE, S. 2016. Readily biodegradable and low-toxic biocompatible ionic liquids for cellulose processing. *RSC Advances,* 6**,** 87325-87331.

MASTERS, J. R. & STACEY, G. N. 2007. Changing medium and passaging cell lines. *Nat Protoc,* 2**,** 2276-84.

MATSUSHIMA, S., ISOGAI, N., JACQUET, R., LOWDER, E., TOKUI, T. & LANDIS, W. J. 2011. The Nature and Role of Periosteum in Bone and Cartilage Regeneration. *Cells Tissues Organs,* 194**,** 320-325.

MATWEB.COM. 2018. *Overview of materials for AISI 4000 Series Steel* [Online]. Available: http://www.matweb.com/search/datasheettext.aspx?matguid=210fcd12132049d0a3e0cabe7d091eef [Accessed 02/08/18].

MILLOT, J. 1926. Contribution à l'histophysiologie des aranéides. Paris.

MOON, M.-J., KIM, C.-S. & KIM, W.-K. 1988a. Ultrastructure of the ampullate gland in the orb web spider, Nephila clavata L. Koch I. Excretory duct of the large ampullate gland. *Applied Microscopy,* 18**,** 77-90.

MOON, M.-J., KIM, C.-S. & KIM, W.-K. 1988b. Ultrastructure of the ampullate gland in the orb web spider, Nephila clavata L. Koch II. Sac and tail portion of the large ampullate gland. *Applied Microscopy,* 18**,** 91-101.

MOON, M.-J. & KIM, W.-K. 1989. Ultrastructure of the ampullate glands in the orb web spider, Nephila clav ata L. Koch III. Excretory duct of the small ampullate gland. *Applied Microscopy,* 19**,** 49-58.

NYFFELER, M. & BIRKHOFER, K. 2017. An estimated 400–800 million tons of prey are annually killed by the global spider community. *The Science of Nature,* 104.

PALMER, J. M. 1985a. The silk and silk production system of the funnel-web mygalomorph spider Euagrus (Araneae, Dipluridae). *Journal of Morphology,* 186**,** 195-207.

PALMER, J. M. 1985b. The silk and silk production system of the funnel-web mygalomorph spiderEuagrus (Araneae, Dipluridae). *Journal of Morphology,* 186**,** 195-207.

PALMER, J. M., COYLE, F. A. & HARRISON, F. W. 1982. Structure and cytochemistry of the silk glands of the mygalomorph spider Antrodiaetus unicolor (Araneae, Antrodiaetidae). *Journal of Morphology,* 174**,** 269-274.

PAN, C., KUMAR, C., BOHL, S., KLINGMUELLER, U. & MANN, M. 2009. Comparative Proteomic Phenotyping of Cell Lines and Primary Cells to Assess Preservation of Cell Type-specific Functions. *Molecular & Cellular Proteomics,* 8**,** 443-450.

PÉREZ-RIGUEIRO, J., VINEY, C., LLORCA, J. & ELICES, M. 2000. Mechanical properties of single-brin silkworm silk. *Journal of Applied Polymer Science,* 75**,** 1270-1277.

PHARTALE, N. N., KADAM, T. A., BHOSALE, H. J., KARALE, M. A. & GARIMELLA, G. 2019. Exploring the antimicrobial potential of Pardosa brevivulva silk. *The Journal of Basic and Applied Zoology,* 80.

PHELAN, K. & MAY, K. M. 2015. Basic techniques in mammalian cell tissue culture. *Current Protocols in Cell Biology,* 66**,** 1.1. 1-1.1. 22.

PHILLIPS, D. M., DRUMMY, L. F., CONRADY, D. G., FOX, D. M., NAIK, R. R., STONE, M. O., TRULOVE, P. C., DE LONG, H. C. & MANTZ, R. A. 2004a. Dissolution and Regeneration of Bombyx mori Silk Fibroin Using Ionic Liquids. *Journal of the American Chemical Society,* 126**,** 14350-14351.

PHILLIPS, D. M., DRUMMY, L. F., CONRADY, D. G., FOX, D. M., NAIK, R. R., STONE, M. O., TRULOVE, P. C., DE LONG, H. C. & MANTZ, R. A. 2004b. Dissolution and regeneration of Bombyx mori silk fibroin using ionic liquids. *J Am Chem Soc,* 126**,** 14350-1.

PIZZI, G., LEWBART 2006. *Invertebrate Medicine*.

POSTGATE, J. R. 1967. Viability Measurements and the Survival of Microbes Under Minimum Stress. *In:* ROSE, A. H. & WILKINSON, J. F. (eds.) *Advances in Microbial Physiology.* Academic Press.

PRINCE, J. T., MCGRATH, K. P., DIGIROLAMO, C. M. & KAPLAN, D. L. 1995. Construction, Cloning, and Expression of Synthetic Genes Encoding Spider Dragline Silk. *Biochemistry,* 34**,** 10879-10885.

RAMÍREZ, M. J. & MICHALIK, P. 2019. The Spider Anatomy Ontology (SPD)—A Versatile Tool to Link Anatomy with Cross-Disciplinary Data. *Diversity,* 11**,** 202.

RATNER, B. D. & ZHANG, G. 2020. 1.1.2 - A History of Biomaterials. *In:* WAGNER, W. R., SAKIYAMA-ELBERT, S. E., ZHANG, G. & YASZEMSKI, M. J. (eds.) *Biomaterials Science (Fourth Edition).* Academic Press.

RISS, T. L., MORAVEC, R. A., NILES, A. L., DUELLMAN, S., BENINK, H. A., WORZELLA, T. J. & MINOR, L. 2004. Cell Viability Assays. *In:* MARKOSSIAN, S., GROSSMAN, A., BASKIR, H., ARKIN, M., AULD, D., AUSTIN, C., BAELL, J., BRIMACOMBE, K., CHUNG, T. D. Y., COUSSENS, N. P., DAHLIN, J. L., DEVANARAYAN, V., FOLEY, T. L., GLICKSMAN, M., GORSHKOV, K., GROTEGUT, S., HALL, M. D., HOARE, S., INGLESE, J., IVERSEN, P. W., LAL-NAG, M., LI, Z., MANRO, J. R., MCGEE, J., NORVIL, A., PEARSON, M., RISS, T., SARADJIAN, P., SITTAMPALAM, G. S., TARSELLI, M. A., TRASK, O. J., JR., WEIDNER, J. R., WILDEY, M. J., WILSON, K., XIA, M. & XU, X. (eds.) *Assay Guidance Manual.* Bethesda

(MD): Eli Lilly & Company and the National Center for Advancing Translational Sciences.

RÖMER, L. & SCHEIBEL, T. 2008. The elaborate structure of spider silk. *Prion,* 2**,** 154-161.

ROUWENHORST, R. J., FRANK JZN, J., SCHEFFERS, W. A. & VAN DIJKEN, J. P. 1991. Determination of protein concentration by total organic carbon analysis. *Journal of Biochemical and Biophysical Methods,* 22**,** 119-128.

RUTHERFORD, A. 2012. Synthetic biology and the rise of the 'spider-goats'. *The Observer , Genetics*.

SATANI, H., KUWATA, M. & SHIMIZU, A. 2020. Simple and environmentally friendly preparation of cellulose hydrogels using an ionic liquid. *Carbohydrate Research,* 494**,** 108054.

SCHARTAU, W. & LEIDESCHER, T. 1983. Composition of the hemolymph of the tarantulaEurypelma californicum. *Journal of comparative physiology,* 152**,** 73-77.

SEBASTIAN, P. 2009. *Spiders of india*, Universities Press.

SEYMOUR, R. S. & HETZ, S. K. 2011. The diving bell and the spider: the physical gill of Argyroneta aquatica. *Journal of Experimental Biology,* 214**,** 2175-2181.

SHEAR, W. A., PALMER, J. M., CODDINGTON, J. A. & BONAMO, P. M. 1989. A Devonian Spinneret: Early Evidence of Spiders and Silk Use. *Science,* 246**,** 479-481.

SPARKES, J. & HOLLAND, C. 2017. Analysis of the pressure requirements for silk spinning reveals a pultrusion dominated process. *Nature Communications,* 8**,** 594.

STARK, M., GRIP, S., RISING, A., HEDHAMMAR, M., ENGSTRÖM, W., HJÄLM, G. & JOHANSSON, J. 2007. Macroscopic Fibers Self-Assembled from Recombinant Miniature Spider Silk Proteins. *Biomacromolecules,* 8**,** 1695-1701.

STARRETT, J., GARB, J. E., KUELBS, A., AZUBUIKE, U. O. & HAYASHI, C. Y. 2012. Early Events in the Evolution of Spider Silk Genes. *PLOS ONE,* 7**,** e38084.

STEHLING, N., ABRAMS, K. J., HOLLAND, C. & RODENBURG, C. 2019. Revealing Spider Silk's 3D Nanostructure Through Low Temperature Plasma Etching and Advanced Low-Voltage SEM. *Frontiers in Materials,* 5.

STEINS, A., DIK, P., MÜLLER, W. H., VERVOORT, S. J., REIMERS, K., KUHBIER, J. W., VOGT, P. M., VAN APELDOORN, A. A., COFFER, P. J. & SCHEPERS, K. 2015. In Vitro Evaluation of Spider Silk Meshes as a Potential Biomaterial for Bladder Reconstruction. *PLOS ONE,* 10**,** e0145240.

STRICKLAND, M., TUDORICA, V., ŘEZÁČ, M., THOMAS, N. R. & GOODACRE, S. L. 2018. Conservation of a pH-sensitive structure in the C-terminal region of spider silk extends across the entire silk gene family. *Heredity,* 120**,** 574-580.

SWATLOSKI, R. P., HOLBREY, J. D. & ROGERS, R. D. 2003. Ionic liquids are not always green: hydrolysis of 1-butyl-3-methylimidazolium hexafluorophosphate. *Green Chemistry,* 5**,** 361-363.

TAHIR, H. M., ZAHRA, K., ZAHEER, A. & SAMIULLAH, K. 2017. Spider silk: An excellent biomaterial for medical science and industry. *Punjab University Journal of Zoology,* 32**,** 143-154.

TAKEDA, S. 2009. Chapter 232 - Sericulture. *In:* RESH, V. H. & CARDÉ, R. T. (eds.) *Encyclopedia of Insects (Second Edition).* San Diego: Academic Press.

TALBOT, H. F. 1834. XLIV. Experiments on light. *The London, Edinburgh, and Dublin Philosophical Magazine and Journal of Science,* 5**,** 321-334.

TANG, C. Y. & YANG, Z. 2017. Chapter 8 - Transmission Electron Microscopy (TEM). *In:* HILAL, N., ISMAIL, A. F., MATSUURA, T. & OATLEY-RADCLIFFE, D. (eds.) *Membrane Characterization.* Elsevier.

TEIXEIRA, R. E. 2012. Energy-efficient extraction of fuel and chemical feedstocks from algae. *Green Chemistry,* 14**,** 419-427.

TEO, A. J. T., MISHRA, A., PARK, I., KIM, Y.-J., PARK, W.-T. & YOON, Y.-J. 2016. Polymeric Biomaterials for Medical Implants and Devices. *ACS Biomaterials Science & Engineering,* 2**,** 454-472.

TERMEYER, R. D. 1866. Researches and Experiments Upon Silk from Spiders, and Upon Their Reproduction. *Essex Institute Proceedings, Salem, MA,* 5**,** 8.

TILLINGHAST, E. K. & TOWNLEY, M. A. 1993. Silk Glands of Araneid Spiders. *Silk Polymers.* American Chemical Society.

TILLINGHAST, E. K. & TOWNLEY, M. A. 1994. Silk glands of araneid spiders: selected morphological and physiological aspects. *ACS symposium series. American Chemical Society,* 544**,** 29-44.

TÓTH, F., ÁRPÁS, K., SZEKERES, D., KÁDÁR, F., SZENTKIRÁLYI, F., SZÉNÁSI, Á. & KISS, J. 2004. Spider web survey or whole plant visual sampling?Impact assessment of Bt corn on non-target predatory insects with two concurrent methods. *Environmental Biosafety Research,* 3**,** 225-231.

TOWNLEY, M. A., TILLINGHAST, E. K. & CHERIM, N. A. 1993. Moult-related changes in ampullate silk gland morphology and usage in the araneid spider Araneus cavaticus. *Philosophical Transactions of the Royal Society of London. Series B: Biological Sciences,* 340**,** 25-38.

TOWNSEND, V. R., SCHAUS, M. H., ZVONAREVA, T., ILLINIK, J. J. & EVANS, J. T. 2017. Leg injuries and wound repair among cosmetid harvestmen (Arachnida, Opiliones, Laniatores). *Journal of Morphology,* 278**,** 73-88.

TU, C., LU, H., ZHOU, T., ZHANG, W., DENG, L., CAO, W., YANG, Z., WANG, Z., WU, X., DING, J., XU, F. & GAO, C. 2022. Promoting the healing of infected diabetic wound by an anti-bacterial and nano-enzyme-containing hydrogel with inflammation-suppressing, ROS-scavenging, oxygen and nitric oxide-generating properties. *Biomaterials,* 286**,** 121597.

TURNBULL, A. 1973. Ecology of the true spiders (Araneomorphae). *Annual review of entomology,* 18**,** 305-348.

UDE, A. U., ESHKOOR, R. A., ZULKIFILI, R., ARIFFIN, A. K., DZURAIDAH, A. W. & AZHARI, C. H. 2014. Bombyx mori silk fibre and its composite: A review of contemporary developments. *Materials & Design,* 57**,** 298-305.

VAGO, C. 2012. *Invertebrate Tissue Culture*, Academic Press.

VANDYK, J. K. 2009. *Entomology 201- introduction to insects* [Online]. iowa state university sylabus: Department of entomology, Iowa state University. Available: https://web.archive.org/web/20090608172729/http://www.ent.iastate.edu/dept/courses/ent201/arthropoda/classarachnidasilk.html [Accessed 23/02/21 2021].

VERT, M., DOI, Y., HELLWICH, K.-H., HESS, M., HODGE, P., KUBISA, P., RINAUDO, M. & SCHUÉ, F. 2012. Terminology for biorelated polymers and applications (IUPAC Recommendations 2012). *Pure and Applied Chemistry,* 84**,** 377-410.

VINEY, C., KERKAM, K., GILLILAND, L., KAPLAN, D. & FOSSEY, S. 1991. Molecular Order in Silk Secretions. *MRS Proceedings,* 248**,** 89.

VOLLRATH, F. 1987. Altered geometry of webs in spiders with regenerated legs. *Nature,* 328**,** 247-248.

VOLLRATH, F. 1994. General properties of some spider silks. ACS Publications.

VOLLRATH, F. & KNIGHT, D. P. 2001. Liquid crystalline spinning of spider silk. *Nature,* 410**,** 541-548.

VOLLRATH, F., PORTER, D. & HOLLAND, C. 2013. The science of silks. *MRS Bulletin,* 38**,** 73-80.

WALKER, P. 2017. Spiders could theoretically eat every human on earth in a year and still be hungry. *The independant*, 6/12/17.

WANG, C., LIANG, C., WANG, R., YAO, X., GUO, P., YUAN, W., LIU, Y., SONG, Y., LI, Z. & XIE, X. 2019a. The fabrication of a highly efficient self-healing hydrogel from natural biopolymers loaded with exosomes for the synergistic promotion of severe wound healing. *Biomaterial Science* 8**,** 313-324.

WANG, P., SHI, R., SU, Y., TANG, L., HUANG, X. & ZHAO, J. 2019b. Hydrated Sodium Ion Clusters [Na+(H2O)n (n = 1–6)]: An ab initio Study on Structures and Non-covalent Interaction. *Frontiers in Chemistry,* 7.

WARBURTON, C. 1890. The spinning apparatus ofgeo-metric spiders. *Quarterly Journal of Microscop-ical Science,* New Series**,** 29–39.

WARD, I. M. 2012. *Structure and properties of oriented polymers*, Springer Science & Business Media.

WIDHE, M., JOHANSSON, J., HEDHAMMAR, M. & RISING, A. 2012. Current progress and limitations of spider silk for biomedical applications. *Biopolymers,* 97**,** 468-478.

WILDER, B. G. 1865. *On the Nephila plumipes: Or silk spider of South Carolina*, Proceedings of the Boston Society of Natural History

WILKES, J. S. 2002. A short history of ionic liquids—from molten salts to neoteric solvents. *Green Chemistry,* 4**,** 73-80.

WILLIAMS, E. R. 1928. Welsh Physicians And The Renaissance. *The British Medical Journal,* 2**,** 1133-1135.

WINKLER, S. & KAPLAN, D. L. 2000. Molecular biology of spider silk. *Reviews in Molecular Biotechnology,* 74**,** 85-93.

WOLFF, J. O. 2021. Evolutionary kinematics of spinneret movements for rapid silk thread anchorage in spiders. *Journal of Comparative Physiology A,* 207**,** 141-152.

WORK, R. W. 1977. Dimensions, Birefringences, and Force-Elongation Behavior of Major and Minor Ampullate Silk Fibers from Orb-Web-Spinning Spiders—The Effects of Wetting on these Properties. *Textile Research Journal,* 47**,** 650-662.

WRAY, J. 1670. A Confirmation of What Was Formerly Printed in Numb. 50. of these Tracts, about the Manner of Spiders Projecting Their Threds; Communicated by Mr. John Wray, to the Publisher. *Philosophical Transactions (1665-1678),* 5**,** 2103-2105.

WRIGHT, S. & GOODACRE, S. L. 2012. Evidence for antimicrobial activity associated with common house spider silk. *BMC Research Notes,* 5**,** 326.

WRINN, K. M. & UETZ, G. W. 2007. Impacts of leg loss and regeneration on body condition, growth, and development time in the wolf spider Schizocosa ocreata. *Canadian Journal of Zoology,* 85**,** 823-831.

YAMADA, H., NAKAO, H., TAKASU, Y. & TSUBOUCHI, K. 2001. Preparation of undegraded native molecular fibroin solution from silkworm cocoons. *Materials Science and Engineering: C,* 14**,** 41-46.

YANG, Y., CHEN, X., SHAO, Z., ZHOU, P., PORTER, D., KNIGHT, D. P. & VOLLRATH, F. 2005. Toughness of spider silk at high and low temperatures. *Advanced Materials,* 17**,** 84-88.

YARGER, J. L., CHERRY, B. R. & VAN DER VAART, A. 2018. Uncovering the structure–function relationship in spider silk. *Nature Reviews Materials,* 3**,** 18008.

YIN, Z., WU, F., ZHENG, Z., KAPLAN, D. L., KUNDU, S. C. & LU, S. 2017. Self-Assembling Silk-Based Nanofibers with Hierarchical Structures. *ACS Biomaterials Science & Engineering,* 3**,** 2617-2627.

YOUNG, R. J., HOLLAND, C., SHAO, Z. & VOLLRATH, F. 2021. Spinning conditions affect structure and properties of Nephila spider silk. *MRS Bulletin,* 46**,** 915-924.

ZEPLIN, P. H., MAKSIMOVIKJ, N. C., JORDAN, M. C., NICKEL, J., LANG, G., LEIMER, A. H., RÖMER, L. & SCHEIBEL, T. 2014. Spider Silk Coatings as a Bioshield to Reduce Periprosthetic Fibrous Capsule Formation. *Advanced Functional Materials,* 24**,** 2658-2666.

ZHAO, Y., LANDAU, S., OKHOVATIAN, S., LIU, C., LU, R. X. Z., LAI, B. F. L., WU, Q., KIEDA, J., CHEUNG, K., RAJASEKAR, S., JOZANI, K., ZHANG, B. & RADISIC, M. 2024. Integrating organoids and organ-on-a-chip devices. *Nature Reviews Bioengineering,* 2**,** 588-608.